SYNTHESIS AND CHARACTERIZATION OF MORDENITE TYPE ZEOLITE USING SILICA FROM CHEMICAL SOURCES AND RICE HUSK ASH

A Thesis Submitted
In Partial Fulfilment of the Requirements
for the Degree of
DOCTOR OF PHILOSOPHY

by

PRAMOD KUMAR BAJPAI

to the

DEPARTMENT OF CHEMICAL ENGINEERING
INDIAN INSTITUTE OF TECHNOLOGY KANPUR

AUGUST 1977

IN MEMORY

of

MY LATE MOTHER

I.I.T. KANPUR
CENTRAL LIBRARY
Acc. No. A 50009
4 MAY 1978

CHE-1977-D-BAD-SYN

I.I.T. Kanpur.
Submitted on 2.2.77

CERTIFICATE

Certified that the work 'SYNTHESIS AND CHARACTERIZATION OF MORDENITE TYPE ZEOLITE USING SILICA FROM CHEMICAL SOURCES AND RICE-HUSK ASH' has been carried out under our supervision and that the work has not been submitted elsewhere for a degre

(K.V.G.K. GOKHALE)
Professor
Department of Civil Engineering

(M. SOMESWARA RAO)
Assistant Professor
Department of Chemical Enginee

Indian Institute of Technology
Kanpur-208016, India

GRADUATE OFFICE
This thesis has been approved for the award of the Degree of Doctor of Philosophy (Ph.D.) in accordance with the regulations of the Indian Institute of Technology Kanpur
30. 1. 1978

ACKNOWLEDGEMENTS

The author had the benefit of continuous valuable guidance and constant encouragement from Professors K.V.G.K. Gokhale and M. Someswara Rao. Their clear, deep insight into many problems encountered during the period of research has enabled the author to accomplish his task in the stipula period of time. The author is deeply indebted to both these supervisors for the same. The author is grateful to Professo E.C. Subba Rao of Materials Science programme for several discussions and timely suggestions.

Dr. D.M. Rao of the geology laboratory has been a source of constant encouragement. The author acknowledges the assistance received from several sources for this work - Dr. T. Prasad Rao for surface area measurements, Shri A.S. Naiyer for thermal analyses, Shri Chaurasia and Shri Basak for flame photometric analyses, Shri R.K. Jain for infrared analyses and Shri D.B. Chakraborty and Shri R.K. Kanaujia for the general technical help. Cooperation received from the staff of the Chemical Engineering Department and that of Glass Blowing Shop is deeply appreciated.

The pleasant association of the colleagues Shri S.C. Shenoy, Shri R.K.Gupta and Dr. N.Choudhary has been of considerable value in keeping the author's schedule.

The author is grateful to Hydronyl Limited (England) for the generous gift of Zeolon. The author acknowledges th continuous help in organization from Pratima (his wife) and the financial assistance received from the Council of Scient and Industrial Research (India) which contributed to the completion of the task.

Author

CONTENTS

	List of Figures ...	vii
	List of Tables ...	x
	Synopsis ...	xii
CHAPTER		
1	INTRODUCTION AND LITERATURE REVIEW	1
	1.1 Structure of Zeolite ...	2
	1.2 Structure and Applications of Mordenite	4
	1.2.1 Structure ...	4
	1.2.2 Applications ...	4
	1.3 Literature Review on the Synthesis and Characterization of Mordenite	8
	1.3.1 General Considerations of Zeolite Synthesis ...	8
	1.3.2 Synthesis of Mordenite	10
	1.4 Characterization of Mordenite	15
2	STATEMENT OF THE PROBLEM ...	22
3	EXPERIMENTAL ...	25
	3.1 Materials ...	25
	3.2 Methods ...	27
	3.2.1 For Synthesis Using Chemical Silica Source ...	27
	3.2.2 For Synthesis Using Rice-Husk Ash ...	29
	3.2.3 Methods of Characterization	29
4	RESULTS AND DISCUSSION ...	33
	4.1 Synthesis ...	33
	4.1.1 synthesis of Mordenite Using Silica from Chemical Source	34

4.1.2 Synthesis of Mordenite Using Silica from Rice-Husk Ash 57

4.1.3 Crystallization Mechanism and Kinetics ... 79

4.2 Characterization of Mordenite 84

4.2.1 X-ray Diffraction Data 85

4.2.2 Infrared Absorption Spectra 94

4.2.3 Thermal Characteristics 102

4.2.4 Chemical Analyses ... 111

4.2.5 Ion-Exchange Characteristics 114

4.2.6 Surface Properties 116

4.2.7 Molecular Sieve Behaviour and Pore Size Determination 121

5 SUMMARY AND CONCLUSIONS ... 123

5.1 Summary ... 123

5.2 Conclusions ... 127

5.3 Recommendations for Future Research 127

REFERENCES ... 129

APPENDIX ... 136

σσσσσσσ

LIST OF FIGURES

FIGURE		
1.1	Mordenite Framework Structure Viewed in the C-direction ...	5
3.1	Line Diagram for the Autoclave Assembly	28
4.1	Reaction Composition Diagrams for 12 Hours Using Silica from Chemical Sources	42
4.2	Reaction Composition Diagrams for 24 Hours Using Silica from Chemical Sources	43
4.3	Effect of Composition of the Starting Batches on Zeolite Crystallizatiom at 135°C for 24 Hours ...	44
4.4	Effect of Composition of the Starting Batches on Zeolite Crystallization at 150°C for 24 Hours	45
4.5	Effect of Composition of the Starting Batches on Zeolite Crystallization at 165°C for 24 Hours ...	46
4.6	Effect of Temperature on Zeolite Synthesis with Starting Batches of Various Compositions (SiO_2/Na_2O Ratios Obtained for constant Al_2O_3, 6.7 per cent from Figures 4.1, 4.2, 4.16 and 4.17	48
4.7	Batch Compositions for Synthesis of Zeolite at 135°C for 24 Hours in the Na_2O-Al_2O_3-SiO_2-H_2O System (Rectangular Coordinates) ...	50
4.8	Batch Compositions for Synthesis of Zeolite at 150°C for 24 Hours in the Na_2O-Al_2O_3-SiO_2-H_2O System (Rectangular Coordinates) ...	51
4.9	Batch Compositions for Synthesis of Zeolite at 165°C for 24 Hours in the Na_2O-Al_2O_3-SiO_2-H_2O System (Rectangular Coordinates) ...	52

4.10	Typical X-ray Diffraction Patterns for Product Obtained after 12 Hours with Batch Composition: $3.5Na_2O \cdot Al_2O_3 \cdot 10\ SiO_2 \cdot 219H_2O$ (Run Nos. 315 and 321) ...	55
4.11	Typical X-ray Diffraction Patterns for Product Obtained after 24 Hours with Batch Composition: $3\ Na_2O \cdot Al_2O_3 \cdot 8SiO_2 \cdot 219H_2O$ (Run Nos. 343, 327 and 347).	56
4.12	Effect of Time on the Stability Fields of Mordenite ...	58
4.13	Typical X-Ray Diffraction Patterns of Products Obtained for Various Reaction Periods at 135°C with Batch Composition $3Na_2O \cdot Al_2O_3 \cdot 6SiO_2 \cdot 219H_2O$ (Run No. 352)	59
4.14	Typical X-Ray Diffraction Patterns of Products Obtained for Various Reaction Periods at 150°C with Batch Composition $4Na_2O \cdot Al_2O_3 \cdot 12SiO_2 \cdot 219H_2O$ (Run No. 330)	60
4.15	Typical X-Ray Diffraction of Products Obtained at 100°C Using Silica from Rice-Husk Ash with Batch Composition: $4Na_2O \cdot Al_2O_3 \cdot 3SiO_2 \cdot 219H_2O$ (Run No. 412)	69
4.16	Reaction Composition Diagrams for 12 Hours Using Silica from Rice-Husk Ash	70
4.17	Reaction Composition Diagrams for 24 Hours Using Silica from Rice Husk Ash	71
4.18	Effect of Silica Source on the Mordenite Synthesis (for 12 Hours Reaction Periods)	72
4.19	Effect of Silica Source on the Mordenite Synthesis (for 24 Hours Reaction Periods)	73
4.20	X-Ray Diffraction Patterns of Products Formed for Different Reaction Periods at 165°C with Batch Composition: $3.5Na_2O \cdot Al_2O_3 \cdot 10SiO_2 \cdot 219H_2O$ (Using Silica from Chemical Sources) ...	77
4.21	X-Ray Diffraction Patterns of Products Formed for Different Reaction Periods at 165°C with Batch Composition: $3.5Na_2O \cdot Al_2O_3 \cdot 10SiO_2 \cdot 219H_2O$ (Using Silica from Rice Husk Ash) ...	78

4.22	Crystallization Curves of Mordenite Using Silica from Chemical Sources	80
4.23	Crystallization Curves of Mordenite Using Silica from Rice-Husk Ash	81
4.24	Dependence of Conversion Rate and Induction Period on Temperatures from Mordenite ...	83
4.25	Typical X-Ray Diffraction Patterns for Synthesized Mordenite and Standard Zeolon ...	88
4.26	Infrared Spectra of Synthesized Mordenite Samples (Range 4000-300 Cm^{-1})	98
4.27	Infrared Spectra of Synthesized Mordenite Samples (Ranges 4000-3000 Cm^{-1} and 1800 - 1500 Cm^{-1}) ...	99
4.28	Thermograms for Na-Mordenite Synthesized from Silica from Chemical Sources	103
4.29	Thermograms for Na-Mordenite Synthesized from Silica from Rice-Husk Ash	105
4.30	Thermograms for H-Mordenite Synthesized from Silica from Rice-Husk Ash	106
4.31	Thermograms for H-Zeolon (Standard)	108
4.32	DTA Pattern for NH_4-Mordenite	109
4.33	Thermograms for Synthesized Analcime	110
4.34	Thermograms for Synthesized Phillipsite	112
4.35	Nitrogen Adsorption Isotherms	117

σσσσσσ

LIST OF TABLES

1.1	Water Sorption Capacity of Zeolites	3
1.2	Experimental Conditions for the Synthesis of Mordenite and Analcime	13
1.3	Some Important Patents on the Synthesis of Mordenite	16
1.4	Zeolite IR Assignments	19
3.1	Chemical Composition of Rice-Husk Ash	26
3.2	Typical Physical Characteristics of Zeolon Molecular Sieves	26
	Synthesis of Zeolites Using Silica from Chemical Sources:	
4.1	At 110 and 120°C	36
4.2	At 135°C	37
4.3	At 150°C	39
4.4	At 165°C	40
4.5	At 175, 190 and 200°C	41
	Synthesis of Zeolites Using Silica from Rice Husk Ash	
4.6	At 90, 100 and 110°C	62
4.7	At 135°C	64
4.8	At 150°C	65
4.9	At 165°C	66
4.10	Activation Energies for Nucleation and Crystal Growth of Mordenite	84
4.11	X-Ray Powder Data for Synthesized Mordenites	86
	X-Ray Powder Data for Ammonium and Hydrogen Mordenite	
4.12	Using Silica From Chemical Sources	89

4.13	Using Silica from Rice-Husk Ash	91
4.14	Lattice Parameters for Mordenite Samples	93
4.15	X-Ray Powder Data for Phillipsite	95
4.16	X-Ray Powder Data for Analcime	96
4.17	Infrared Spectral Data for Mordenite Samples	100
4.18	Chemical Composition of Various Mordenite Samples	113
4.19	Ammonium Ion-Exchange Results	115
4.20	Nitrogen Adsorption Data	118
4.21	Surface Area of Various Mordenite Samples	120
4.22	Acidity Measurements of Mordenite Samples	121
A-2	X-Ray Powder Data for SodiumSilicate	137
A-3	X-Ray Powder Data for Sodium Hydroxide	138
A-4	X-Ray Powder Data for Aluminium Hydroxide	138
A-5	X-Ray Powder Data for Natural Mordenite	139

σσσσσ

SYNTHESIS AND CHARACTERIZATION OF MORDENITE TYPE ZEOLITE USING SILICA FROM CHEMICAL SOURCES AND RICE-HUSK ASH

A Thesis Submitted
In Partial Fulfilment of the Requirements
For the Degree of

DOCTOR OF PHILOSOPHY

by

PRAMOD KUMAR BAJPAI
to the
Department of Chemical Engineering
Indian Institute of Technology, Kanpur

August 1977

SYNOPSIS

Mordenite, the high silica zeolite species, is increasingly being used in recent times as a molecular sieve in the adsorptive separation of gas/liquid mixtures involving acidic components. It also finds extensive application as a catalyst for various industrially important reactions like hydrocracking, hydroisomerization, alkylation, reforming and cracking. In spite of such wide usage, a detailed study of mordenite, dealing with its synthesis, stability and characterization has not been adequately undertaken so far by the earlier workers.

The present work deals with the study of synthesis and characterization of mordenite type zeolite. The mordenite was synthesized separately from two types of gels. While sodium silicate, sodium hydroxide, silica gel and aluminium hydroxide constituted the materials for one gel, in the other one silica has been largely supplied as silica solution (with sodium hydroxide) derived from the rice-husk ash. The latter approach was meant to utilize the rice-husk, an agricultural waste product, as a source of silica. The ash obtained on burning rice-husk contains amorphous silica upto 90 per cent by weight. In agricultural countries like India, the rice-husk produced in enormous quantities is available at a very low-cost price. As such the utilization of rice-husk ash in the synthesis of mordenite offers tremendous scope in countries like India, Burma, Sri Lanka, Thailand and Japan.

The thesis has five chapters. A brief review of the structures of the zeolites with an emphasis on the mordenite structure followed by the review of the existing literature on the synthesis, stability and characterization of mordenite has been presented in Chapter 1. Based on this literature survey, the aspects that have received inadequate attention in the synthesis and characterization of mordenites, have been brought into focus and the objectives of the work with a statement of the problem are given in Chapter 2. The materials

utilized and the methods adopted for the synthesis as also the characterization are outlined in Chapter 3.

The results obtained in the present study and the discussion of the same are presented in Chapter 4. This chapter has been divided into two parts - one part dealing with the synthesis and the other one with the characterization. Around 250 runs have been carried out with the gels containing silica from chemical sources and also those with silica derived from rice-husk ash with composition, time and temperature as variables. The ranges for the same are as follows:

Temperature of crystallization	:	90 - 200°C
Time of crystallization	:	1 hr - 7 days
SiO_2/Al_2O_3 (molar ratio) in the starting mix	:	1 - 20
Na_2O/Al_2O_3 (molar ratio) in the starting mix	:	0.8 - 6.0
H_2O/Na_2O (molar ratio) in the starting mix	:	40 - 220

The compositional stability diagrams for mordenite with various temperatures and times of synthesis have been presented. The rate of crystallization of mordenite as also the formation of other phases at different stages of investigation and under different conditions have been tracked using x-ray diffraction technique. The crystallization proceeds through a sequence: amorphous product ⟶ mordenite/phillipsite ⟶ analcime.

The best temperature for the crystallization of mordenite has been found to be in the range 135 - 165°C. The crystallization of mordenite is controlled by the composition of initial gel and also by the type of silica in the gel. Within the synthesis range, as the temperature of synthesis increased the field for mordenite crystallization shifted towards higher SiO_2 and lesser Na_2O in the initial gel compositions. With greater alkalinity in the initial gel, analcime crystallized even at lower temperatures preceded by the formation of phillipsite. It has also been observed that the gels containing silica solution from rice-husk ash are more reactive compared to the gels with silica from chemical sources. The rate curves for the mordenite synthesis from both types of gels presented and the activation energies obtained in the present investigations are in conformity with the reported values.

The cell constants for the synthesized mordenites (a = 18.06, b = 20.34 and c = 7.54 Å) correspond closely to the standard mordenite and the chemical analyses indicated its composition to be $Na_2O \cdot Al_2O_3 \cdot 10.8\ SiO_2$. The dehydration and dehydroxylation characteristics obtained with the differential thermal patterns have been discussed for the synthesized sodium mordenite and also its hydrogen form. The weight loss measurements indicated a total loss of 13.6 per cent for sodium form (corresponding to a total of 26.7 H_2O per unit

cell) and 14.8 per cent for the hydrogen form. These values are in conformity with the earlier reports. The infrared absorption spectra for the sodium and hydrogen forms have been presented with a discussion on the different bands in various frequency regions as related to the mordenite framework structure and the association of water. The water adsorption capacity was found to be 15.2 per cent for the sodium form and 16 per cent for the hydrogen form. The surface area estimations by the BET method revealed the values around 450 m^2/g for the sodium form and 500 m^2/g for the hydrogen form. These closely agreed with the reported values for the standard mordenite. The acidity as a measure of its catalytic activity was also determined.

The utilization of synthesized mordenite in its sodium and hydrogen forms as molecular sieves has been established using toluene and p-xylene, toluene and o-xylene, o-xylene and p-xylene and o-xylene and triethyl benzene mixtures. The sodium form adsorbed p-xylene and toluene and excluded o-xylene, while the hydrogen form adsorbed o-xylene and excluded triethylbenzene. Thus the mordenite synthesized in the present case is of a large port variety.

A summary of the results achieved in the present study has been presented in Chapter 5 alongwith the conclusions and suggestions for future work.

CHAPTER 1

INTRODUCTION AND LITERATURE REVIEW

The utilization of synthetic crystalline zeolites as molecular sieves and as catalysts offers considerable potential in industry [1-5] such as in adsorption separations, ion-exchange, hydrocarbon catalysis, recovery of radioactive ions from waste solutions and separation of hydrogen isotopes, and other purifications. Zeolites are known as molecular sieves because of their selective adsorption behaviour. The term molecular sieve was first used by McBain [6] to define porous solid materials which exhibit the property of acting as sieves towards the gas molecules. The dehydrated zeolite crystals act as sieves by the selective adsorption or the rejection of gas/liquid molecules due to the differences in the sizes and structural characteristics of such materials. The internal pore spaces available in zeolites are governed by the individual zeolite structure.

The present work deals with the synthesis and characterization of the mordenite type zeolite and as such the literature reviewed in this chapter is essentially confined to the same. However, as an introduction to the subject, a brief account of the structure of zeolites in general and of mordenite in particular is presented.

1.1 Structure of Zeolite:

Zeolites are crystalline crosslinked, polymeric macromolecules having repeating units given by the formula [7]:

$$M_{x/n}\ [(AlO_2)_x\ (SiO_2)_y]\cdot wH_2O$$

where M is the exchange cation of valency n, w is the number of water molecules, and x + y is the total number of tetrahedra per unit cell. The ratio y/x ranges between 1 to 10 for natural and synthetic zeolites. The framework structure is composed of chains of $Si(0/2)_4$ and $Al(0/2)_4^-$ tetrahedra in which 0/2 represents the shared oxygen atom [8]. Because the formula charge of oxygen is -2 and of aluminium is +3, each $Al(0/2)_4^-$ tetrahedra bears one unit of excess negative charge which is neutralized by the other metal cations. These metal cations which neutralize the excess anionic charge on the aluminosilicate framework are usually alkali metal and alkaline earth metal cations and at least some of them must be able to undergo reversible ion exchange if the material is to be classified as a zeolite. The water molecules fill the remaining volume in the interstices of the zeolite.

The seven structural classes of zeolites [9] have been arranged (Table 1.1) according to the openness of their framework as measured by their water sorption capacity [10]. The structure of many zeolites can be obtained by simple arrangement of polyhedra in a three-dimensional array.

TABLE 1.1: WATER SORPTION CAPACITY OF ZEOLITES

Group	Water sorption capacity (Cm^3H_2O/Cm^3 Zeolite)
Analcime	0.18
Natrolite	0.21 - 0.33
Mordenite	0.27 - 0.33
Heulandite	0.33 - 0.37
Phillipsite	0.34 - 0.49
Chabazite	0.36 - 0.46
Faujasite	0.46 - 0.54

For stability reasons, the maximum substitution of aluminium for silicon is in the ratio of 1:1. In this event, a complete ordering of the aluminium and silicon is present. However, zeolites with a Si/Al ratio of greater than 100 have been reported [11].

The zeolite structures are open and they contain large cavities filled with the water molecules. The cavities may be interconnected in one, two or three directions. The metallic ions which are needed for the charge compensation occupy sites in the channel or adjacent to the cavities and are generally available for exchange by other cations.

1.2 Structure and Applications of Mordenite:

1.2.1 Structure:

The mordenite lattice consists of micropore system essentially with parallel elliptical cylinders of major and minor crystallographic free diameters of 6.95 and 5.81 Å respectively. The main channels are interconnected by small side channels of 2.9 Å free diameter. These side channels prohibit the motion of hydrocarbon molecules from one main channel to another.

The structure of the hydrated sodium form of mordenite was studied in detail by Meier [12]. The crystal structure consists of chains of 4- and 5- membered rings of $Si(O/2)_4$ and $Al(O/2)_4^-$, in which 5- membered rings predominate (as shown in Figure 1.1). This structure of mordenite is unique among the zeolites. The unit cell of the sodium form of mordenite has dimensions: a = 18.13 Å, b = 20.49 Å, and c = 7.52 Å and the same is represented by:

$$(Na_2O)_4 \cdot (Al_2O_3)_4 \cdot (SiO_2)_{40} \cdot 24H_2O$$

which shows a silica/alumina ratio of 10:1.

Several forms of mordenite reported in literature are the derivatives from the original sodium form by ion-exchange process.

1.2.2 Applications:

The two major applications of these zeolites are

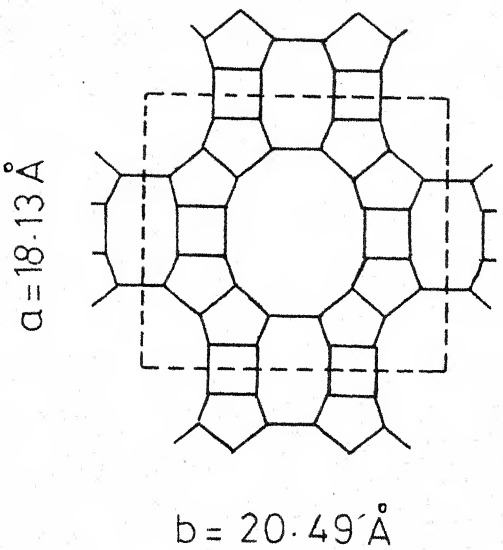

Fig. 1.1 - Mordenite framework structure viewed in the c-direction.

in adsorption and catalysis for which closely controlled specifications in terms of their purity, mechanical properties and porosity are essential. Although mordenite as a mineral occurs in nature, synthetic mordenites are better suited to meet these stringent requirements imposed on molecular sieve adsorbents in adsorption and catalytic processes, owing to their high purity.

Adsorption:

These zeolites are high capacity, selective adsorbents for two reasons:

1. They separate molecules based upon molecular size and configuration of the molecule relative to the size and geometry of the zeolite structure.

2. They adsorb molecules, in particular, those with a permanent dipole moment and other interaction effects, with a selectivity that is not found with conventional adsorbents.

Two types of separations may occur, one based upon the molecular sieve effect and the other upon the preferential adsorption. The sodium form of mordenite readily adsorbs materials such as water, CO_2, SO_2, cyclohexane and p-xylene. O-xylene, cumene and other hydrocarbons of bigger molecular diameter are physically excluded from them. When the sodium is replaced by hydrogen, the effective pore diameter of the mordenite molecular sieve increases and it adsorbs o-xylene,

cumene etc.

Of the available commercial molecular sieve adsorbents currently in use, the mordenite molecular sieves being high in silica/alumina ratio, are preferred for use in adsorption where acidic components are present. They can also be used at higher temperatures. In addition, synthetic mordenite molecular sieves are also suitable for use where resistance to strong alkali solution is required. They are stable in environments with pH as high as 12.

Catalysis:

As in adsorption, the catalytic reactions take place within the cavities of these crystalline zeolites. Hence the voids must be accessible to the reactants and zeolites with largest pore sizes and maximum available void volume are the most suitable ones. The sieving effects occur in catalysis as in adsorption. Not only the reactants permeate the zeolite structure but the products, likewise, must exit through the pores. Mordenite satisfies the important properties, for its use as a catalyst, such as structure, pore size, charge and locations, acidity and Si/Al ratio.

Zeolite catalysts are best known in hydrocarbon catalysis particularly in cracking [13-15]. In catalytic cracking, catalyst containing mordenite molecular sieve exhibits higher activity and better selectivity as compared to the conventional

silica-alumina cracking catalyst. Typically higher gasoline yields (upto 20 per cent) are obtained. In isomerization reactions, hydrogen mordenite catalysts are used to upgrade the low-octane number of normal paraffins. These catalysts have a long life and resistance to sulfur poisoning and unlike the conventional types, are non corrosive. The hydrogen mordenite is used for isomerization of xylenes [16,17] and cyclohexane [18,19]. The mordenite catalysts are also used for alkylation [20, 21], disproportionation, trans-alkylation [22], dehydration [13], steam reforming for hydrogen manufacture [23], polymerization [21, 24, 25] and a host of other reactions.

1.3 Literature Review on the Synthesis and Characterization of Mordenite:

1.3.1 General Considerations of Zeolite Synthesis:

The zeolites are synthesized under hydrothermal conditions. The term 'hydrothermal' includes the crystallization of zeolites from aqueous systems which contain the necessary chemical components. The growth of crystalline aluminosilicate first requires the formation of a nucleus. The important conditions for the synthesis are [26, 27]:

1. Reactive starting materials, such as freshly co-precipitated gels (hydrous metal aluminosilicates) or amorphous solids. The gel preparation and the subsequent crystallization

are represented by the fcllowing reaction steps:

$$Na(OH)\ (aq.) + NaAl(OH)_4\ (aq.) + Na_2SiO_3\ (aq.)$$

$$\downarrow \quad T_1 = 25 - 100^{\circ}C$$

$$[Na_a(AlO_2)_b(SiO_2)_c \cdot NaOH \cdot H_2O]\ \text{gel}$$

$$\downarrow \quad T_2 = 25 - 200^{\circ}C$$

$$Na_x[(AlO_2)_x(SiO_2)_y] \cdot m\ H_2O + \text{solution}$$

(Zeolite crystals)

2. Relatively high pH introduced in the form of an alkali metal hydroxide or other strong base.

3. Hydrothermal conditions

4. A high degree of supersaturation of the components of the gel leading to the formation of the nucleus of a large number of crystals.

The zeolites are formed in the early stages as a metastable phase which left for a longer time in the system, is converted to a more stable species. The type of zeolite formed depends upon the composition of the starting mix, the temperature and the time of crystallization.

Several investigators have synthesized the zeolites under high temperature and pressure (i.e. natural conditions) [28-31]. Extensive, pioneering and systematic research on hydrothermal chemistry of aluminosilicates was started by Barrer [32-35]. Barrer and his coworkers have been active in making significant contributions on zeolite synthesis for the last three decades.

Synthesis of zeolites at low temperature under low pressure starting from very reactive components was first reported by Milton and his associates [36,37]. They synthesized several zeolites at temperatures ranging from about room temperature to the boiling point of water. Synthesis of zeolites at low temperature has also been reported involving different starting materials under different conditions [38-41]. Since the present study is concerned mainly with the synthesis of mordenite, a literature survey on the synthesis of the same is given in the following section.

1.3.2 Synthesis of Mordenite:

Enough literature exists on the synthesis of mordenite type zeolite [30, 33, 35, 40-66]. Several starting materials of both chemical and natural (mineral) sources have been used in the synthesis. First report on synthesis of mordenite was by Leonard [42] who obtained Na-Li mordenite by reacting feldspars and alkali carbonates for 7 days at 200°C and 15 atm pressure.

Using ingredients of chemical source, Barrer and coworkers [33, 35] have reported the ideal temperature range for the mordenite synthesis to be 265 - 295°C with the initial compositions: SiO_2/Al_2O_3 = 8-12, Na_2O/Al_2O_3 = 1 under alkaline conditions (pH = 8 to 10). Barrer and Denny [40] obtained low yields of calcium mordenite using different silica sources (sol. and powdered silica glass) in the temperature range of

125 - 450°C. Ames and Sand [44] reported the synthesis of sodium and calcium mordenites at 330 - 455°C under 1000 atm pressure approaching the natural environmental conditions of the occurrence of these minerals. The mordenite type zeolite was synthesized by Ellis [45] from obsidian glass at 230°C at pH of 5-7 after 17 days of reaction. Strontium mordenite has been synthesized in the system $SrO-Al_2O_3-nSiO_2$ (n=1 to 9) in the temperature range 110-450°C [46].

With the variation of the conditions of the synthesis, Sand [41] has obtained two types of synthetic mordenites which are termed as the large port-type and the small port-type. The small port-type mordenite exhibited an adsorption diameter of about 4 Å, while the large port one could adsorb molecules of about 7 Å diameter. While the type of starting materials was found to be critical in the temperature range of 275 - 300°C for the synthesis of small port mordenite equivalent to the zeolite Na-D of Barrer [35], the water content, however, was found to be critical for the synthesis of large port variety at 100-260°C for 12 to 168 hours. The large port variety could not be successfully distinguished from the small port one by x-ray diffraction techniques.

A high purity mordenite type zeolite was synthesized by Domine and Quobex [47] using a SiO_2/Al_2O_3 ratio of 12 to 13 in the starting mixture. Starting with amorphous sodium alumino-silicate at 300°C, the rate of crystallization was increased

with increase in pH upto 12.8, beyond which the mordenite was apparently converted to analcime-type zeolite. At a pH of 12.6, the induction period varied from one hour at 350°C to 4 weeks at 100°C and two days at 200°C. The rate of crystallization from gels was slower than that from amorphous aluminosilicate. The experimental conditions for the synthesis of mordenite are presented in Table 1.2 together with those for analcime, which also appears often as one of the products.

Mordenite has also been synthesized from alumino silicate gels in periods varying from 2 to 12 hours at 150-200°C in the presence of 0.05 to 10 wt. per cent of an alkyl phenol and alkyl sulfonate or a HCHO-naphthalene sulfonic acid condensate [48]. The synthesis of mordenite from an inexpensive raw material, pitchstone, at 200°C within 4 hours of duration has been reported [49].

Culfaz and Sand [50] indicated that the induction period can be eliminated by seeding the starting mixture with the mordenite crystals. They have also found that the addition of NaCl in the starting mixture decreased the rate of crystallization of mordenite at 90-135°C.

The most suitable conditions for the synthesis of Li-mordenite were reported by Sand and coworkers [51] to be around 150-200°C using the colloidal silica sol., aluminium hydroxide and lithium carbonate as the starting materials. Sand and Sand [52] prepared the Li-Na mordenite from the

TABLE 1.2: EXPERIMENTAL CONDITIONS FOR THE SYNTHESIS OF MORDENITE AND ANALCIME

Zeolite Type	Typical Reactant composition (mol /mol of Al_2O_3)			Reactants	Conditions		Ref.
	Na_2O	SiO_2	H_2O		Temp., °C	Time	
1	2	3	4	5	6	7	8
Na-D (mordenite)	1	8.2-12.3	-	$NaAlO_2$, silicic acid	265-295 pH=8-10	2-3 days	33, 3 47
Large port mordenite	6.3	27	61	$NaAlO_2$, diatomite, sodium silicate	100	168 hr	41, 5
Large port mordenite	2.6	15.5	56	$NaAlO_2$, diatomite, sodium silicate	175	16 days	41, 5
Large port mordenite	12	10.7	53	$NaAlO_2$, silicic acid, sodium silicate	260	24 days	54
Mordenite	1+x x=20-40 mg/g.H_2O	10	-	$NaAlO_2$, NaOH, silica-gel	150-200	7 days	55
Mordenite	2	12	-	$NaAlO_2$, silica gel	300 150	1 day 4-8 days	47
Mordenite	8.5 $NaCl/Al_2O_3$ = 4.5	3.5	182	Sodium silicate, an amorphous substrate of near-mordenite composition	90-135	200-700 hr	50

Table 1.2 (contd)

1	2	3	4	5	6	7	8
Mordenite	8.5 (26 per cent mordenite $NaCl/Al_2O_3=4.5$)	3.5	182	Sodium silicate, an amorphous substrate of near-mordenite composition	150-300	10-20 hr	50
Na-B (Analcime)	>1.0	4.0	-	$Al_2O_3 \cdot 3H_2O$, NaOH, silicic acid	180	-	35
Analcime	1.0	2.6	-	$Na_2O \cdot Al_2O_3 \cdot SiO_2$ glass	200	1 day	56,57
Analcime	1.0	2-10	-	Silica glass, $NaAlO_2$	300	24 hr	58
Analcime	≈1	2.5-13	-	$Na_2O \cdot Al_2O_3 \cdot SiO_2$ gels			59,60

lithia-soda system at 200°C in 300 hours. Kimura and Nakajima [53] have synthesized a mixed mordenite with $K_2O/(K_2O + Na_2O + CaO)$ mol. ratio of 0 - 0.5 at 1000 bars fluid pressure and 300 - 400°C temperature in the $K_2Al_2Si_{10}O_{24}$ $(Na_2, Ca)Al_2 \cdot Si_{10}O_{24} \cdot H_2O$ system.

The extensive literature on mordenite synthesis is available in patent form, part of which is condensed in Table 1.3.

1.4 Characterization of Mordenite:

Crystalline zeolite molecular sieves are complex materials chemically and structurally, comprising the major group of the framework silicates. A complete characterization of a zeolite involves the work on the framework structure, cation content, chemical composition and various structure related properties such as the ion exchange behaviour and physical adsorption characteristics. Thus to characterize a zeolite several tools of analysis are being used. These include the x-ray diffraction analysis, infrared absorption, nuclear magnetic resonance, electron spin resonance in addition to many other conventional chemical techniques.

Extensive x-ray studies since 1955 have enabled the determination of the detail framework structure of about 40 species and a classification of the various structure types and groups has been proposed by Smith [67], Fisher and Meier [68] and Meier [9]. X-ray analysis has been used to

TABLE 1.3: SOME IMPORTANT PATENTS ON THE SYNTHESIS OF MORDENITE

S.No.	Reactants and their composition	Temp., ^{o}C	Time	Ref.
1	2	3	4	5
1.	240 parts of amorphous SiO_2, 50 parts of 28 per cent sod. silicate solution, 100 parts of sod. aluminate	150	24 hr	63
2.	Diatomaceous earth, sod. aluminate, sod. silicate Na_2O/SiO_2 = 0.07 - 0.3 SiO_2/Al_2O_3= 6 - 180 Na_2O/Al_2O_3= at least 1	75-175	24 hr	64
3.	Siliceous, aluminous, aluminosiliceous sources in presence of organic compounds.	150-200	2-12 hr	48
4.	Pitch stone, Na_2CO_3, $NaNO_3$, sod. silicate	200	4 hr	49
5.	Silica-alumina gel, Na_3PO_4	100-150	72-240 hr	54
6.	Sodium and lithium system: 0.34 Li_2O·0.36 Na_2O·Al_2O_3· 10.2 SiO_2·6.6 H_2O. Lithium system: $3Li_2O \cdot Al_2O_3 \cdot 40SiO_2 \cdot 314H_2O$	200	300 hr	52

Table 1.3 (contd)

1	2	3	4	5
7.	Silica containing material, NaOH etc.			
	SiO_2/Al_2O_3 = 9 - 18,	100	-	65
	Na_2O/SiO_2 = 0.1-0.25			
	H_2O/Na_2O = 5 - 70			
8.	Amorphous aluminosilicates, and aluminium salt solution	200-280	24-48 hr	66
	SiO_2/Al_2O_3 = 10-12			
	Na_2O/Al_2O_3 = 0.5-2.0			

determine the crystallinity of the zeolite, the distribution of cation sites and the structural changes caused during ion-exchange and calcination etc. In fact x-ray diffraction technique has attained an important place in the characterization of zeolites. The loss in the crystallinity of the large port mordenite as a function of aluminium extraction from it has been studied by Krainich and coworkers [11]. Weeks and coworkers [69] have investigated the effects of the heating rate and heating conditions on the crystallinity of the mordenites using x-ray diffraction. The cell constants for the Na-, NH_4- and H- forms of mordenite have been reported in the literature [69].

The non-availability of large single crystals of synthetic zeolites limits the structural investigations using x-ray diffraction technique. The polyhedral building units present in the zeolite framework can be best understood with infrared spectroscopy. The mid infrared region (200-1300 Cm^{-1}) of the spectrum is used since it contains the fundamental vibrations of the framework (Si, Al)O_4 tetrahedra. Infrared data for this region for synthetic zeolites (including mordenite) are available [70-73]. The IR spectra for zeolites indicate peaks that can be assigned to (1) internal vibrations of the TO_4 tetrahedron, not sensitive to structural variations and (2) vibrations related to the linkages between the tetrahedra which are sensitive to overall structure. These are presented

in Table 1.4. The number of Al atoms in the framework structure influence the variation of frequency in both the asymmetric stretching in the region 970-1020 Cm^{-1} as also the symmetric stretching in the region 670 - 725 Cm^{-1} [72, 73].

TABLE 1.4: ZEOLITE IR ASSIGNMENTS, CM^{-1} [73]

1. Internal Tetrahedra	-Asym. stretch	1250 - 950
	-Sym. stretch	720 - 650
	-T-O bend	500 - 420
2. External linkages	-Double rings	650 - 500
	-Pore Opening	420 - 300
	-Sym. stretch	820 - 750
	-Asym. stretch	1150 - 1050

Removal of zeolite water did not modify the infrared spectra within the mid infrared region of several synthetic zeolites containing alkali metal ions [73]. The association of water molecules with the cation and/or with the framework oxygen ions of a zeolite is dependent upon the openness of the structure. The three typical bands observed are the broad band characteristics of hydrogen bonded OH around 3400 Cm^{-1}, the sharp band typical of isolated OH at 3700 Cm^{-1} and the usual bending vibration of the water at 1645 Cm^{-1}. The isolated OH stretching is attributed to the interaction of the water

hydroxyl with the cation. The other bands are assigned to the hydrogen bonding of the water molecules to a surface oxygen and to the bending mode of the water [74].

Structurally similar zeolites can be distinguished by the differential thermal analysis patterns and DTG data [75-78]. Barrer and Peterson [79] have reported the DTA and TGA patterns for the hydrogen mordenite. According to them, the initial endotherm from slightly above room temperature to 350°C is characteristic of its dehydration and the exotherm around 1000°C corresponds to its crystal collapse. The total weight loss is reported to be around 15 per cent. Ammonium mordenite exhibits a sharp endotherm at 130°C due to water desorption and a large exotherm at 525°C due to NH_3 oxidation. A shallow endotherm was also reported around 400°C indicating some NH_3 desorption prior to oxidation. The dehydroxylation event is characterized by an endotherm around 700°C and the crystal collapse by an exotherm around 1030°C [69].

The ion-exchange process in synthetic zeolites have been extensively studied [80-85]. Since the hydrogen form of the mordenite has more catalytic activity, efforts have been made by earlier workers to derive this form through a two-stage operation; first by ammonium exchange of sodium mordenite to form ammonium mordenite and later by converting the ammonium form to hydrogen form by heating. Work in this direction has been reported by Barrer [33] and Weeks and coworkers [69].

Adsorption studies on natural mordenites were reported by several workers for argon, oxygen, nitrogen, water, CO_2, CO, CH_4, C_2H_4, C_2H_6 and C_3H_8 [86, 87]. Adsorption on sodium and hydrogen form of zeolon for CO_2, SO_2, Ar, O_2, N_2 and Kr was also studied [88-91]. The adsorption of several gases and hydrocarbons was studied by Barrer and Peterson [79].

The catalytic activity and selectivity of mordenite for several reactions have been extensively studied. The BET surface area of mordenite has been reported to be around 400 m^2/g for Na-form and 500 m^2/g for H-form [92, 93]. Hopper and Shigemura [17] have reported that H-mordenite is a very good catalyst for the liquid phase isomerization of xylene. They achieved 88 per cent of p-xylene equilibrium. Studies on mordenite as a catalyst were also reported for reactions such as cumene cracking [15], cyclohexane hydroisomerization [18], dehydrogenation and isomerization of cyclohexane [19], benzene alkylation with ethylene and propylene [20] and benzene alkylation and polymerization of ethylene [21].

CHAPTER 2

STATEMENT OF THE PROBLEM

The high silica zeolites and especially the mordenite type, as already stated earlier, find extensive industrial applications in adsorptive separations and also in catalysis of hydrocarbon reactions. As evident from the literature review presented in the previous chapter, the information on the synthesis of mordenite has been inadequate in its detail. No systematic work has been reported in the published literature on the synthesis and stability of mordenite as also the role of the different parameters in its formation.

In the earlier work on the synthesis of mordenite, the starting materials for silica and alumina have been from chemical sources. Efforts have also been made by some workers to use clay mineral like montmorillonite as a source for alumina and silica in the synthesis of some zeolites though not for mordenite.

In agricultural countries such as India, Sri Lanka, Thailand and Japan, rice-husk is obtained in enormous quantities as a byproduct. This material, as experiences in India reveal, is easily available in large quantities on an extremely low-cost basis. This husk, on complete burning yields porous, cellular and light grey coloured ash which on analysis has been found to be containing amorphous silica upto around 90 per cent

by weight of the ash composition. Being cellular, this silica is in a highly reactive state. As such the rice-husk ash is an important source of silica which on leaching with an alkali like sodium hydroxide offers great potentialities for its use in the synthesis of sodium zeolites. In developing countries like India, with a need for the development of indigeneous technology, the possibility of using this rice-husk (an agricultural waste) in the synthesis of zeolites offers a great potentiality.

All these considerations generate thoughts on the following lines:

1. Can synthesis of sodium mordenite be attempted using silica from the rice-husk ash source?
2. What is the nature of the product in such a case during synthesis under different conditions?
3. The role of different parameters like composition of the starting mix, temperature and time on the formation of mordenite and its stability.
4. Are there any possible differences in the role of such parameters for mordenite synthesis from rice-husk ash silica source when compared to the same for the formation of mordenite from silica chemicals?

5. A comparison of the mordenite synthesized from both these sources with regard to their characteristics.
6. Possibilities of usage of these synthesized mordenites as molecular sieves.

An attempt has been made in the present work to answer these points.

CHAPTER 3

EXPERIMENTAL

3.1 Materials:

For the synthesis of zeolites, silica has been used in the form of sodium silicate, silica gel and silica solution derived from rice-husk ash. The sodium silicate contained 29.2 weight per cent of Na_2O and 28.3 weight per cent of SiO_2 as supplied by M/S Chemilon of Bombay, India. The silica gel was used in conjunction with the sodium silicate to obtain the required silica content in the initial mixture. The silica gel as supplied by Sarabhai-Merck Chemicals of Baroda, India, was finely ground in a ball mill to obtain the particle size fraction passing through 200 mesh. The x-ray powder pattern for the same indicated only a broad hump with no definite reflections.

Rice-husk used as a silica source was obtained from a rice-mill in Utripura situated around 40 kms from Kanpur city. The husk was burnt for 3 hours at 1000°C to get a carbon free ash. The ash thus obtained was ground in a ball mill to the size passing through 200 mesh. X-ray diffraction patterns of the ash indicated the amorphous nature of the same. The chemical composition of the ash is presented in Table 3.1.

TABLE 3.1: CHEMICAL COMPOSITION OF RICE-HUSK ASH

Components	Per cent by wt.
SiO_2	88.86
Al_2O_3	6.40
Fe_2O_3	0.35
Alkalies	1.16
Loss on ignition	3.23

Aluminium hydroxide used was of an extra pure grade (alkali free) as supplied by M/S E. Merck AG Darmstadt, Germany. Sodium hydroxide pellets, supplied by Sarabhai,Merck Chemicals of Baroda, India were utilized. The x-ray diffraction data for the sodium and aluminium chemicals are presented in Appendices A-2, A-3 and A-4.

Zeolon of Norton Company, U.S.A. make was chosen for use as a standard to compare the synthesized mordenites. This is a large port synthetic mordenite with the physical characteristics as listed in Table 3.2.

TABLE:3.2 TYPICAL PHYSICAL CHARACTERISTICS OF ZEOLON MOLECULAR SIEVES

Mineral class:	Synthetic mordenite	Bulk density (g/Cm^3)	0.64
Theoretical SiO_2/Al_2O_3 ratio	10/1	Surface area (m^2/g)	440
Effective pore diameter	7 Å	Static H_2O capacity (wt. per cent)	14
		Available form	5-12 μ (powder)

3.2 Methods:

3.2.1 For Synthesis of Mordenite Using Chemical Silica Sources:

Sodium aluminosilicate gel of varying $Na_2O:Al_2O_3:SiO_2$ was prepared by mixing two solutions individually prepared earlier, one containing sodium metasilicate in distilled water heated to boiling and the other an aqueous sodium-hydroxide solution to which an appropriate amount of $Al(OH)_3$ was added and heated to boiling. If more silica was required in the mixture, silica gel in appropriate quantities was added to the former solution. Several such mixes with varying $Na_2O:Al_2O_3:SiO_2$ proportions adopted for the synthesis are listed in Table 4.1 of the next chapter.

The hot solution of the starting mix was kept in the autoclave for the hydrothermal reaction. The autoclave used in the present investigation is a high pressure type of Parr make (Series 4500) (Figure 3.1). This unit consists of a vertical stainless steel vessel B of one litre capacity designed for operating upto 1000 psig pressure and 350°C. A stirrer S is provided which is motor driven. The pressure in the autoclave at the end of a run can be released through a gas release valve V_1. Liquid samples containing fine solid particles could be collected during the run through the sample port V_2 of the vessel. The autoclave tightly sat inside the heater assembly H and the temperature controlled to an accuracy of $\pm$ 2°C with a variac. The desired reaction

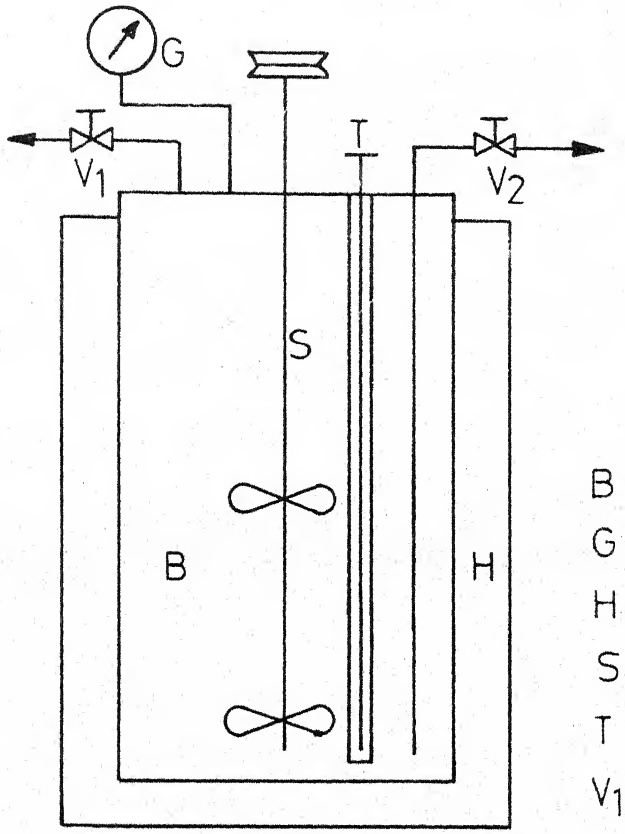

B - Stainless steel vessel
G - Pressure gauge
H - Heating assembly
S - Stirrer
T - Dial thermometer
V_1 - Gas release valve
V_2 - Sampling valve

Fig. 3.1 - Line diagram for the autoclave assembly.

temperature was attained within 30-50 minutes. The zero time of the reaction was corrected adopting the method suggested by Freund [94]. At the end of each run conducted for specific period of reaction, the material obtained was filtered in a sintered glass disk funnel under vacuum and the solid product washed with hot distilled water till the pH of the filtrate reached 7. The solid product was then dried at 120°C in an oven for 12 hours.

3.2.2 For Synthesis Using Rice-Husk Ash:

The silica solution was prepared by treating rice-husk ash with 1-2 molar aq. NaOH solution maintained at 60°C for 24 hours with continuous shaking. The silica dissolved in NaOH solution was estimated. The silica solution thus prepared was mixed with the solution containing sodium hydroxide and appropriate amounts of $Al(OH)_3$. Several compositions of starting mix were prepared by an appropriate mixing of these solutions listed in Table 4.2.

The procedure adopted for the synthesis is identical to the one described in previous section.

3.2.3 Methods of Characterization:

X-ray diffraction analyses were carried out on G.E. unit fitted with XRD-6 diffractometer using Ni-filtered Copper K_α radiations. Scanning was done in the range of 6-60°(2 θ) at a rate of 2°/min with a chart speed of 1''/min. The exact

peak positions were checked by obtaining the counts from point to point within the peak range. The interplanar spacings (d) were obtained for all the synthesized samples and the cell constants were also determined for the mordenite using formula for the orthorhombic system.

The infrared spectra for the samples were recorded using a Perkin Elmer 521 IR spectrophotometer using KBr pellet technique [95]. The spectra were obtained in the range 4000-300 Cm^{-1} which covers the frequency ranges for the framework structure as also water association.

Differential thermal analysis (DTA), differential thermogravimetric (DTG) and thermogravimetric (TG) analysis of the samples were carried out simultaneously using the Derivatograph of MOM make (Budapest) with 10^{o}/min. heating rate using α Al_2O_3 as an inert material. Few samples were also analyzed on DuPont 900 DTA unit fitted with $1200^{o}C$ furnace assembly using Pt-Pt 13 per cent Rh thermocouples.

The silica, alumina and sodium estimations were done by standard analytical procedures [96-98].

For preparing ammonium mordenite, samples of sodium mordenite synthesized were kept in an excess of 2 M aqueous solution of NH_4Cl in a constant temperature shaker bath maintained at $70^{o}C$. The exchanged zeolites after equilibration were filtered and dried. These samples were once again treated with NH_4Cl solution and this process was repeated several times.

The degree of exchange was determined from the concentration of sodium ions in the equilibrated solutions with the help of flame photometry and the coordinates of Na^+-NH_4^+ exchange isotherm were calculated by the method reported by Sherry [84].

The water adsorption capacity is estimated as the increase in weight of dehydrated zeolite samples placed in a dessicator containing saturated NH_4Cl solutions (until they reach constant weight). The water adsorption capacity of a zeolite is the measure of its void volume available for adsorption.

The nitrogen adsorption isotherms for the mordenite samples were obtained with standard BET apparatus (Numinco Surface Area Analyzer) at the boiling point of N_2 and the surface areas were calculated from the same.

The acidity measurements for the zeolite samples, characterizing their catalytic activities, were determined by the procedure reported by Holm and coworkers [99], and Plank [100]. The method involves the estimation of pH for the filtrate obtained of a solution containing 0.2 g of the zeolite in 20 ml of 0.1 N aqueous ammonium acetate kept at 35°C for 24 hours. This procedure was repeated for several time intervals and the respective values of pH determined. The pH at zero time was obtained by extrapolation. The corresponding acidity measurement for the zeolite mordenite was determined using a calibration curve of pH values for

known quantities of acetic acid added to the ammonium acetate solution.

The pore size as an expression of molecular sieve property was determined for dehydrated zeolite samples by passing through them several mixtures of known compositions of toluene and o-xylene, toluene and p-xylene, O- and p-xylenes and O-xylene and triethylbenzene. The effluents were analyzed with a gas chromatograph (of C.I.C. make, Baroda, India) equipped with a TC detector using a column (maintained at 100°C) of copper tubing 1/8'' O.D. packed with 5 per cent Bentone-34 and 6 per cent diethylene glycol succinate on 60-80 mesh chromosorb W and the flow rate of the carrier gas (N_2) being maintained at 15 ml/min.

CHAPTER 4

RESULTS AND DISCUSSION

The investigations undertaken in the present study fall into two categories. The syntheses of mordenite using silica from chemical source as also silica derived from rice-husk ash are dealt with in the first part. Effects of variables viz., the temperature, the duration of reaction and the compositional variations on the synthesis and the stability of mordenite are included in this part. The second part comprises the characterization studies on synthesized mordenites and their operational performance as molecular sieves.

4.1 Synthesis:

On the basis of preliminary investigations, it has been found that the starting materials in the form of an alumino-silicate gel rather than in the form of individual oxides facilitate better synthesis of mordenite. A few instances, however, exist in the literature for the synthesis of mordenite directly from the oxide mixtures [33,44]. But in the present investigation, sodium aluminate was prepared from the reaction of sodium hydroxide and aluminium hydroxide. This aluminate was mixed with sodium silicate to form the sodium alumino-silicate gel to be used as the starting material for the crystallization of mordenite. The ranges of operating variables

were as follows:

Temperature of reaction:	90 - 200°C
Synthesis time:	1 hr - 7 days
SiO_2/Al_2O_3 (molar ratio in the starting mix):	1 - 20
Na_2O/Al_2O_3 (molar ratio in the starting mix):	0.8 - 8.0

H_2O/Al_2O_3 molar ratio has been kept constant at 219 in most of th runs and where this ratio was changed, this has been indicated in the appropriate place.

The products obtained from each run have been identified by x-ray powder analysis after their separation from the mother liquor. In the present study, in addition to mordenite the reaction products often included either analcime or phillipsite. All these products were identified on the basis of their characteristic intense reflections as indicated in Section 4.2. In the runs where crystallization of the products was far from completion, the x-ray diffraction patterns indicated absence of peaks and a broad hump for the amorphous material was seen. The per cent composition of the mordenite in the product was determined by quantitative x-ray analysis using standard mordenite (zeolon) of Norton Company as the reference.

4.1.1 Synthesis of Mordenite Using Silica from Chemical Source:

The details for the various runs conducted with varying compositions and times, together with the reaction products

for different reaction temperatures are indicated in the Tables 4.1 through 4.5.

Effect of Starting Composition:

Initial composition of any mix is of paramount importance in governing the type of zeolite crystallized. In the present investigations, composition was varied in the starting material in the following ranges:

Na_2O(mol per cent)	:	12 - 50
Al_2O_3 (mol per cent)	:	4.0 - 18.8
SiO_2(mol per cent)	:	32.8 - 80.0
H_2O/Na_2O(molar ratio)	:	40 - 220

To represent the stability fields of mordenite as a function of composition in the system Na_2O-Al_2O_3-SiO_2-H_2O at constant H_2O/Al_2O_3 ratio, triangular diagrams for the temperatures 135, 150 and 165°C were plotted. These diagrams are given for 12 hr and 24 hr of synthesis period for these temperatures (Figure 4.1 and 4.2).

Since three end members are involved, the SiO_2/Al_2O_3 and Na_2O/Al_2O_3 ratios have been plotted against each other for reaction temperatures of 135, 150 and 165°C (Figures 4.3 - 4.5). It is evident that with temperature and time as constants, a higher SiO_2/Al_2O_3 ratio in the starting mixture requires a higher ratio of Na_2O/Al_2O_3 for the formation of mordenite. At constant temperature and time, in any starting

TABLE 4.1: SYNTHESIS OF ZEOLITES USING SILICA FROM CHEMICAL SOURCES

Run No.	Composition of starting Mixture[a] (anhydrous basis) Na_2O (mol per cent)	Al_2O_3 (mol per cent)	SiO_2 (mol per cent)	Reaction Time (hr)	Reaction product
		Reaction temperature: 110°C			
211	37.8	10.6	52.60	4	Am+P
212	50.0	14.3	35.70	4	P
213	46.7	13.3	40.00	4	P
214	43.75	12.5	43.75	4	P
215	41.2	11.7	47.10	4	P
216	38.9	11.1	50.00	4	P+Am
217	35.0	10.0	55.00	4	Am+P
218	33.3	9.5	57.2	4	Am
		Reaction Temperature 120°C			
323	24.1	6.9	69.00	24	Am
324	24.1	6.9	69.00	48	Am

[a] $H_2O/Al_2O_3 = 219$

Am = Amorphous

P = Phillipsite

TABLE 4.2 SYNTHESIS OF ZEOLITES USING SILICA FROM CHEMICAL SOURCES

Run No.	Composition of Staring Mixture[a] (Anhydrous basis)			Reaction time, hr	Reaction Product
	Na_2O (mol per cent)	Al_2O_3 (mol per cent)	SiO_2 (mol per cent)		
1	2	3	4	5	6
	Reaction Temperature: 135°C				
321	24.10	6.90	69.00	8	Am
				16	Am
				20	M
				24	M
				36	M
				48	M
333	19.10	4.76	76.14	12	Am
				24	Am
336	21.75	8.70	69.60	12	Am
				24	M
338	18.50	7.40	74.10	12	Am
				24	Am
339	26.70	6.67	66.63	12	M
				24	M
340	16.10	6.45	77.40	12	Am
				24	Am
341	21.45	7.15	71.50	12	Am
				24	Am
342	15.40	7.70	77.00	12	Am
				24	Am
343	24.96	8.34	66.70	12	M
				24	M

Table 4.2 (contd)

1	2	3	4	5	6
352	30.00	10.00	60.00	4	Am
				12	P
				24	P
				96	An
353	17.50	12.50	70.00	12	Am
				24	Am
354	22.50	12.50	65.00	12	M
				24	M
355	25.00	5.00	70.00	12	M
				24	M
356	29.50	6.00	64.50	12	M
				24	M

Am = Amorphous P = Phillipsite M = Mordenite

An = Analcime

[a] $H_2O/Al_2O_3 = 219$

TABLE 4.3: SYNTHESIS OF ZEOLITES USING SILICA FROM CHEMICAL SOURCES

Run No.	Composition of starting mixture[a] (Anhydrous basis) Na_2O (mol per cent)	Al_2O_3 (mol per cent)	SiO_2 (mol per cent)	Reaction Time (hr)	Reaction Product
		Reaction Temperature: 150°C			
315	24.10	6.90	69.00	4	Am
				12	M
				24	M
316	24.10	6.90	69.00	16	M
				48	M
325	13.33	6.66	80.01	12	Am
				24	Am
326	18.18	9.10	72.72	12	Am
				24	M
327	24.96	8.34	66.70	12	M
				24	An
328	18.75	6.25	75.00	12	M
				24	M
330	23.53	5.87	70.60	4	Am
				12	M
				24	An+M
331	16.00	4.00	80.00	12	Am
				24	Am
332	15.00	5.00	80.00	12	Am
				24	Am
357	20.00	10.00	70.00	12	M
				24	M
358	12.50	10.00	77.50	12	Am
				24	Am
359	15.00	15.00	70.00	12	Am
				24	Am

Am=Amorphous M= Mordenite An = Analcime

[a] $H_2O/Al_2O_3 = 219$

TABLE 4.4: SYNTHESIS OF ZEOLITES USING SILICA FROM CHEMICAL SOURCES

Run No.	Composition of starting mixture[a] (Anhydrous basis) Na_2O (mol per cent)	Al_2O_3 (mol per cent)	SiO_2 (mol per cent)	Reaction Time, hr	Reaction Product
		Reaction Temperature: 165°C			
319	24.10	6.90	69.00	8 12 16 24	Am + A M M M
334	27.78	5.55	66.66	12 24	An An
335	21.70	8.70	69.60	12 24	M M
337	16.13	6.45	77.42	12 24	Am M
344	22.72	4.55	72.73	12 24	M An
345	26.70	6.67	66.63	12 24	An An
346	15.30	7.70	77.00	12 24	Am Am
347	24.96	8.34	66.60	12 24	M An
348	12.00	11.00	77.00	12 24	Am Am
349	20.00	12.00	68.00	12 24	M M
350	20.00	8.00	72.00	12 24	M M
351	16.00	14.00	70.00	12 24	M M

[a] H_2O/Al_2O_3 = 219

Am = Amorphous
An = Analcime
M = Mordenite

TABLE 4.5: SYNTHESIS OF ZEOLITES USING SILICA FROM CHEMICAL SOURCES

Run No.	Composition of starting mixture (Anhydrous basis)			$\frac{H_2O}{Al_2O_3}$	Reaction Time, hr	Reaction Product
	Na_2O (mol per cent)	Al_2O_3 (mol per cent)	SiO_2 (mol per cent)			
	Reaction Temperature: 175°C					
317	24.10	6.90	69.00	219	24	M
318	24.10	6.90	69.00	219	48	M+An
	Reaction Temperature: 190°C					
320	24.10	6.90	69.00	219	24	M+An
	Reaction Temperature: 200°C					
111	46.30	18.80	34.90	80	4	An
112	50.00	17.20	32.80	95	2	An
113	50.00	17.20	32.80	95	1	An
119	33.33	11.11	55.56	201	4	An
120	33.33	11.11	55.56	201	1 2	An An
314	24.10	6.90	69.00	219	4 6 24	Am M An
322	24.10	6.90	69.00	219	7 12 16	M M M+An

Am=Amorphous M = Mordenite An=Analcime

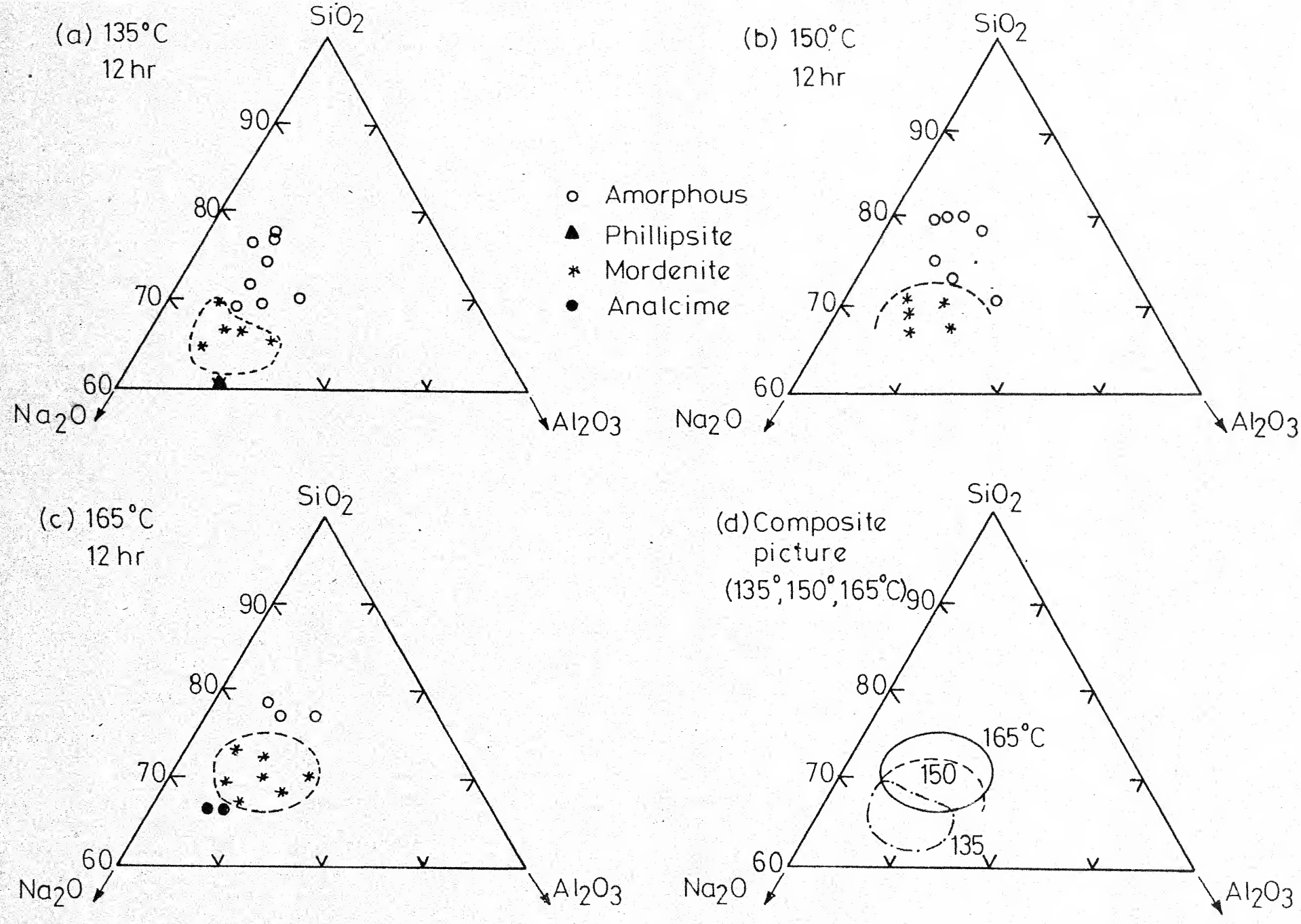

Fig. 4.1 - Reaction composition diagrams for 12 hours using silica from chemical source

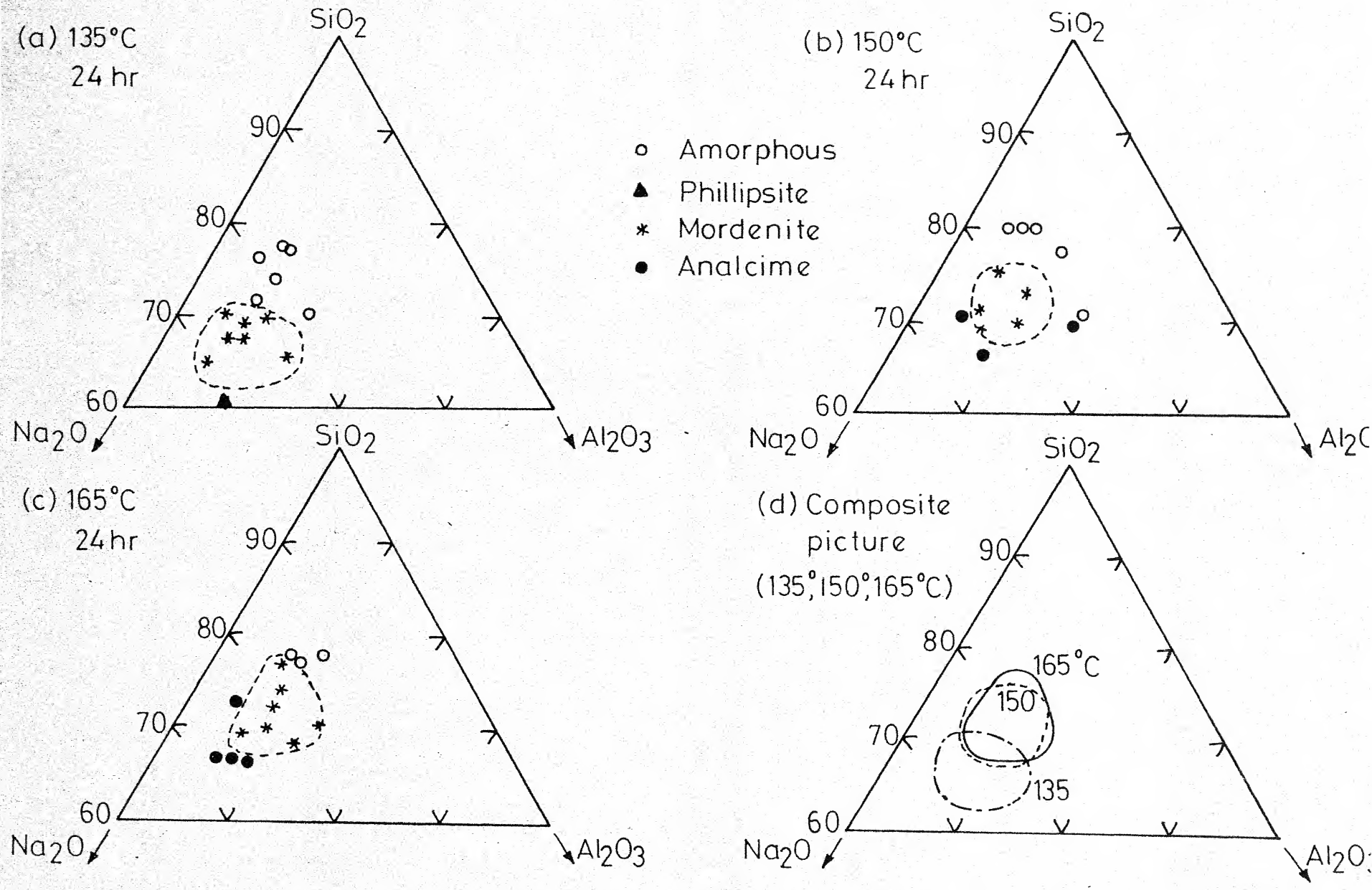

Fig. 4.2 - Reaction composition diagram for 24 hours using silica from chemical sources.

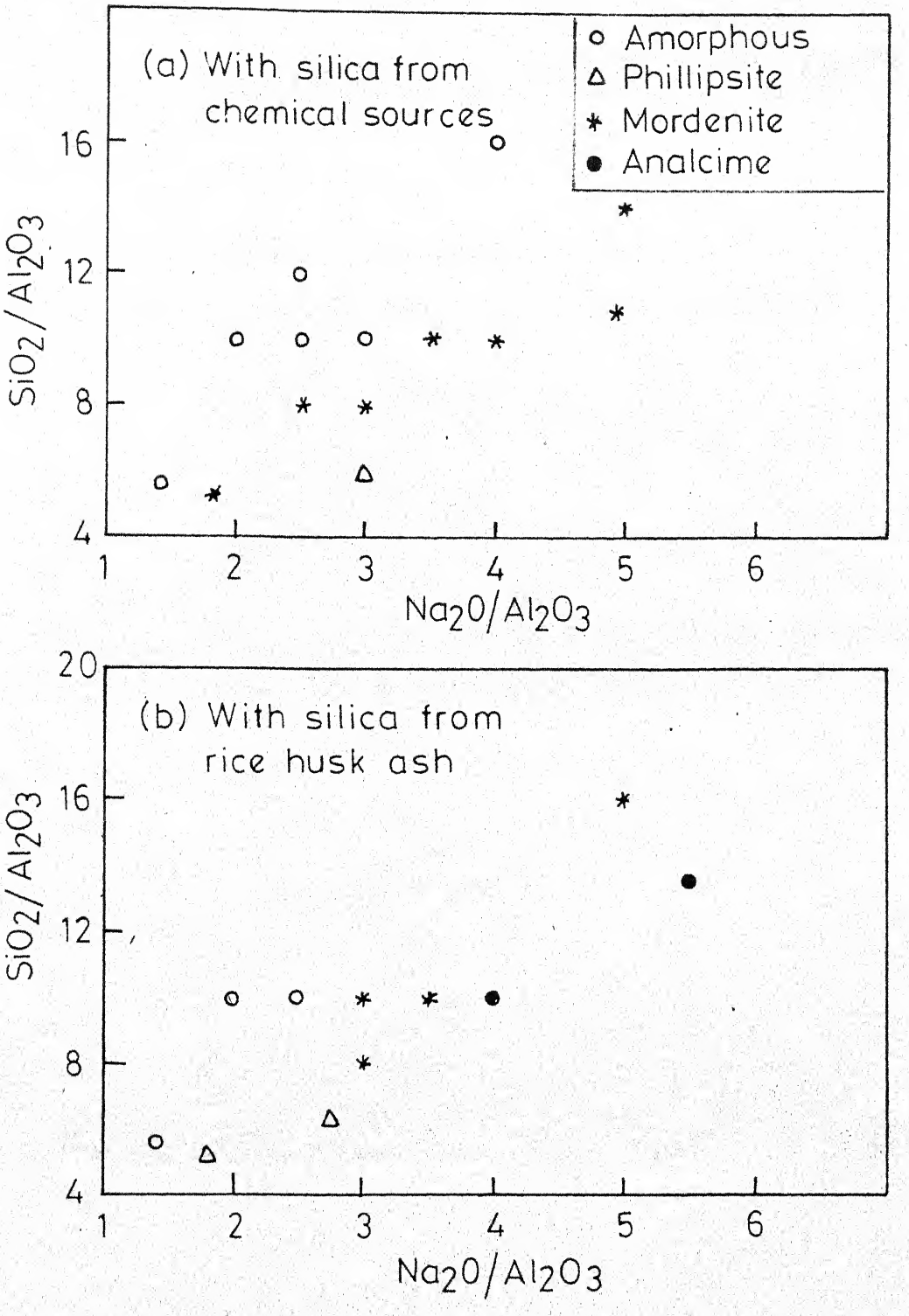

Fig. 4.3 - Effect of composition of the starting batches on zeolite crystallization at 135°C for 24 hr.

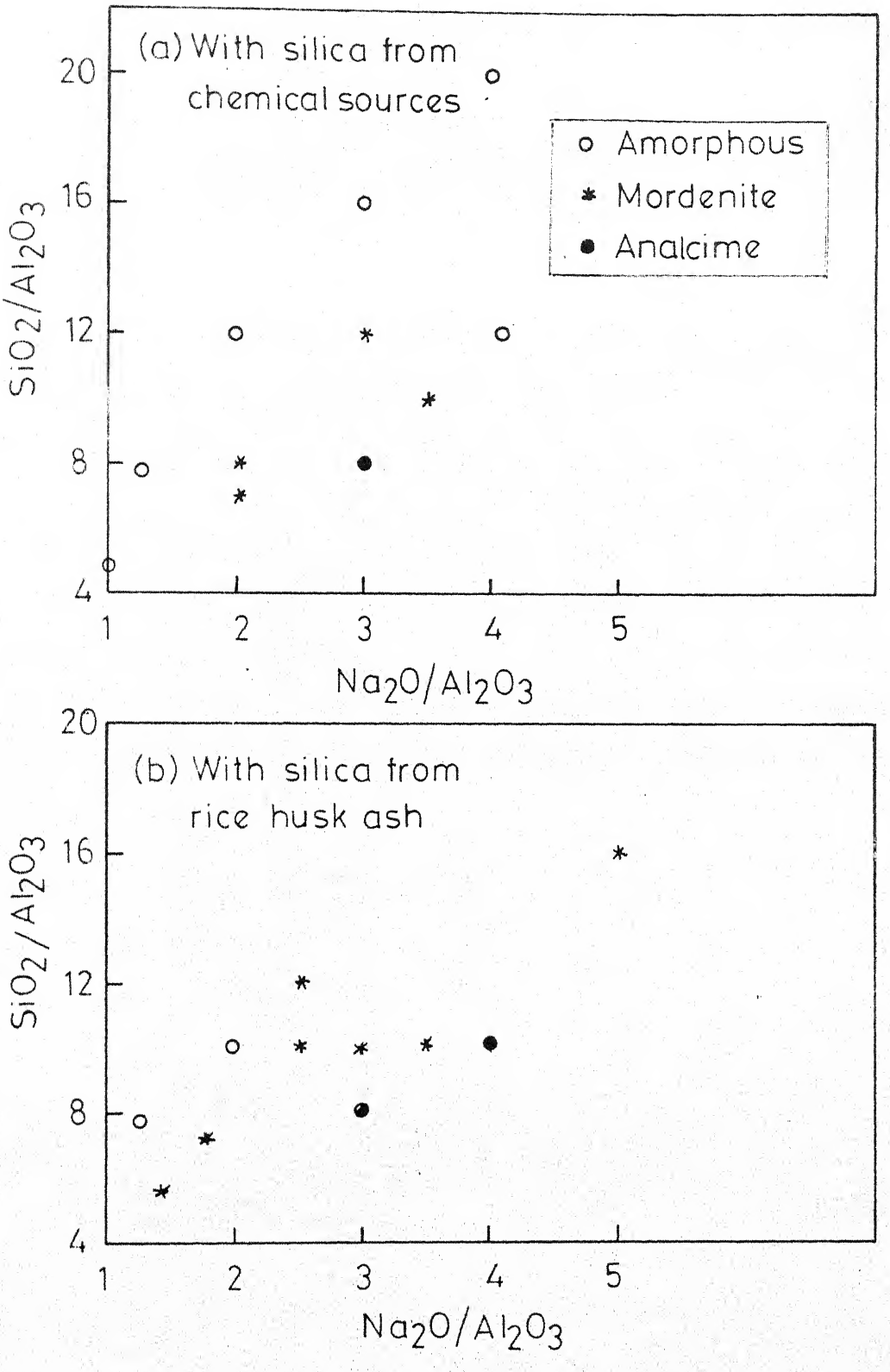

Fig. 4.4 - Effect of composition of the starting batches on zeolite crystallization at 150°C for 24 hr.

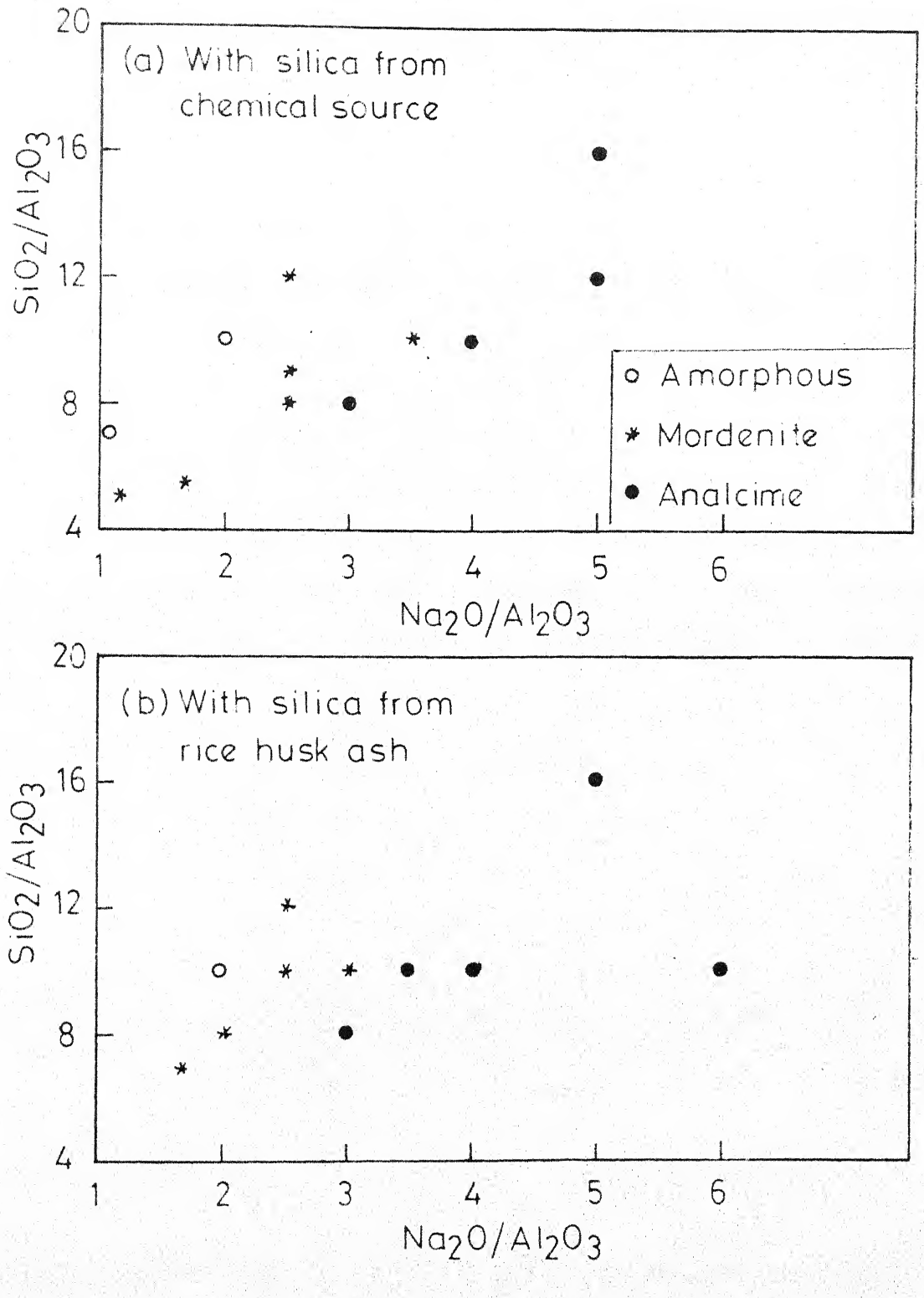

Fig. 4.5 - Effect of composition of the starting batches on zeolite crystallization at 165°C for 24 hr.

mixture with a particular SiO_2/Al_2O_3 ratio, the shift from mordenite to analcime crystallization results with the increase in Na_2O/Al_2O_3 ratio. Similarly an increase in SiO_2/Al_2O_3 for any particular Na_2O/Al_2O_3 ratio favours the crystallization of mordenite instead of analcime. Similar observations were reported by Barrer [33, 35].

From the triangular diagrams (Figures 4.1 and 4.2), the effect of composition can also be examined by choosing the tie lines for any particular Al_2O_3 per cent and obtaining the SiO_2 and Na_2O contents in the starting mixture for different temperatures. The SiO_2/Na_2O ratios are plotted against temperature with the corresponding product phases indicated (Figure 4.6). From such plots, it is clear that a higher ratio of SiO_2/Na_2O is required for the formation of mordenite at higher temperatures and that at any particular temperature, a decrease in the SiO_2/Na_2O ratio shifts the sequence of product formation in the direction of amorphous to phillipsite/mordenite to analcime. The appearance of mordenite or phillipsite is guided by the availability of silica during the zeolite crystallization. Mordenite in its composition has an SiO_2/Al_2O_3 ratio around 10 while in phillipsite the same is around 3-5.

In many of the earlier investigations [33, 43, 44], the effect of water content in the mixture has not been studied. The concentration of the reacting components in the initial mixture if expressed inversely with the water content is of

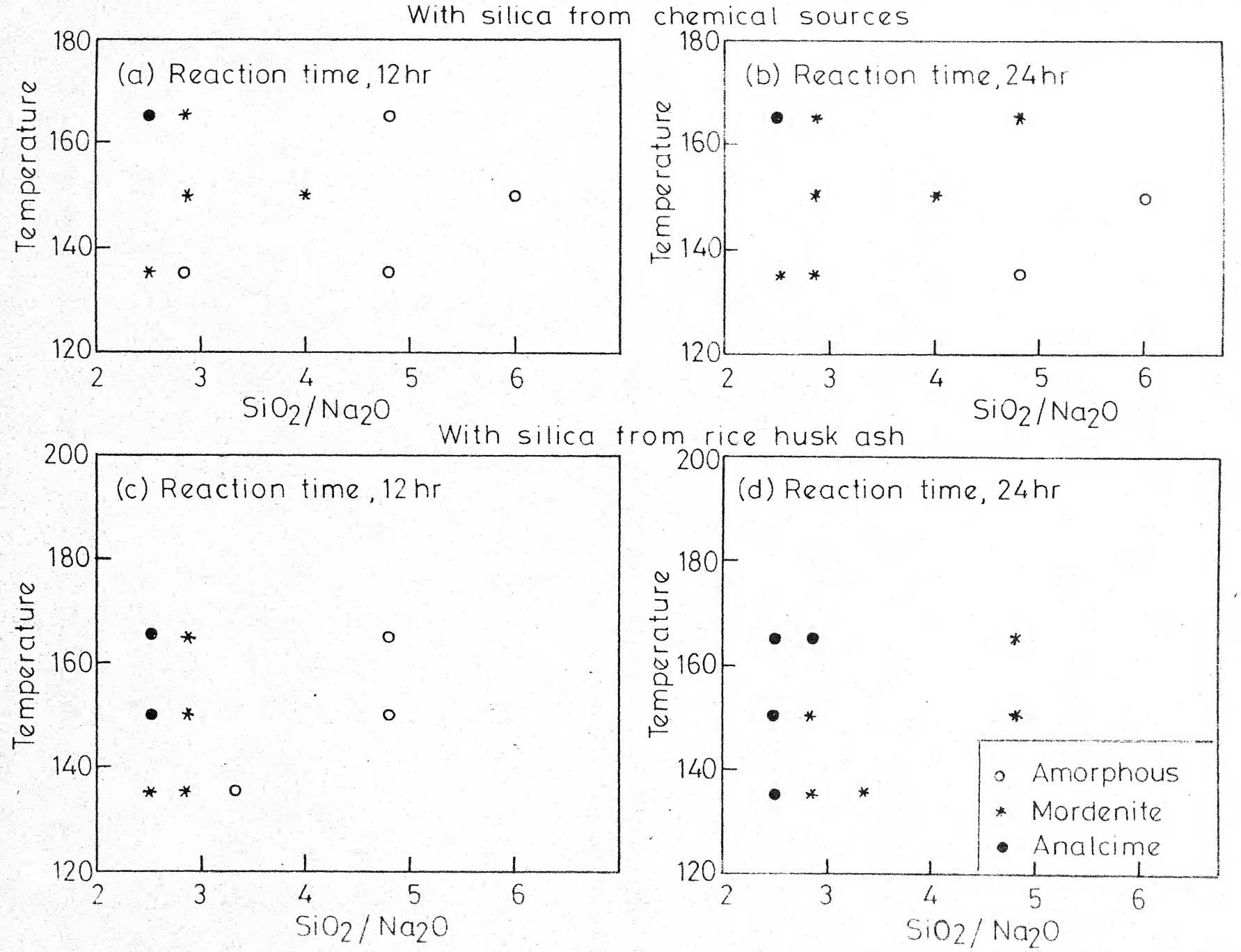

Fig. 4-6 - Effect of temperature on zeolite synthesis with starting batches of various compositions (SiO_2/Na_2O ratio obtained for constant Al_2O_3, 6·7%, from figs. 4·1, 4·2, 4·15 and 4·17).

significance in the determination of the species crystallized [4]. For example, the H_2O/Na_2O ratio in the starting mixture represents the inverse of the alkalinity. The effect of this ratio on the stability of formation of mordenite is presented in rectangular coordinates in Figures 4.7, 4.8 and 4.9 for the reaction temperatures of 135, 150 and 165°C respectively. It has been observed that the temperature, reaction time and SiO_2/Al_2O_3 being constant, the trends of stability were in the direction: analcime to mordenite to amorphous phases with the increase in H_2O/Na_2O ratio. A higher H_2O/Na_2O ratio in the initial mixture corresponds to lower concentrations of various components (aluminate and silicate) in the liquid phase. This in turn results in the formation of a less stable phase, conversely lower ratios of H_2O/Na_2O in the starting mixture correspond to higher concentrations of the various components in the liquid phase, resulting in the formation of a more stable zeolite phase.

Effect of Temperature and Time of Reaction:

Although experiments were conducted at several temperature levels, only three temperatures (135, 150 and 165°C) are used for discussion on the various aspects of the synthesis of mordenite, since it was observed that no mordenite was formed at temperatures less than 135°C. Beyond 175°C analcime appears.

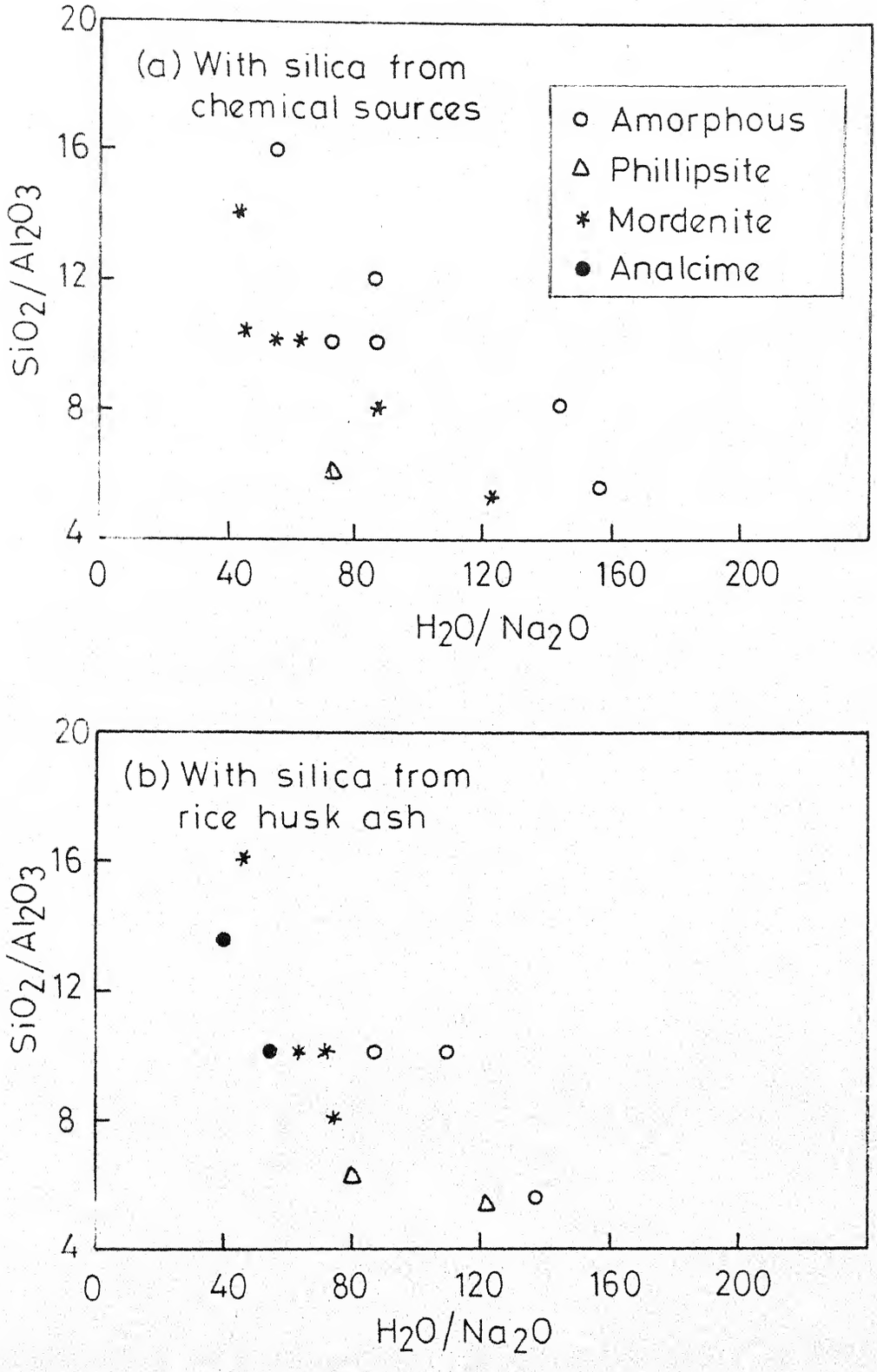

Fig. 4.7 - Batch compositions for synthesis of zeolite at 135°C for 24 hr in the $Na_2O-Al_2O_3-SiO_2-H_2O$ system (rectangular coordinates)

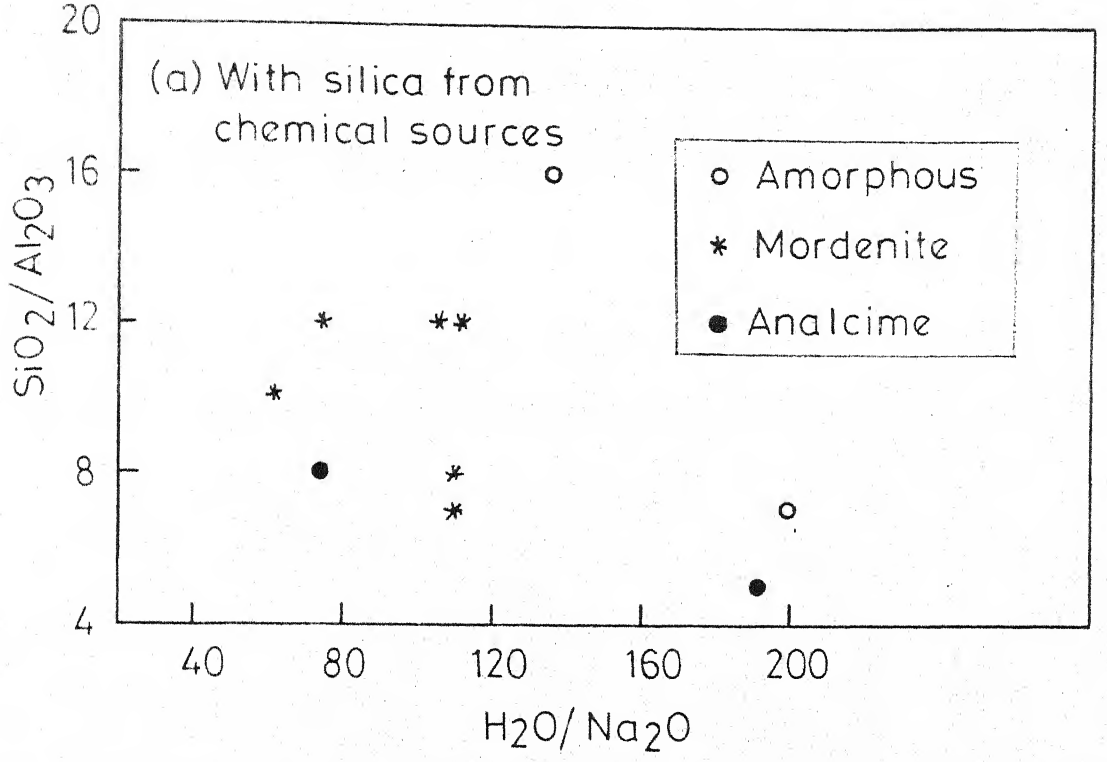

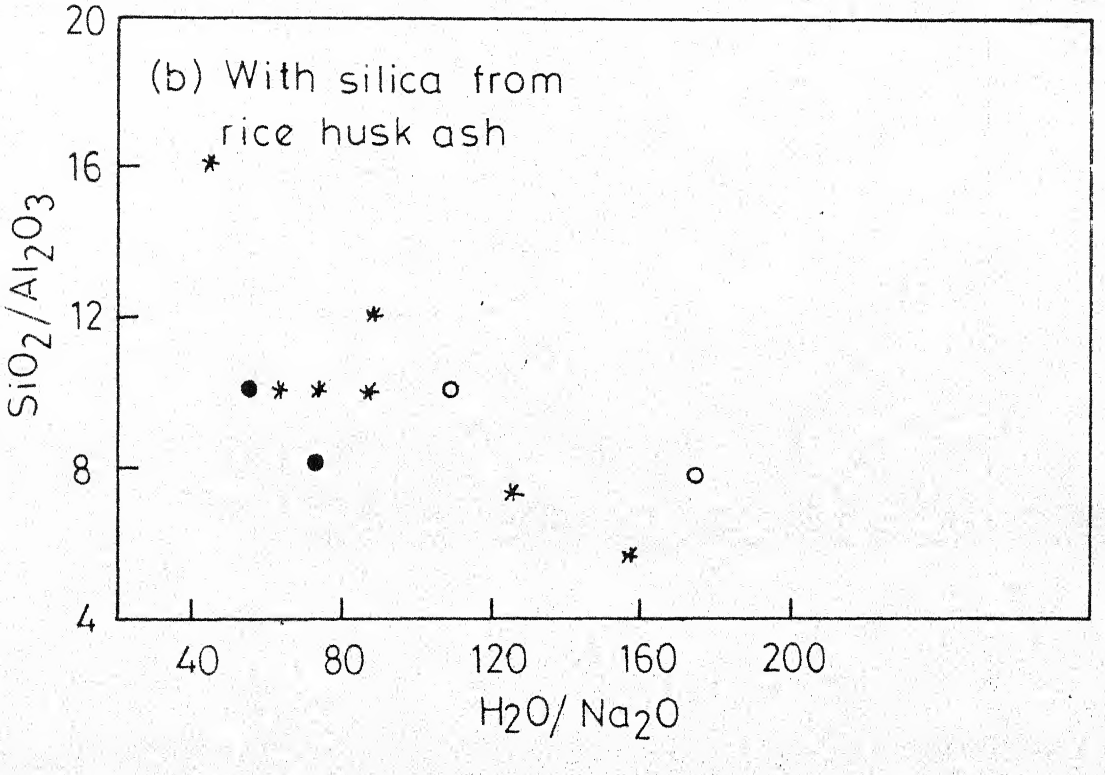

Fig. 4.8 - Batch composition for synthesis of zeolite at 150°C for 24 hr in the $Na_2O-Al_2O_3-SiO_2-H_2O$ system (rectangular coordinates)

CENTRAL LIBRARY
Acc. No. A 54009

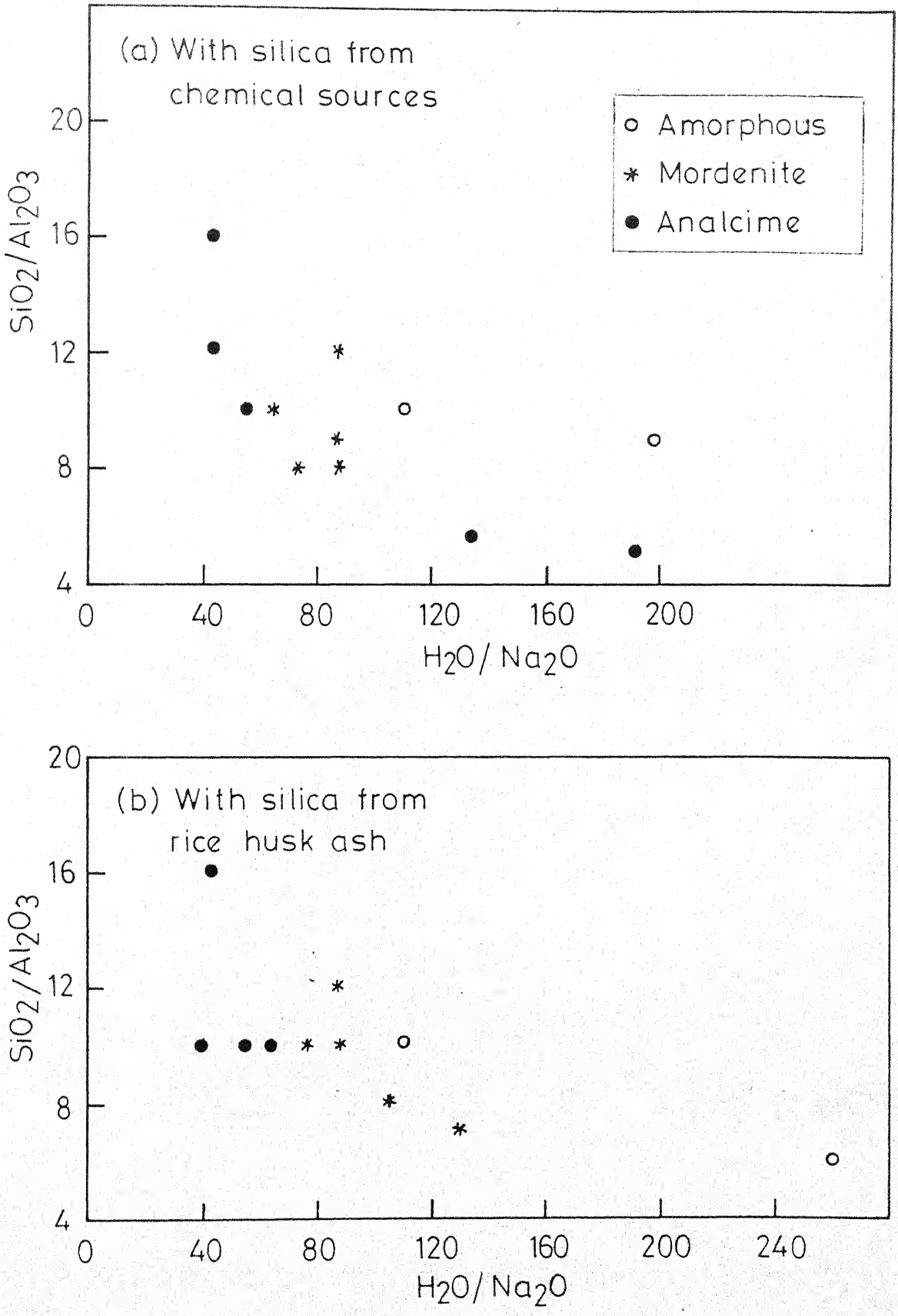

Fig. 4.9 - Batch composition for synthesis of zeolite at 165°C for 24hr in the $Na_2O-Al_2O_3-SiO_2-H_2O$ system (rectangular coordinates)

In the triangular diagrams (Figures 4.1 and 4.2) a, b and c in each of these two figures, the field for mordenite is indicated. To bring out the trends of changes with increase in temperature, the diagram d is obtained by superimposition of these three diagrams. It can be observed that at higher temperatures, mordenite starts crystallizing from starting mixes containing more of silica or less of Na_2O content (Figure 4.1(d) and 4.2(d)). This shift in crystallization field for mordenite with an increase in temperature of synthesis can be explained as follows: The concentration of components (aluminate and silicate) in the liquid phase of the gel is the main controlling factor in the formation of a zeolite [101]. As the temperature increases, the solubilities of the aluminate and silicate ions increase causing a shift in the concentration of the liquid phase. This results in the formation of analcime in place of mordenite. Hence if the mordenite has to be crystallized at higher temperatures, the starting mixtures should have relatively higher SiO_2 or lower Na_2O contents which means the reduction of the alkalinity.

The sequence of formation of the products with an increase in temperature is in the direction:

Amorphous ⟶ Mordenite ⟶ Analcime

For instance, for the runs numbered 321 and 315 (Tables 4.2 and 4.3) at temperatures of 135 and 150°C respectively, the products after 12 hours of reaction have been found to be

amorphous material in the first case and mordenite in the other (Figure 4.10), although the composition of the initial mix was the same in both the cases. Similarly, for a reaction period of 24 hr., the products obtained were mordenite for run no. 343 at 135°C, analcime for run no. 327 at 150°C and run no. 347 at 165°C, the initial composition being same in all the mixes (Figure 4.11).

For any mix, as the temperature increases, the rate of crystallization of mordenite increases. The rate curves established on the basis of a quantitative analysis of the x-ray diffraction data together with a discussion on the kinetic aspects of the synthesis are presented in Section 4.1.3. The effect of temperature on the mordenite stability can be obtained from the plots of SiO_2/Na_2O ratio versus temperature keeping the other component constant. Such plots (Figure 4.6) are informative in indicating the sequence of formation of different zeolites. Since compositional variations are involved, these are already presented there.

The present study indicated that for an initial composition of the reaction mixture of 3.5 $Na_2O \cdot Al_2O_3 \cdot 10SiO_2 \cdot 219H_2O$, the best temperature range for the synthesis of mordenite to be 135 - 175°C. Barrer [33, 35] has reported the same to be 265 - 295°C for a different initial composition $Na_2O \cdot Al_2O_3 \cdot 8\text{-}10SiO_2$.

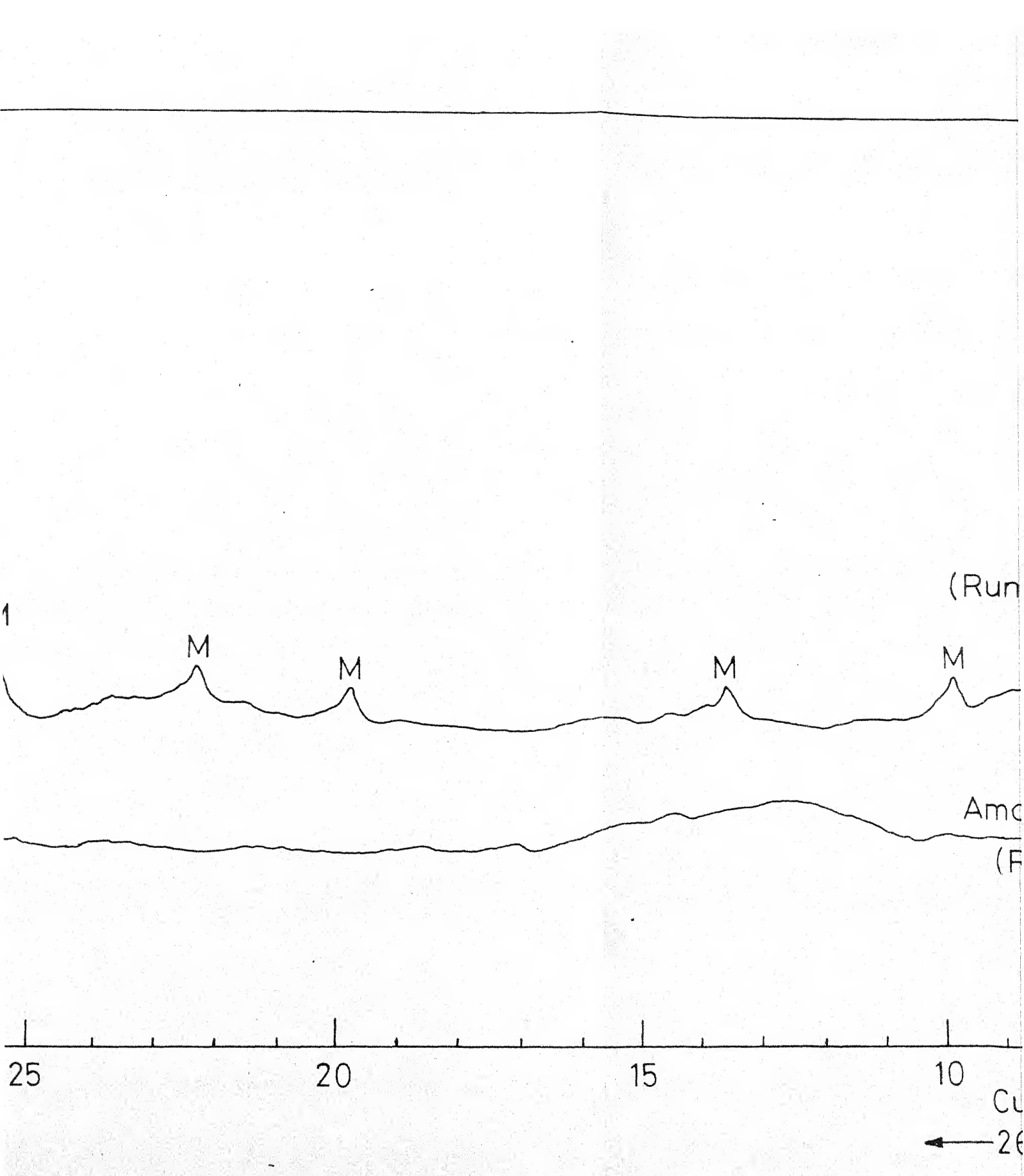

ducts obtained after 12 hr with batch composition: 3·5 Na_2O·
SiO_2· 219 H_2O (run nos. 315, 321)

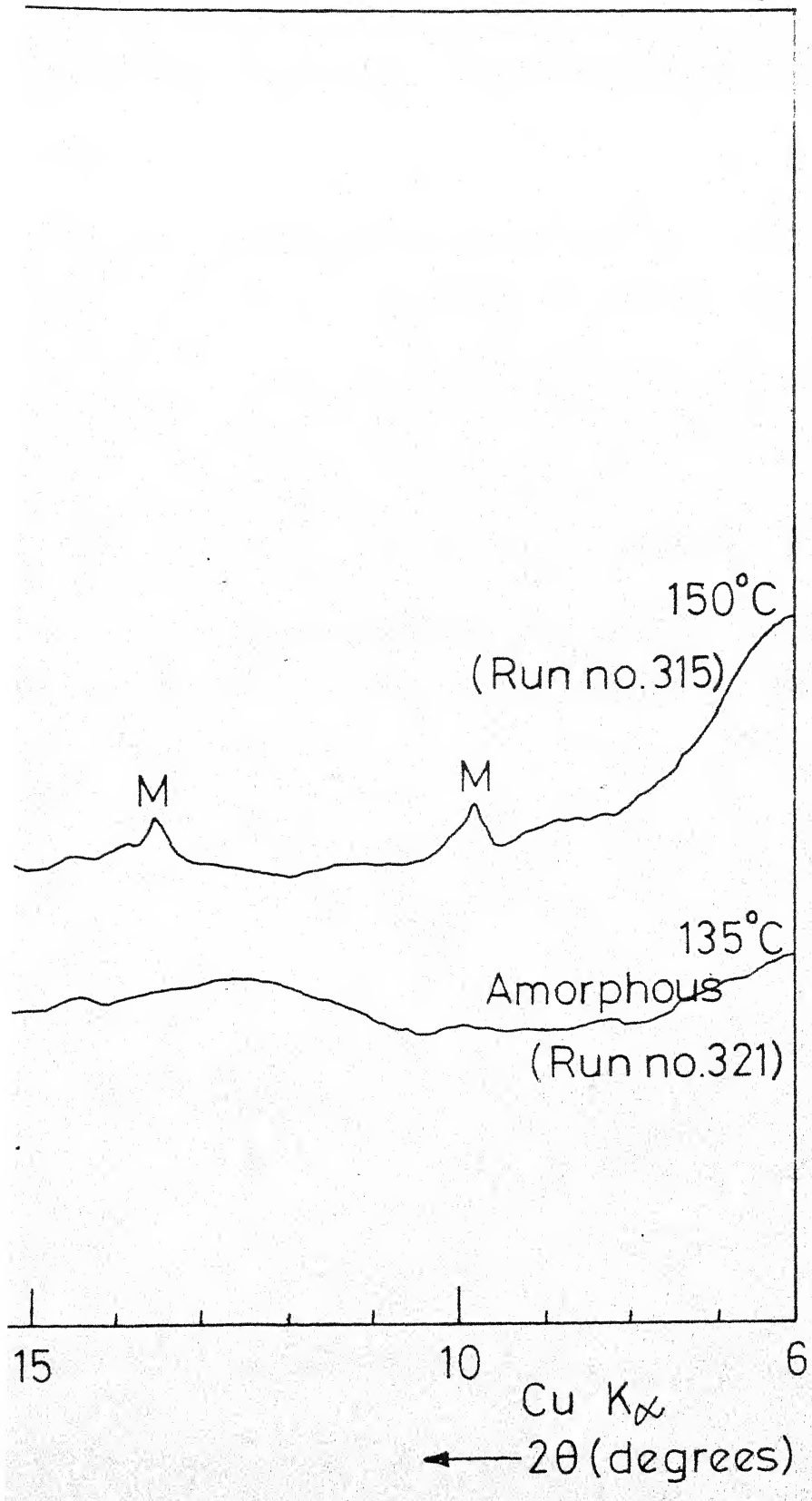

:h composition: 3·5 $Na_2O \cdot Al_2O_3 \cdot$

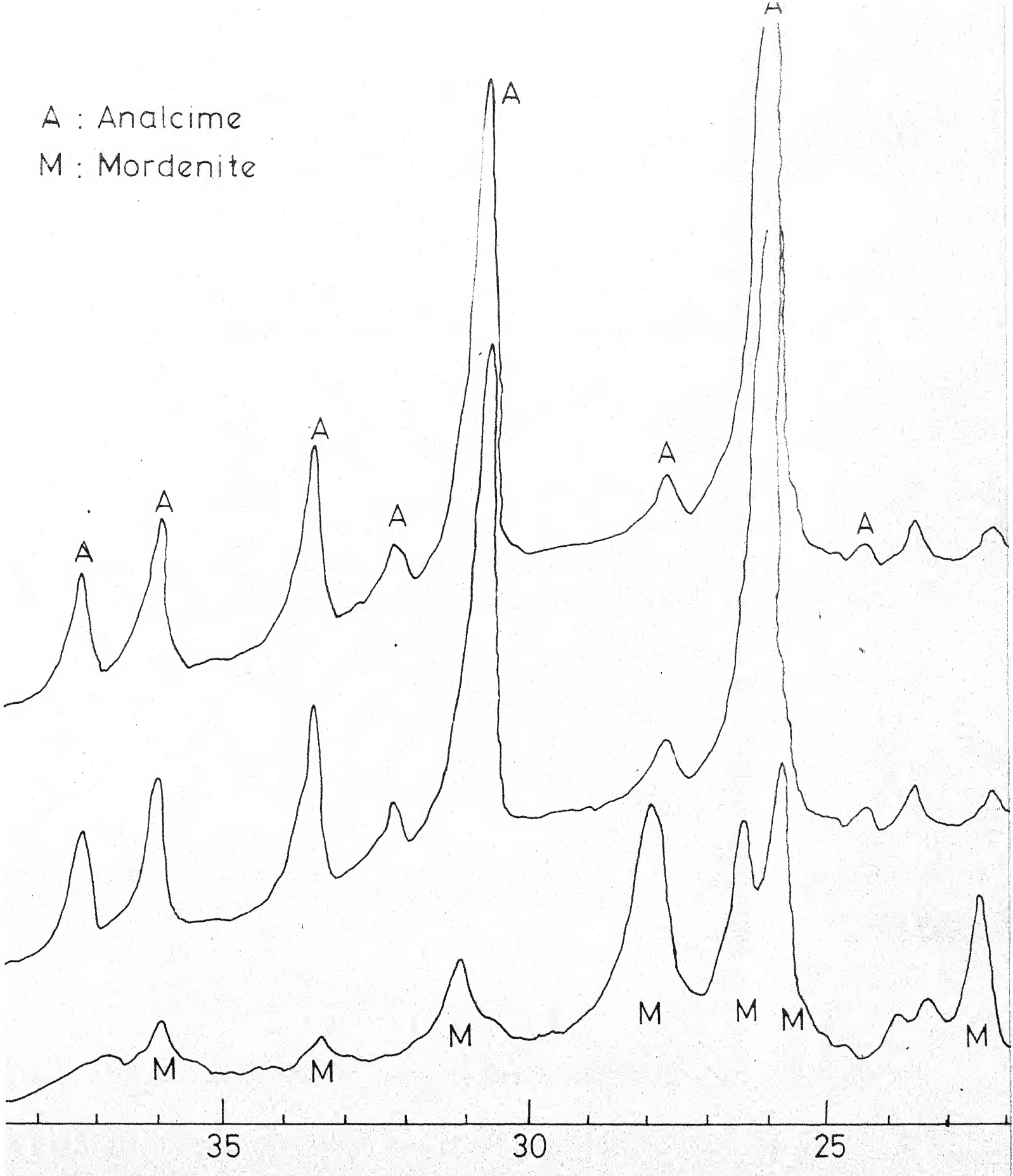

g. 4·11 - Typical X-ray diffraction patterns of products obt
$8SiO_2 \cdot 219 H_2O$

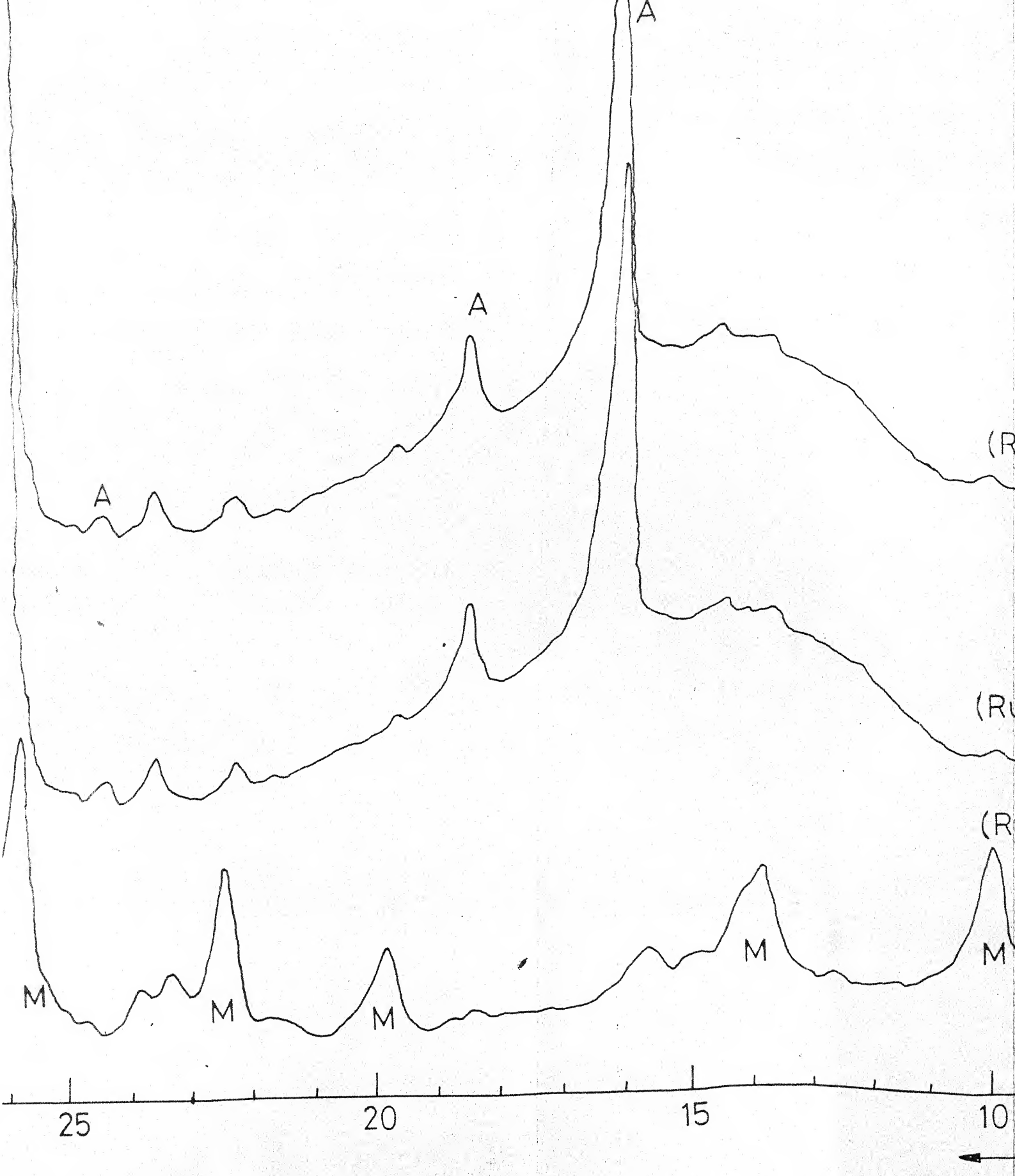

f products obtained after 24 hr with batch composition: 3 N
$8\,SiO_2 \cdot 219\,H_2O$ (run nos. 343, 327, 347)

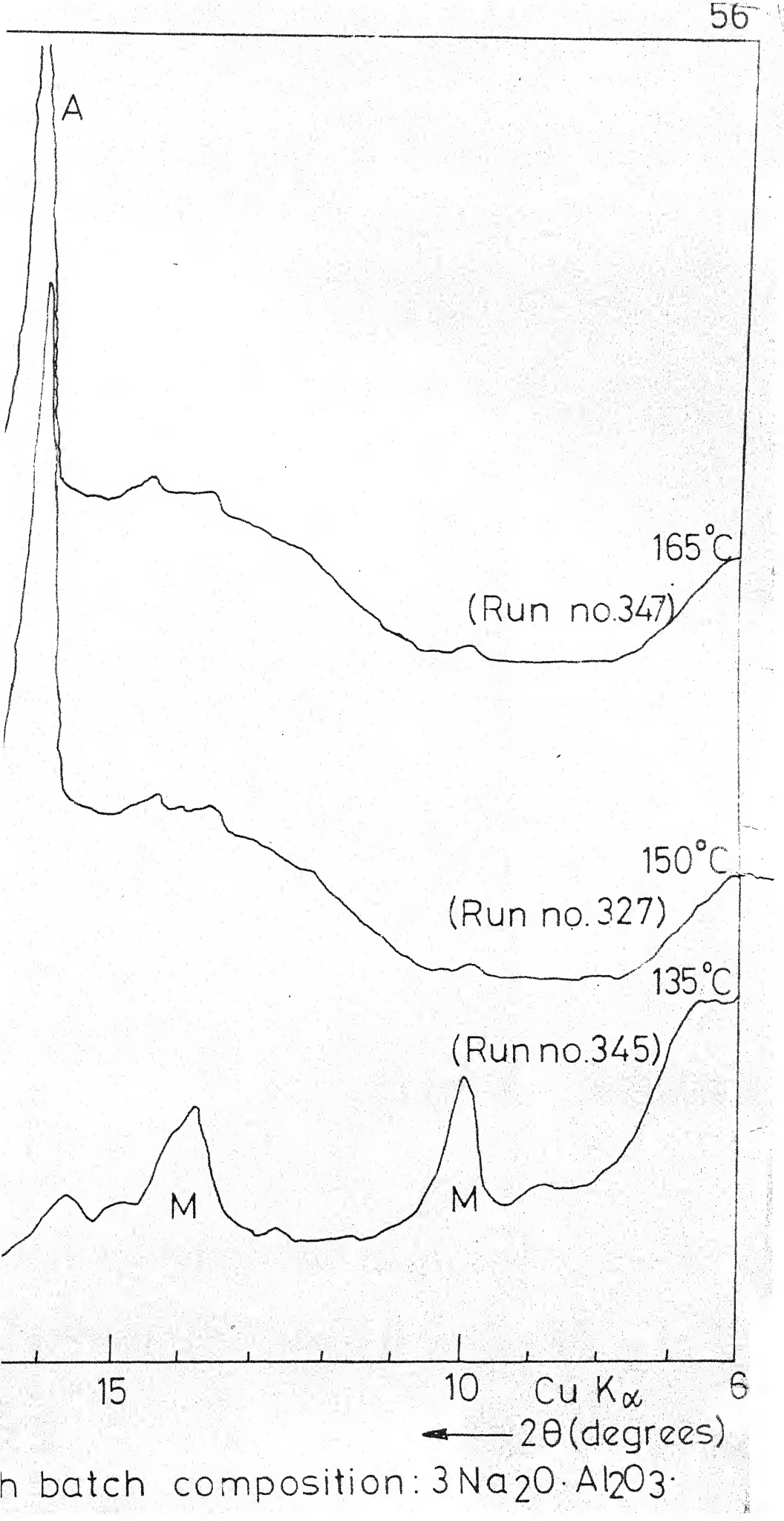

h batch composition: $3Na_2O \cdot Al_2O_3 \cdot$

For the temperatures 135, 150 and 165°C, the mordenite crystallization fields for 12 hr. and 24 hr. of reaction time are indicated in the triangular diagrams (Figure 4.12). As the reaction time increased, the sequence of changes in the product was in the direction: amorphous ⟶ phillipsite/ mordenite ⟶ analcime (Figure 4.13 and 4.14). Such an observation is in conformity with the earlier work [33, 35, 47, 51]. In the above, analcime was the most stable phase. This trend indicates that less stable species nucleate more rapidly than the more stable ones. According to the Ostwald's law of successive transformations [4], the most stable state may not be reached at once, but passes through a succession of intermediate and less stable states. This correlates with the idea that the phases tend to appear in the order of decreasing simplexity or entropy [102]. Ready nucleation may be favoured by high simplexity or entropy. However, the energy as well as the entropy changes ultimately determine the relative stabilities of the phases formed and hence the final product.

4.1.2 Synthesis of Mordenite Using Silica from Rice-Husk Ash:

As explained earlier, amorphous silica available in the rice-husk ash was obtained in solution with sodium hydroxide and this silica solution in alkali was reacted with prepared sodium aluminate solution to make a fresh sodium aluminosilicate gel of the desired composition. The synthesis

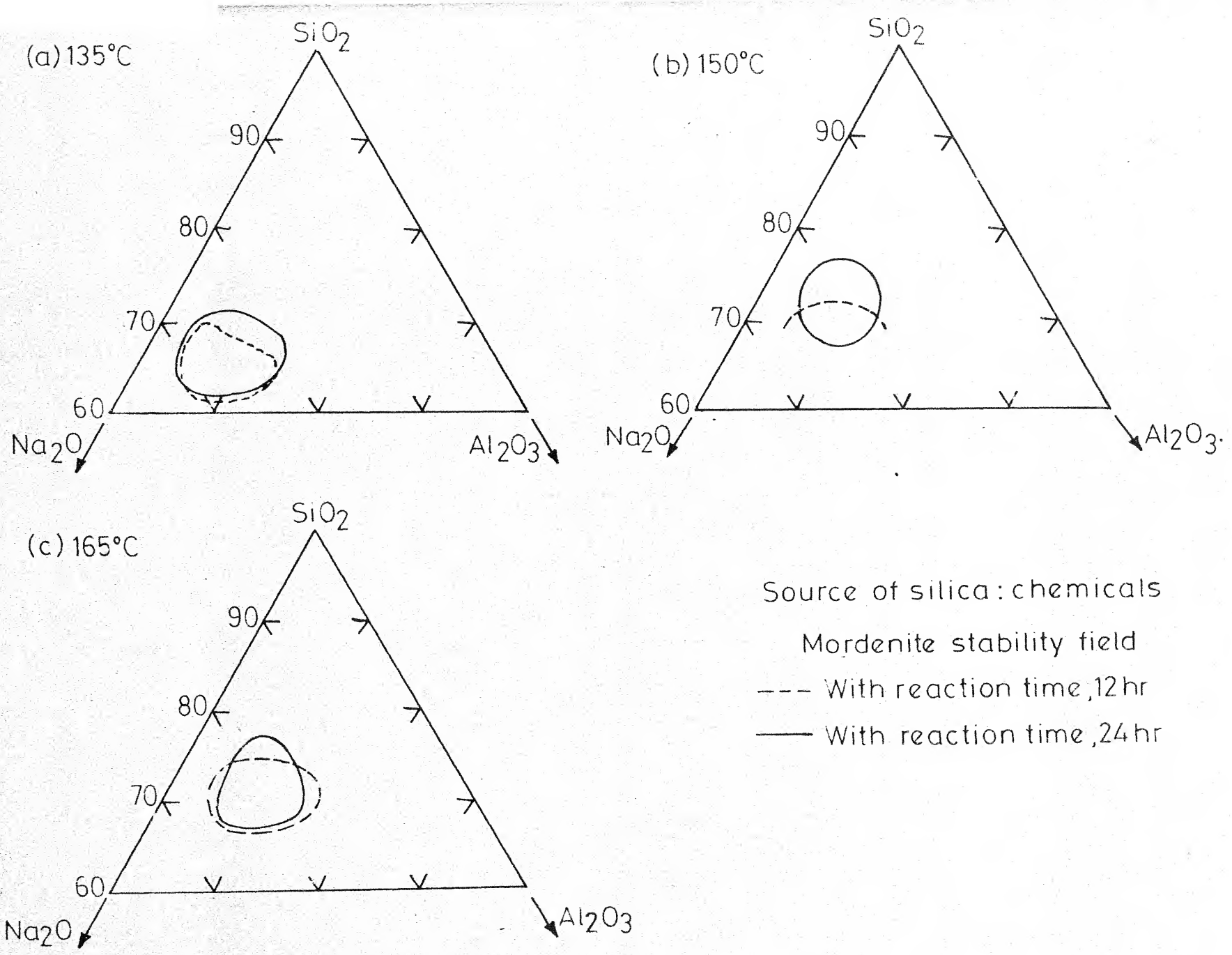

Fig. 4.12 - Effect of time on the stability field of mordenite

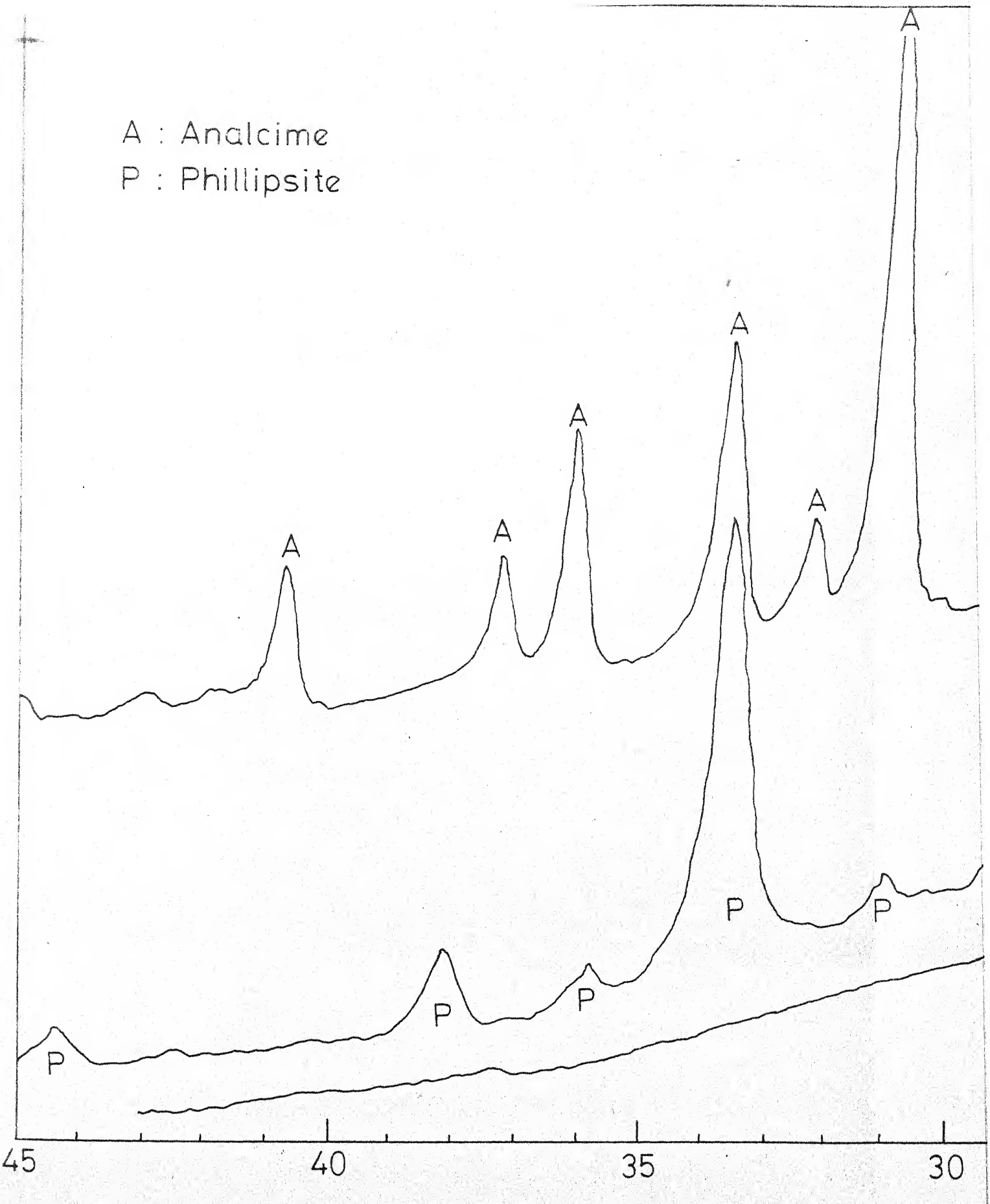

Fig. 4.13 - Typical X-ray diffraction patterns of products 3 Na_2O

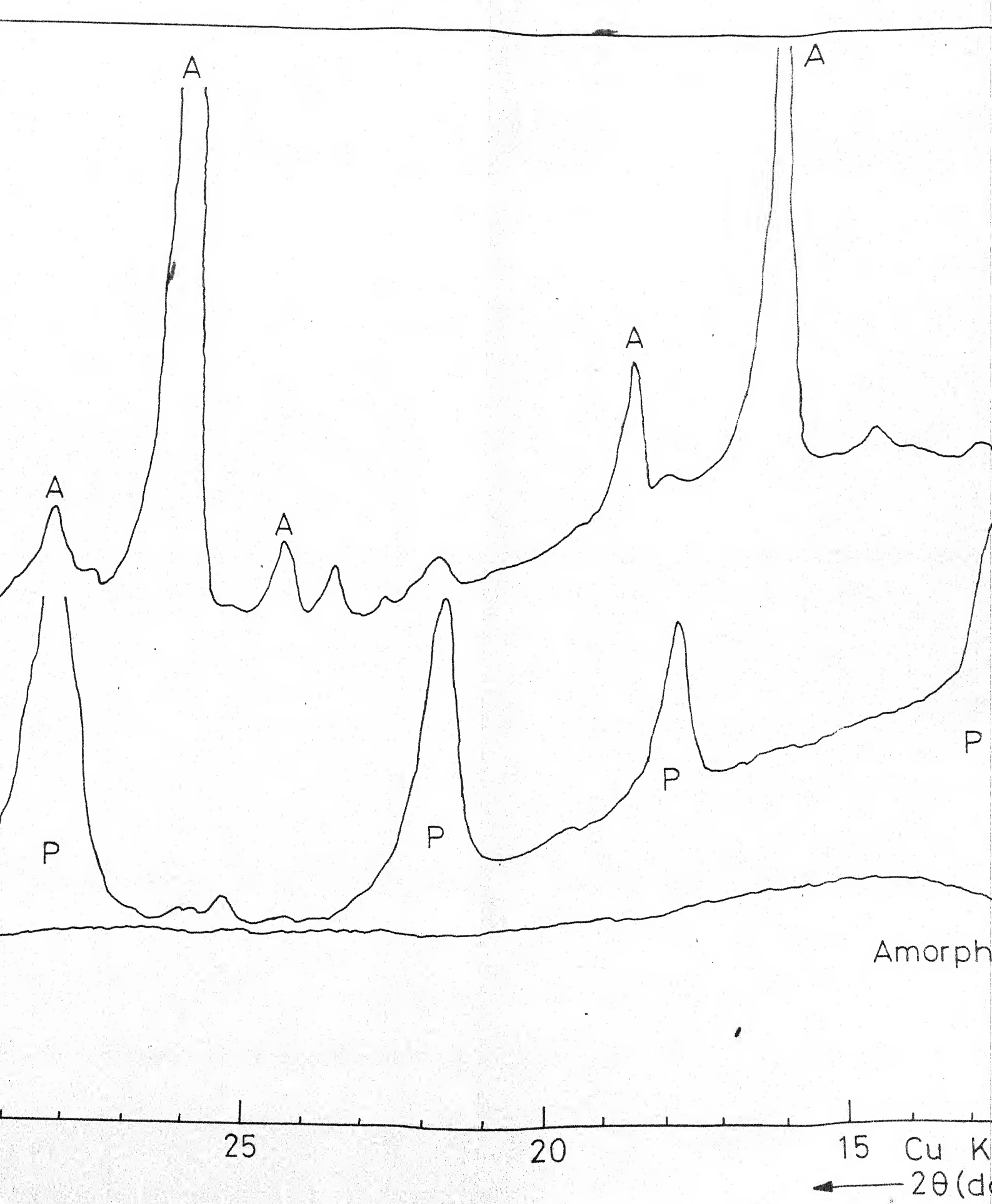

obtained for various reaction periods at 135°C with batch
$Al_2O_3 \cdot 6\ SiO_2 \cdot 219\ H_2O$ (run no. 352)

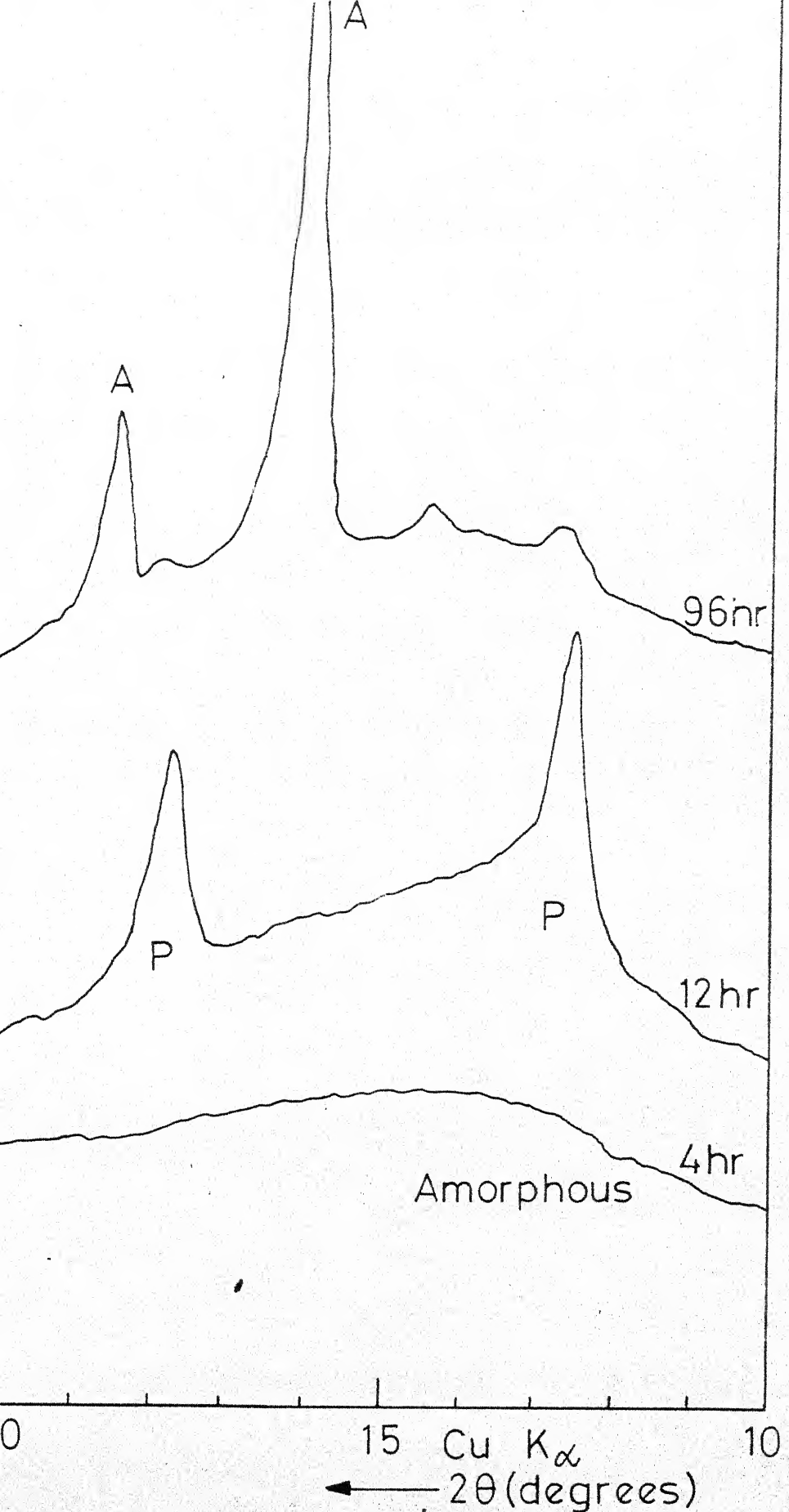

riods at 135°C with batch composition:

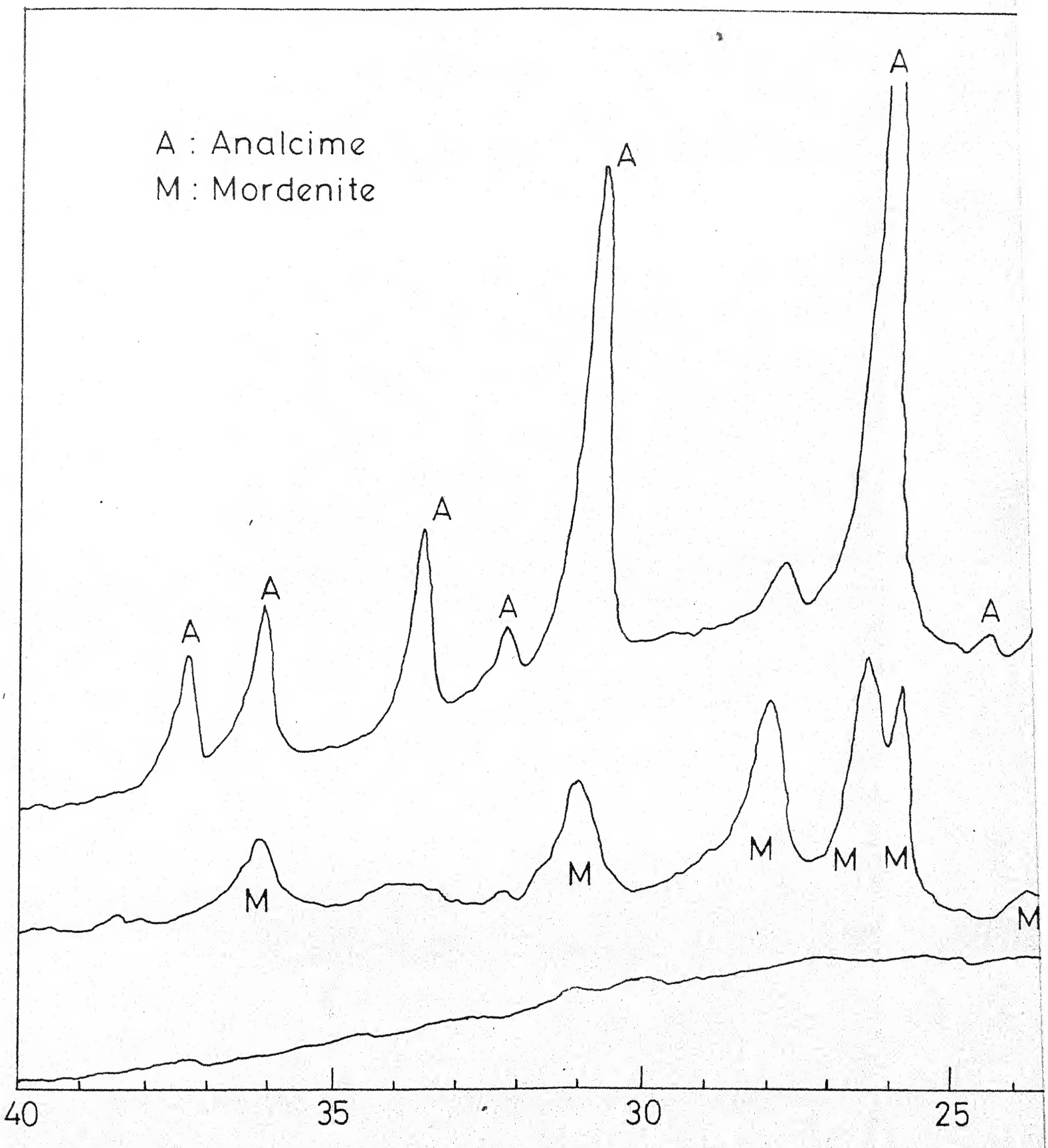

Fig. 4·14– Typical X-ray diffraction patterns of products ob
composition: 4 Na_2O·A

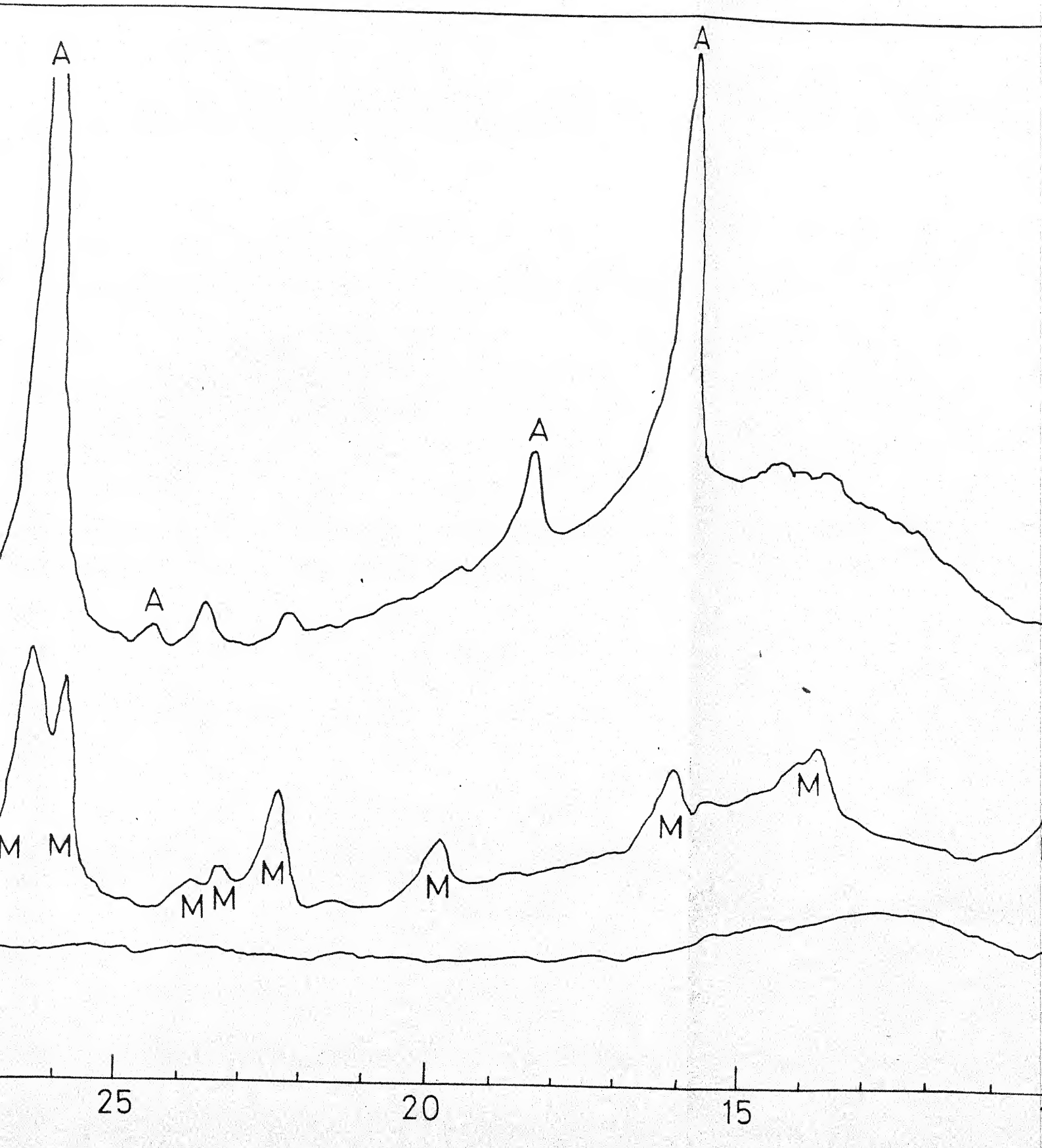

products obtained for various reaction periods at 150°C v

ion: $4\,Na_2O \cdot Al_2O_3 \cdot 12\,SiO_2 \cdot 219\,H_2O$ (run no. 330).

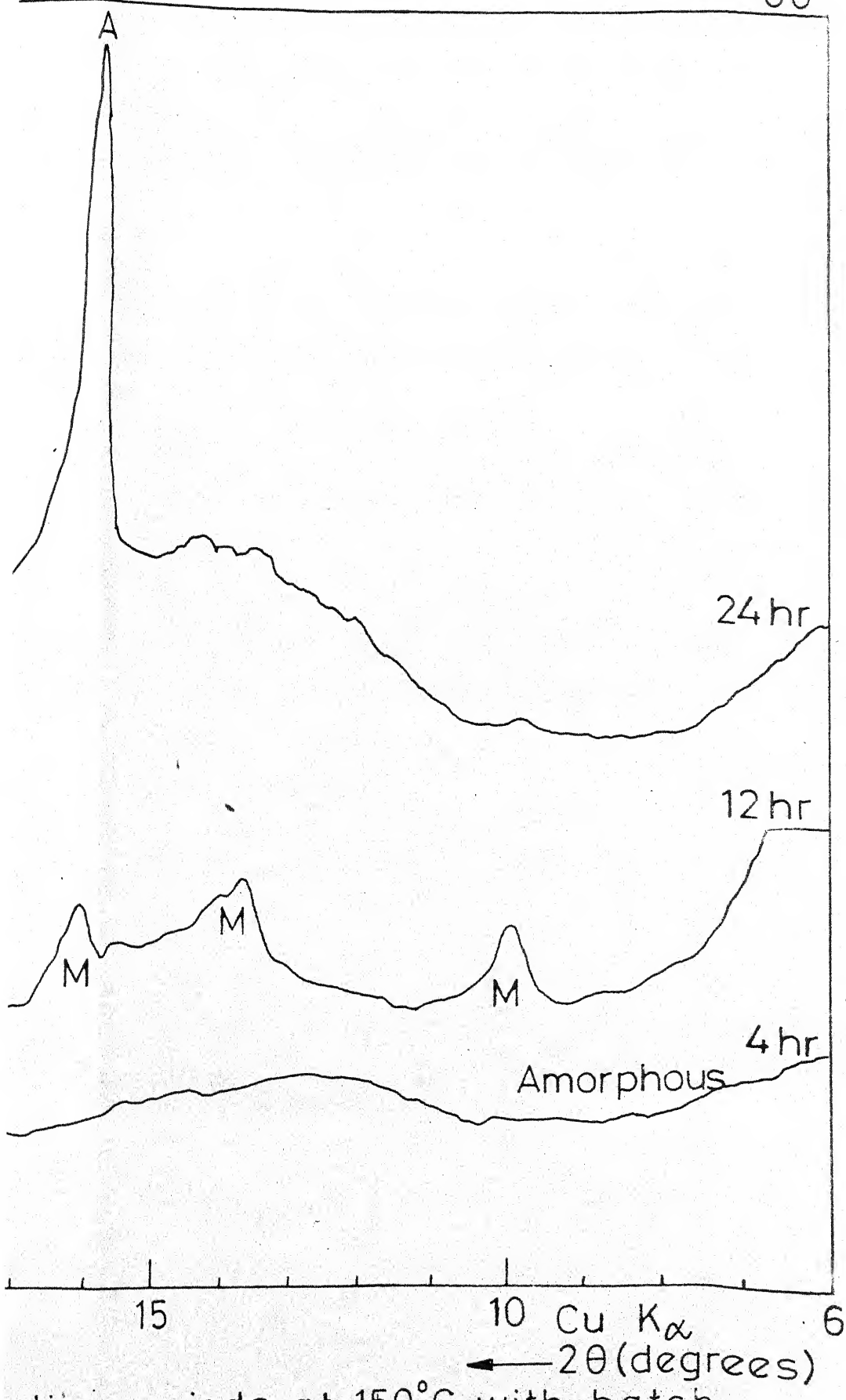

ction periods at 150°C with batch
n no. 330).

was carried out on identical lines as in the previous case. However, the ranges of variations of the chemical constituents involved in the starting mixture were slightly different compared to the previous runs. The ranges of operating variables were as follows:

Temperature of reaction	:	90 - 165°C
Synthesis time	:	1 hr - 7 days
Na_2O (mol per cent in the starting mix)	:	10.5 - 50.0
SiO_2 (mol per cent in the starting mix)	:	36.8 - 77.4
Al_2O_3 (mol per cent in the starting mix)	:	3.34 - 21.1
H_2O/Na_2O (mol ratio)	:	40 - 220

It may be noted here that in the present case since analcime has appeared in the runs conducted at 165°C under different conditions, the experiments for synthesis were scheduled only upto this temperature.

The nature of products obtained in several runs involving starting mixtures of different compositions and for reaction periods ranging from an hour to 7 days for several temperatures are indicated in Tables 4.6 - 4.9. It has been observed that for all the runs with varying conditions conducted at 90 and 100°C for varying periods of time (even upto 7 days in some cases), mordenite did not crystallize. The x-ray diffraction patterns revealed either the amorphous material or the crystallization of phillipsite. Typical x-ray

TABLE 4.6: SYNTHESIS OF ZEOLITES USING SILICA FROM RICE-HUSK ASH

Run No.	Composition of Starting Mixture (Anhydrous basis) Na_2O (mol per cent)	Al_2O_3 (mol per cent)	SiO_2 (mol per cent)	$\frac{H_2O}{Al_2O_3}$	Reaction Time (hr)	Reaction Product
1	2	3	4	5	6	7
			Reaction Temperature: 90°C			
407	22.25	3.75	74.00	320	24	Am
					48	Am
					96	Am
					168	Am
409	25.60	6.40	68.00	160	24	Am
					48	Am
					96	Am
					168	Am
418	50.00	12.50	37.50	176	4	Am
					8	P
					24	P
419	42.10	21.10	36.80	70	1	Am
					2	Am
					4	P
					24	P
			Reaction Temperature: 100°C			
405	30.00	3.34	66.66	200	12	Am
					24	Am
406	35.30	5.88	58.82	320	24	Am
					48	Am
					96	Am
					120	Am
412	50.00	12.50	37.50	176	4	Am
					8	P
					24	P
413	42.10	21.10	36.80	70	2	P
					4	P
					8	P

Table 4.6 (contd)

1	2	3	4	5	6	7
417	42.10	21.10	36.80	70	½ 1	Am P
		Reaction Temperature: 110°C				
404	40.00	6.67	53.33	290	4 8 24	Am Am P
411	22.25	3.75	74.00	320	24 48 96 168	Am Am+M M M
415	27.60	3.40	69.00	320	24	P

Am = Amorphous P = Phillipsite M = Mordenite

TABLE 4.7: SYNTHESIS OF ZEOLITE USING SILICA FROM RICE-HUSK ASH

Run No.	Composition of Starting Mixture[a] (Anhydrous basis) Na_2O (mol per cent)	Al_2O_3 (mol per cent)	SiO_2 (mol per cent)	Reaction Time (hr)	Reaction Product
		Reaction Temperature: 135°C			
421	24.10	6.90	69.00	12 24	M M
440	15.40	7.70	77.00	12 24	Am Am
441	18.50	7.40	74.10	12 24	Am Am
442	21.45	7.15	71.50	12 24	Am M
443	24.96	8.34	66.70	12 24	M M
444	26.70	6.67	66.63	12 24	M An
445	22.72	4.55	72.73	12 24	Am M
446	17.50	12.50	70.00	12 24	Am Am
453	27.50	5.00	67.50	12 24	Am Am
454	22.50	12.50	65.00	12 24	P P
455	27.50	10.00	62.50	12 24	P P

[a] $H_2O/Al_2O_3 = 219$

Am = Amorphous P = Phillipsite
M = Mordenite An = Analcime

TABLE 4.8: SYNTHESIS OF ZEOLITES USING SILICA FROM RICE-HUSK ASH

Run No.	Composition of Starting Mixture[a] (Anhydrous basis) Na_2O (mol per cent)	Al_2O_3 (mol per cent)	SiO_2 (mol per cent)	Reaction Time (hr)	Reaction Product
		Reaction Temperature: 150°C			
420	24.10	6.90	69.00	12 24	M M+An
424	16.10	6.45	77.40	12 24	Am M
426	15.40	7.70	77.00	8 24 48	Am Am Am
425	21.45	7.15	71.50	8 16 24	M+Am M M
428	18.50	7.40	74.10	12 24	Am M
429	26.70	6.67	66.63	12 24	An An
430	24.96	8.34	66.70	12 24	M An
431	22.75	4.55	72.70	8 16 24	M M M
450	17.50	12.50	70.00	12 24	Am M
451	12.50	10.00	77.50	12 24	Am Am
452	17.50	10.00	72.50	12 24	Am M

[a] H_2O/Al_2O_3 = 219

Am = Amorphous
An = Analcime

M = Mordenite

TABLE 4.9: SYNTHESIS OF ZEOLITES USING SILICA FROM RICE-HUSK ASH

Run No.	Composition of Starting Mixture[a] (Anhydrous basis) Na_2O (mol per cent)	Al_2O_3 (mol per cent)	SiO_2 (mol per cent)	Reaction Time (hr)	Reaction Product
1	2	3	4	5	6
		Reaction Temperature: 165°C			
403	35.30	5.88	58.82	12 24	An An
408	24.10	6.90	69.00	24 48	An An
410	24.10	6.90	69.00	4 8 12 16	Am M+Am M M+An
423	16.10	6.50	77.40	12 24	Am M+Am
432	24.96	8.34	66.70	12 24	An An
433	26.70	6.67	66.63	12 24	An An
434	22.72	4.55	72.73	12 24	M An
435	18.50	7.40	74.10	12 24	M M
436	15.40	7.70	69.90	12 24	Am Am
437	18.50	9.00	72.50	12 24	M M
438	21.45	7.15	71.50	12 24	M M

Table 4.9 (contd)

1	2	3	4	5	6
447	10.50	12.50	77.00	12 24	Am Am
448	15.00	15.00	70.00	12 24	M M
449	17.50	10.50	72.00	12 24	M M

[a] H_2O/Al_2O_3 = 219

Am=Amorphous
M=Mordenite
An=Analcime

diffraction patterns for a representative run (412) at 100°C are indicated in Figure 4.15.

Effect of Composition of the Starting Mixture:

The triangular diagrams plotted with SiO_2, Al_2O_3 and Na_2O as three end members indicating the field for crystallization of mordenite are presented in Figures 4.16 and 4.17 for the three temperatures 135, 150 and 165°C and for 12 and 24 hr of reaction time. To facilitate a comparison of the results obtained in the experimental runs using silica from chemical source with those using silica derived from rice-husk ash under identical conditions of temperature and time, the diagrams (Figure 4.18 and 4.19) are plotted superimposing the respective fields.

It has been observed that for the synthesis of mordenite with silica from rice-husk ash, relatively lesser Na_2O or greater SiO_2 content in the starting mixture is required compared to the synthesis of mordenite using silica from chemical source. It can be seen that a higher H_2O/Na_2O ratio is involved in the former case (Figure 4.7 - 4.9). This possibly can be attributed to the form of silica in the initial mixture. Where silica from chemical sources was used, part of it was in the form of sodium silicate in solution with the remaining part as silica gel. In the runs that involved the silica from rice-husk ash, the silica was in the form of a silica solution in sodium hydroxide. Since the

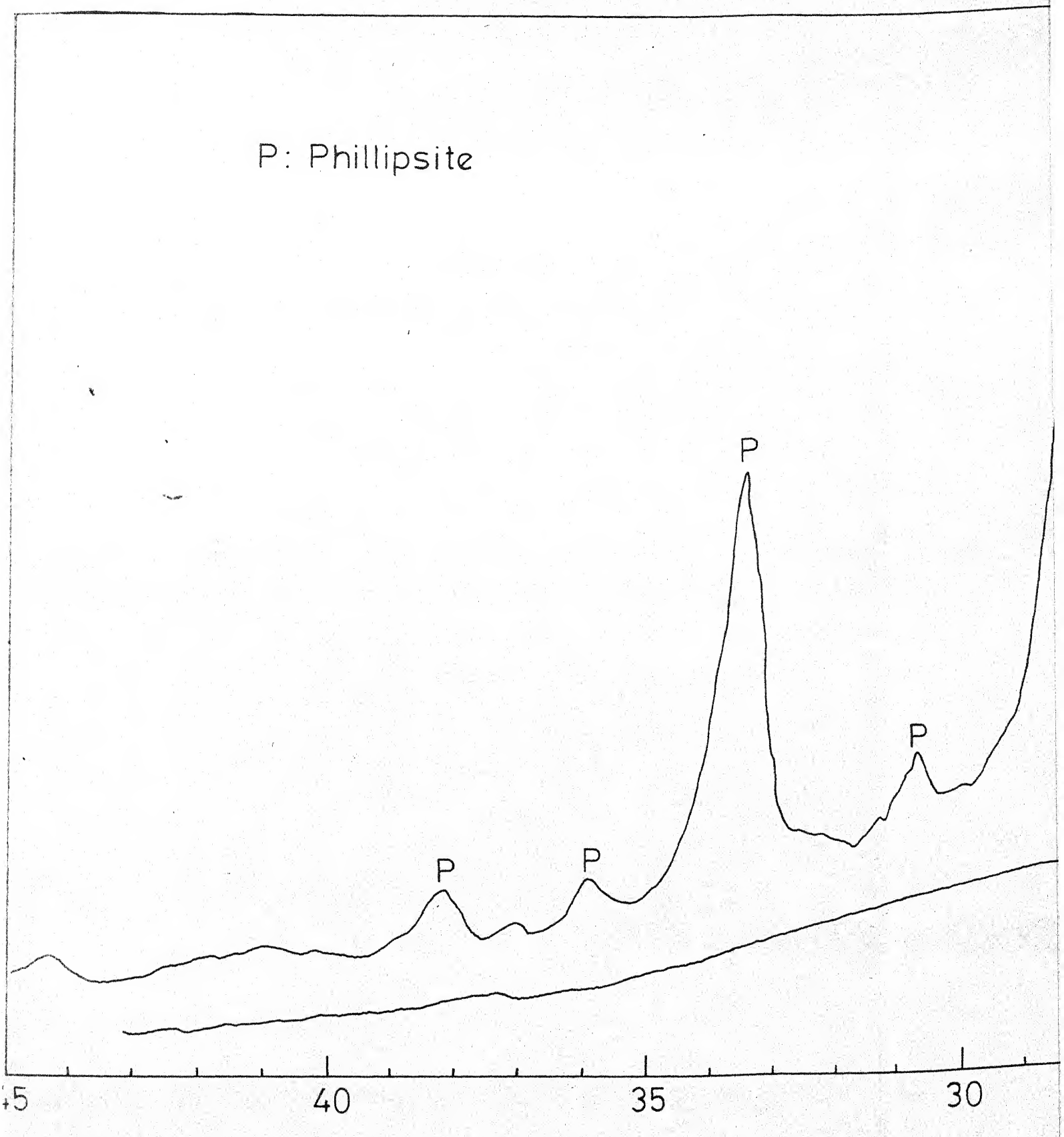

Fig. 4·15– Typical X-ray diffraction patterns for products fo

$4\,Na_2O \cdot Al_2$

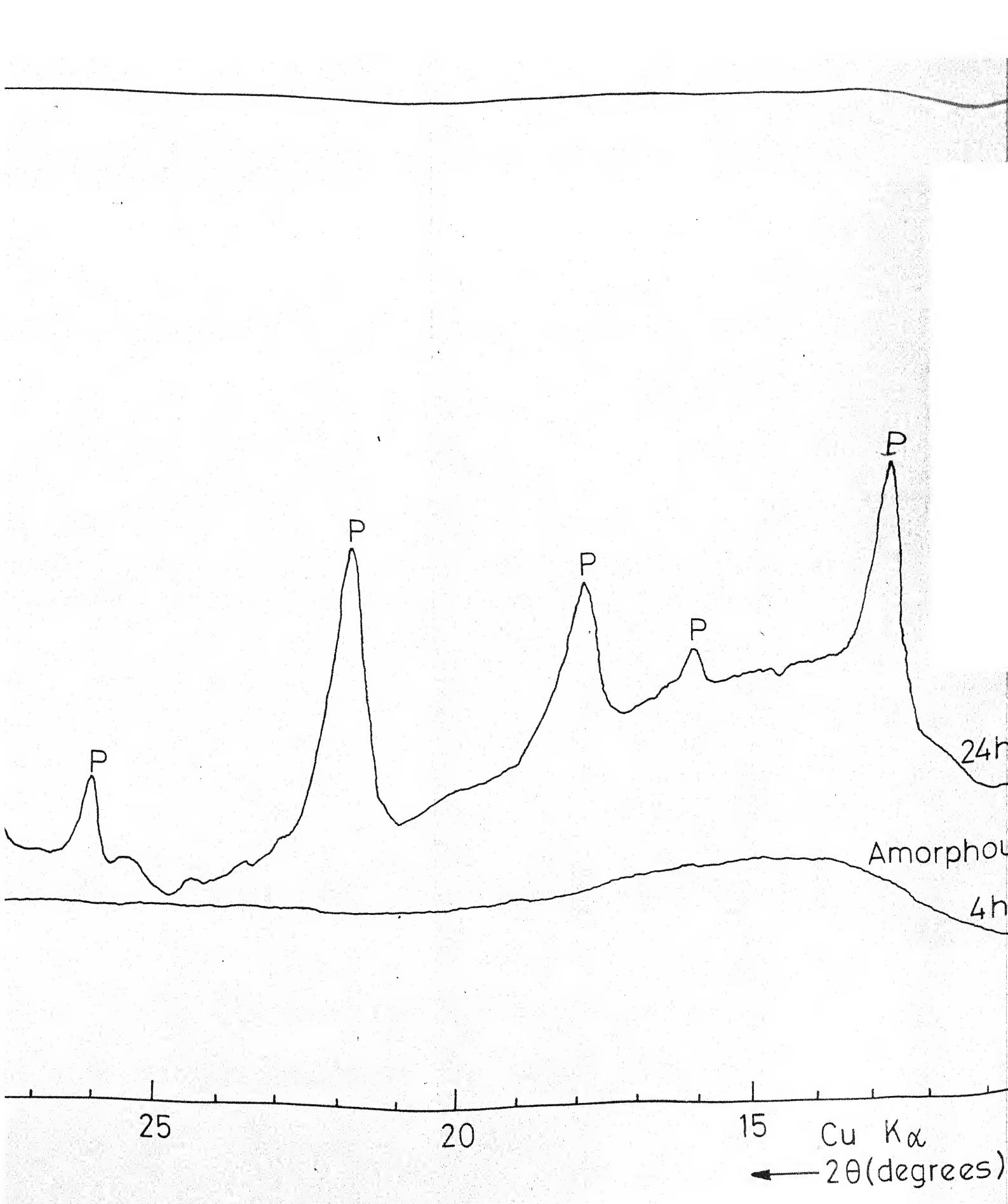

:d at 100°C using silica from rice husk ash with batch composition
3 SiO_2 · 219 H_2O (run no. 412).

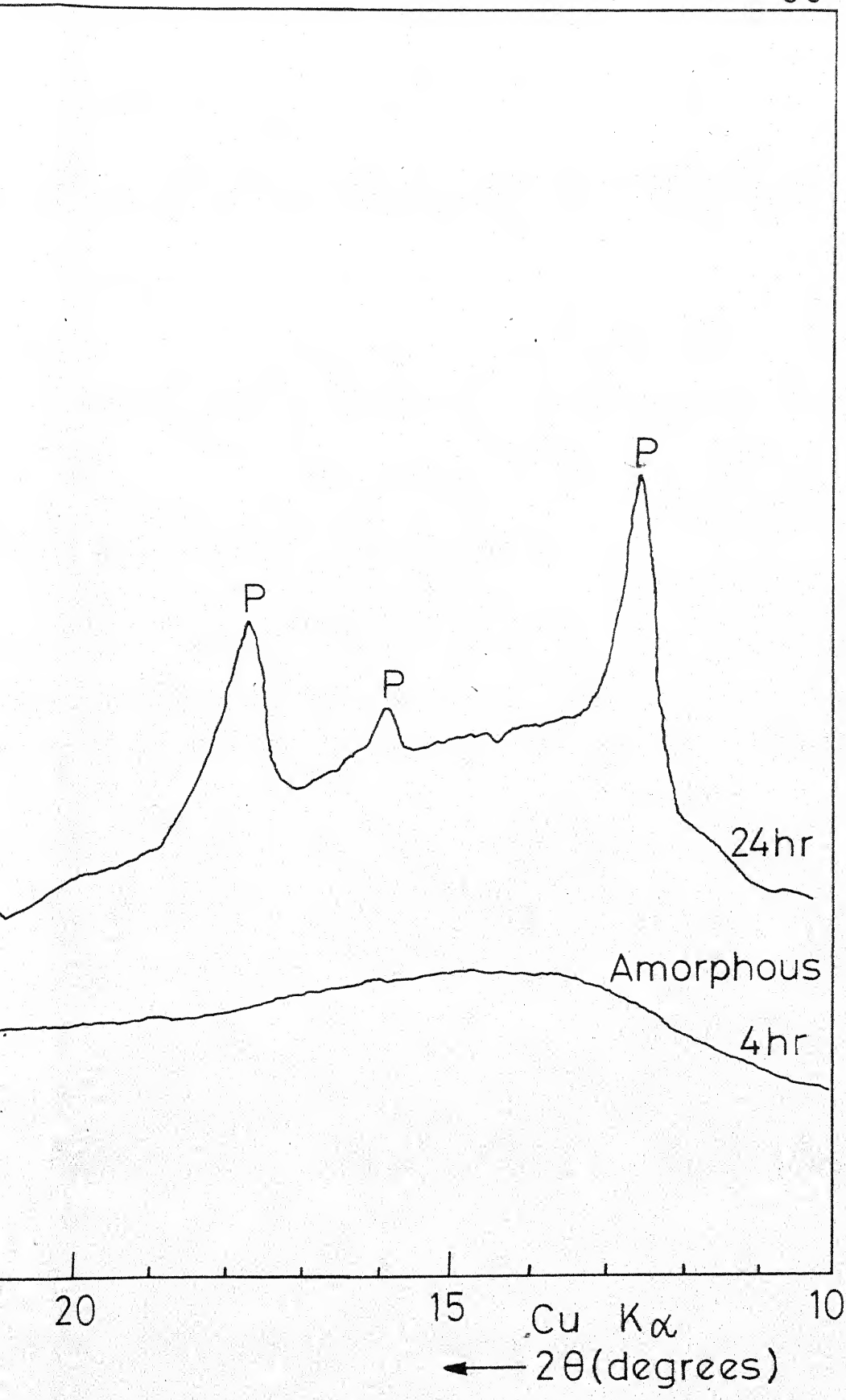

rom rice husk ash with batch composition:

412)..

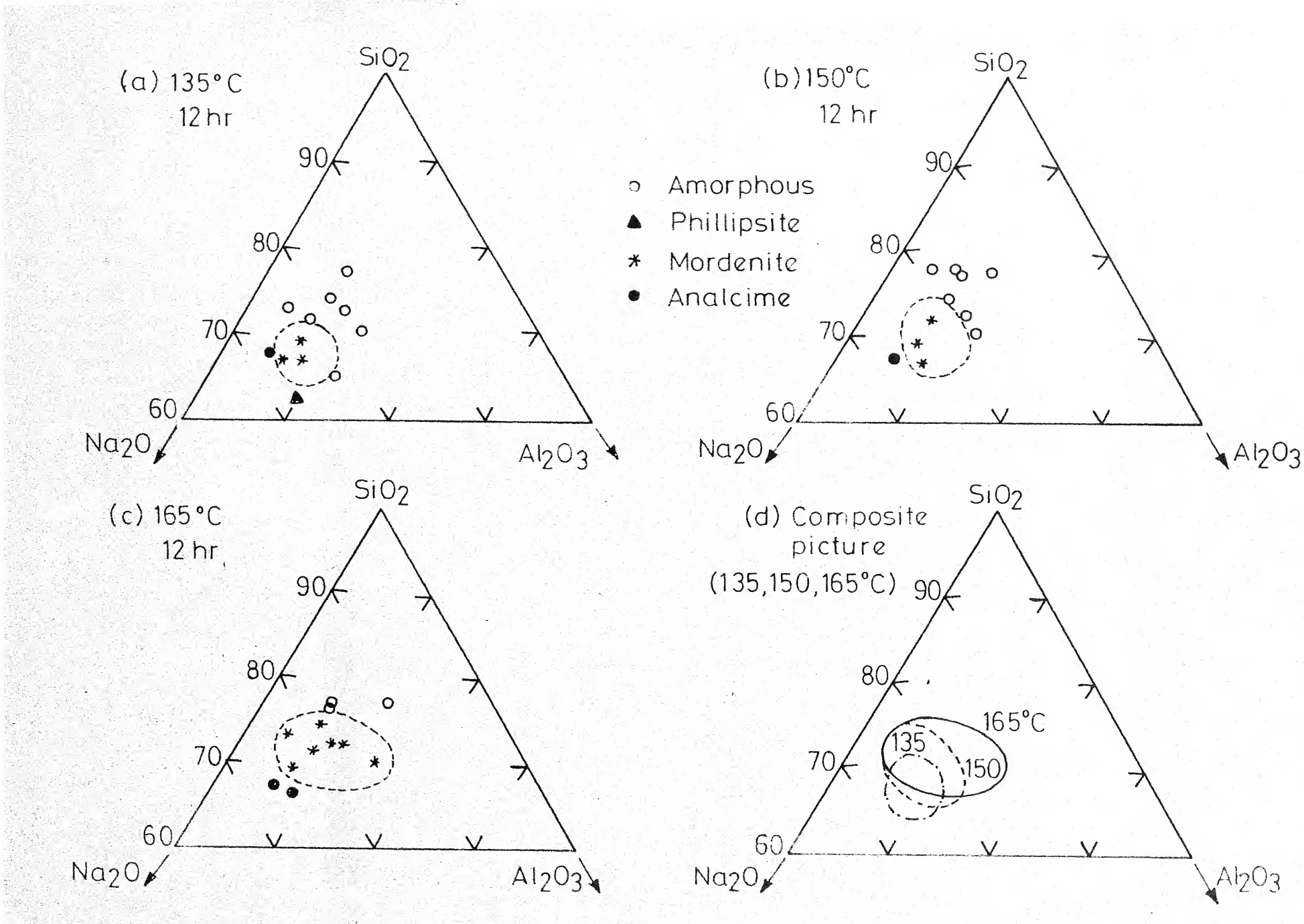

Fig 4.16 - Reaction composition diagrams for 12 hr using silica from rice husk ash.

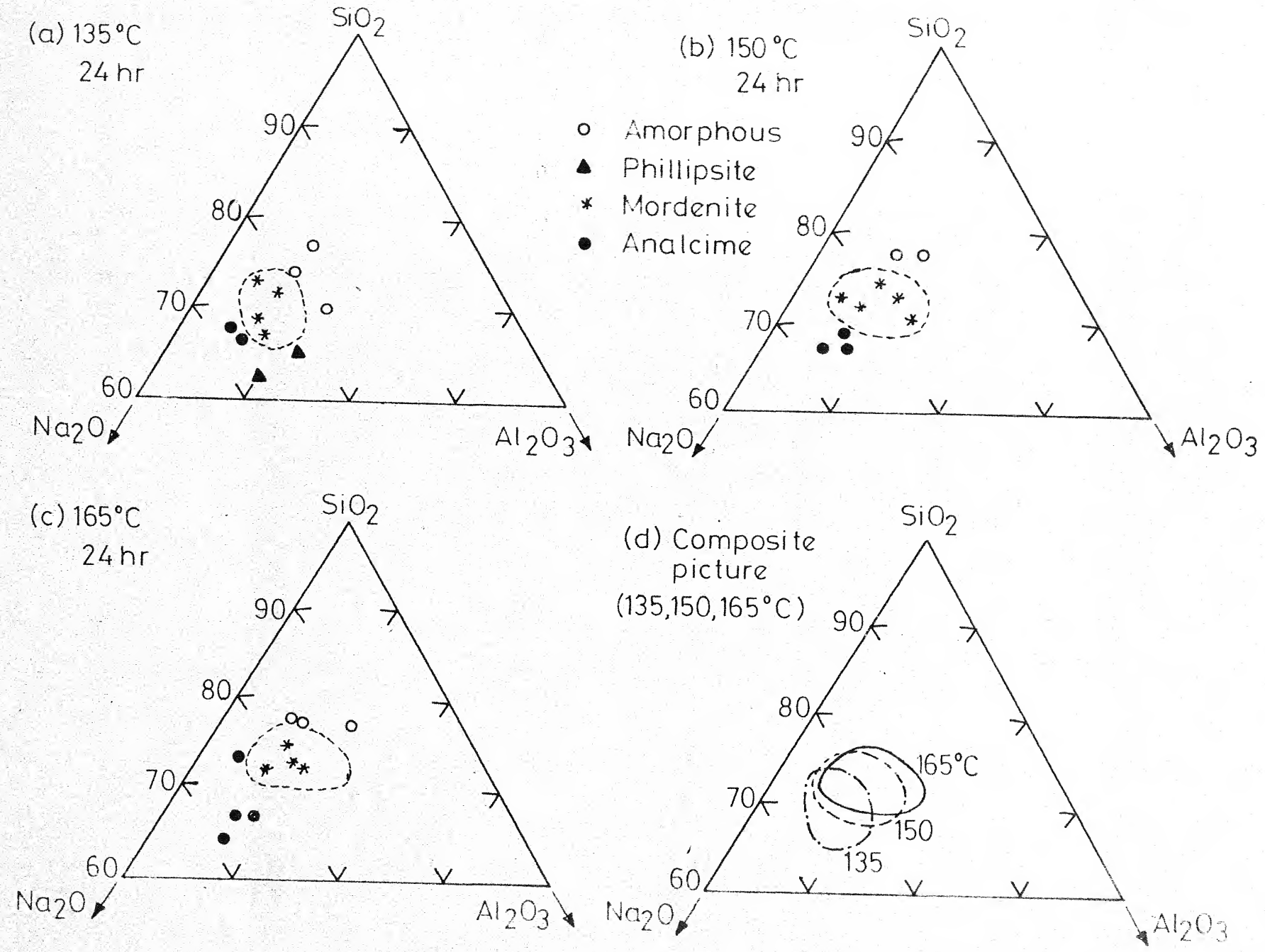

Fig 4.17 - Reaction composition diagrams for 24 hr using silica from rice husk ash.

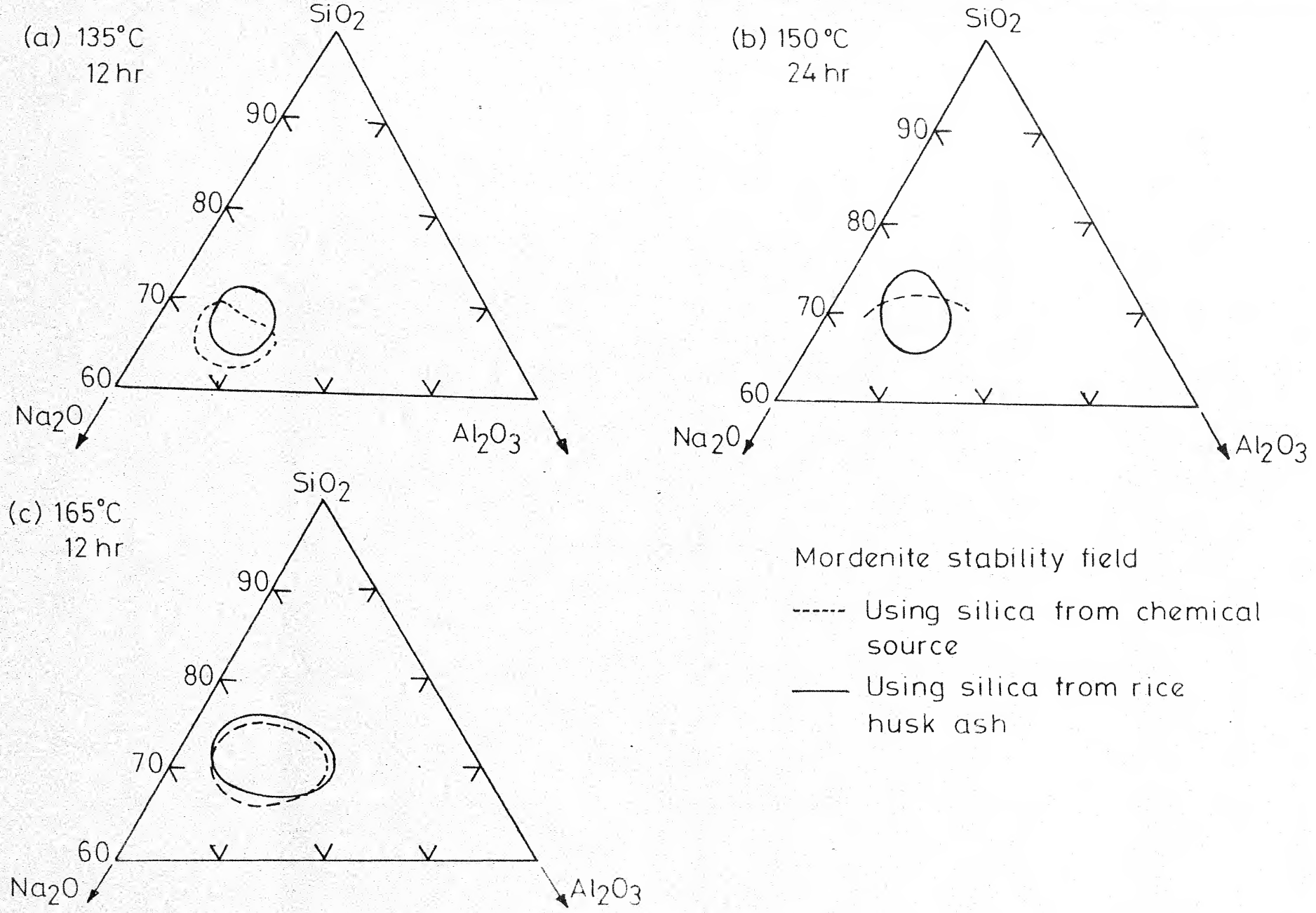

Fig 4-18 – Effect of silica source on the stability field of mordenite (reaction period 12 hr)

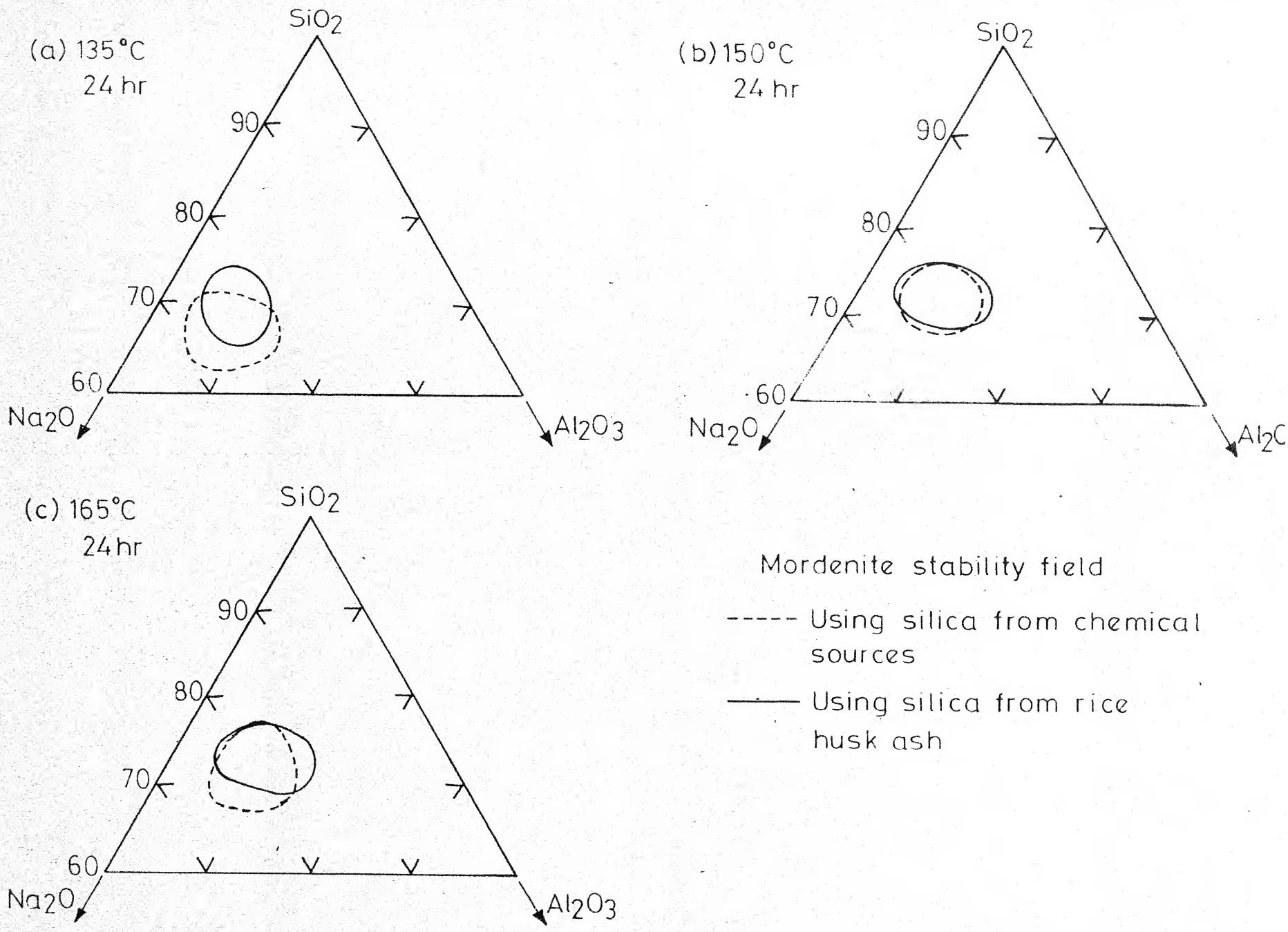

Fig. 4.19 - Effect of silica source on the stability field of mordenite (reaction period 24 hr)

crystallization of mordenite starts from the liquid phase of the starting sodium alumino-silicate gel, the solubilities of the materials in the final mixture to form the liquid phase that contributes to the mordenite crystallization appear to be different in both the cases.

The activity of silica during the crystallization of aluminosilicate of variable silica content was reported by Coombs et al. [61]. According to these workers, the use of a more reactive amorphous silica is important for the synthesis of high silica zeolite. Breck [4] indicated that when the reaction mixtures are prepared using a colloidal silica sol or amorphous silica as the silica source, the products that are formed can be different from those crystallized from the homogeneous sodium aluminosilicate gel. The reason attributed by him is the solubilization of silicate anions and the resulting interaction with the aluminate ions present in the solution.

The interrelationship between the SiO_2 and Na_2O contents have been indicated in the graph (Figures 4.3 to 4.5) by plotting SiO_2/Al_2O_3 ratio against Na_2O/Al_2O_3 ratio. These when compared with the corresponding plots for the runs in the synthesis using silica from chemical sources (indicated as part a in the same figures) reveal certain differences. At 135°C, the mordenite formation is restricted to a narrow range of both these ratios. Analcime starts appearing in

the mixtures containing Na_2O/Al_2O_3 around 4 and with SiO_2/Al_2O_3 around 10 at this temperature. However, the results obtained in the experiments using silica from chemical sources, indicate that mordenite continues to crystallize in the mixtures with Na_2O/Al_2O_3 and SiO_2/Al_2O_3 ratios even beyond these values (5 and 14 respectively). At 165°C also analcime could be obtained with relatively smaller values of these ratios in the runs with silica from rice-husk ash when compared to those with silica from chemical sources.

Effect of Temperature and Time:

The effect of temperature of reaction on the mordenite synthesis is indicated in Figures 4.18(d) and 4.19(d). With increase in temperature, the mordenite field shifts towards a higher silica and alumina direction. A gradual shifting could be noticed in these figures as compared to Figure 4.1(d) and 4.2(d) which are for mordenite synthesized from chemical silica sources. In the latter case, there is a drastic shift between the mordenite field at 135°C and the same at 150 and 165°C. The fields at 150 and 165°C more or less coincide in the case of mordenite synthesized from chemical sources for 24 hr of duration.

It has also been observed that in the range less than 3 for SiO_2/Na_2O at temperatures of 150°C and above, analcime appeared as a product in the runs with silica from rice-husk ash while mordenite could be seen in this range for the runs

with silica from chemical sources (Figure 4.6).

The plots of SiO_2/Al_2O_3 versus H_2O/Na_2O revealed interesting trends in the case of experiments using silica from rice-husk ash. While the mordenite field is restricted within narrow ranges for these ratios for the runs at 135°C, the same is within the broader range of H_2O/Na_2O ratio at 150 and 165°C. For the runs using silica from chemical sources, the mordenite field is restricted at 165°C within narrow ranges of SiO_2/Al_2O_3 and H_2O/Na_2O ratios. In general, the scatter for the mordenite plots is wider at 150 and 165°C on these graphs for runs with rice-husk ash silica compared to those with chemical silica source (Figures 4.7 - 4.9). This implies that in the case of runs using silica from chemical sources the mordenite could be formed only when the initial mixture has high alkalinity while it could be crystallized even with a relatively low alkalinity in the synthesis using silica from rice-husk ash.

It was also observed that the crystallization of mordenite at any particular temperature is attained faster using silica from rice-husk ash in synthesis. Further, the appearance of analcime was noticed at relatively shorter time of reaction in such cases when compared to the runs conducted with starting mixtures of identical compositions and at similar temperatures but with silica from chemical sources. The x-ray diffraction patterns presented in Figures 4.20 and 4.21

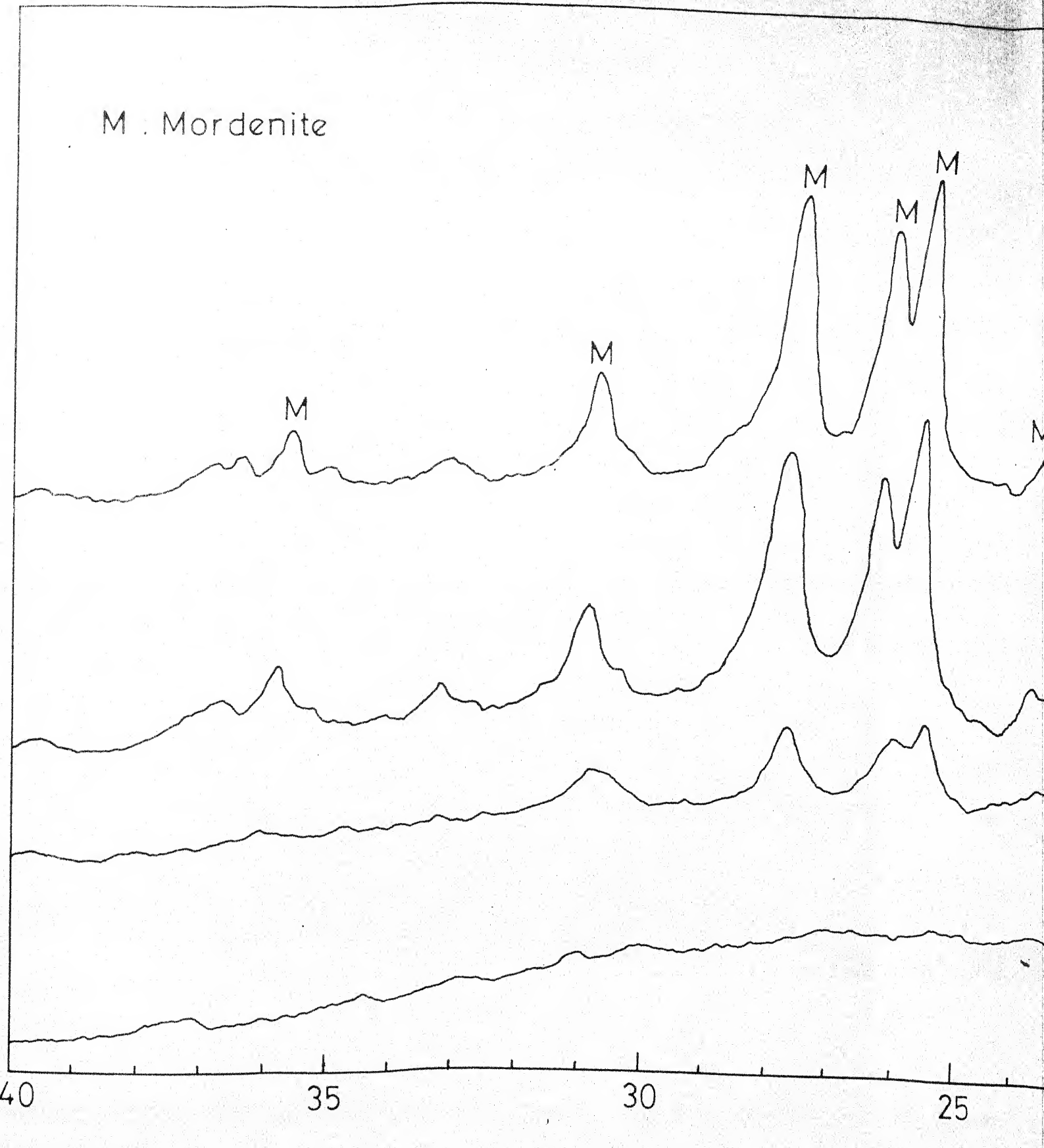

Fig. 4·20– X-ray diffraction patterns of products for differe

$Al_2O_3 \cdot 10\,SiO_2$

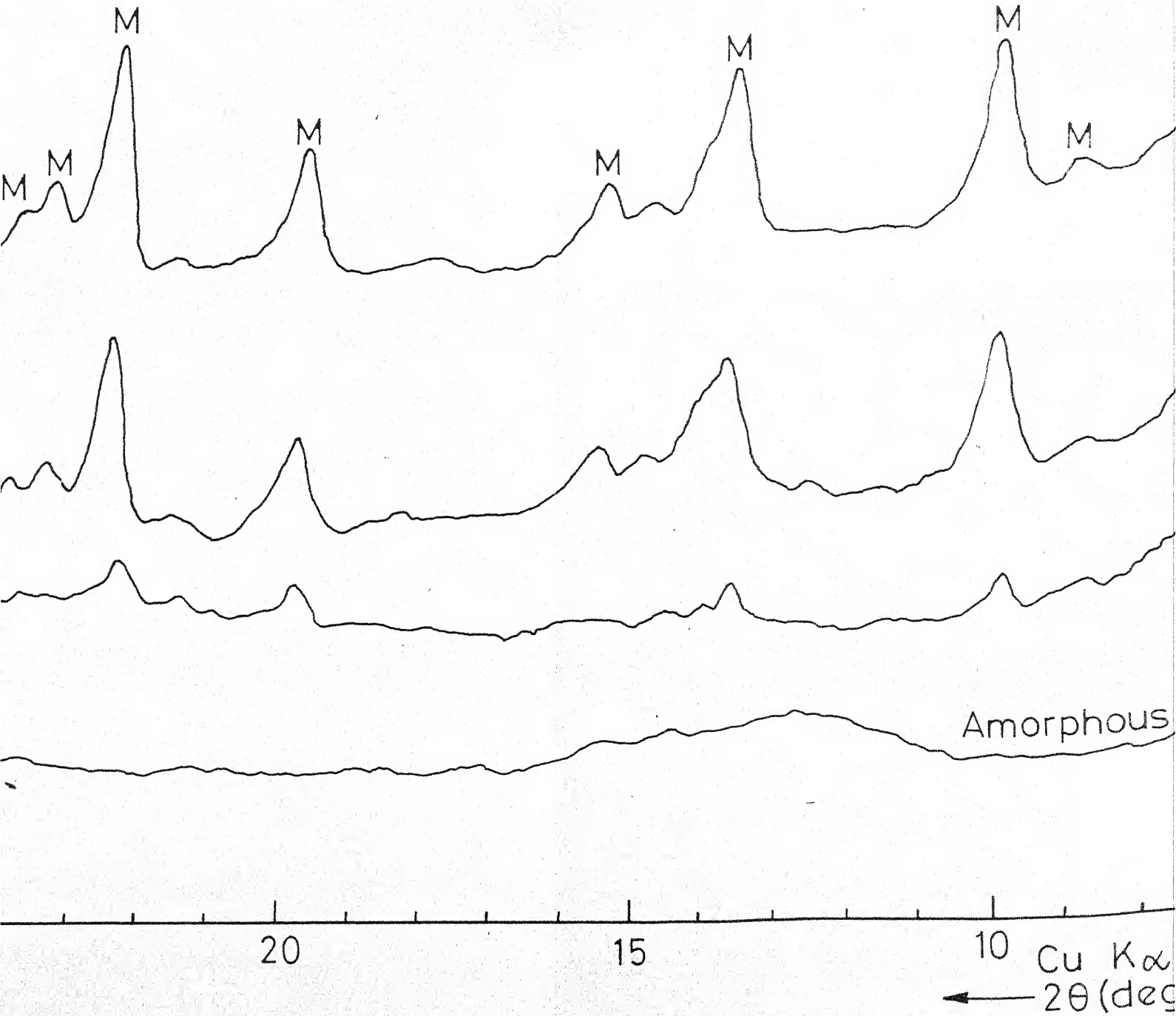

rent reaction periods at 165°C with batch composition: 3·5 N

O_2· 219 H_2O (using silica from chemical source)

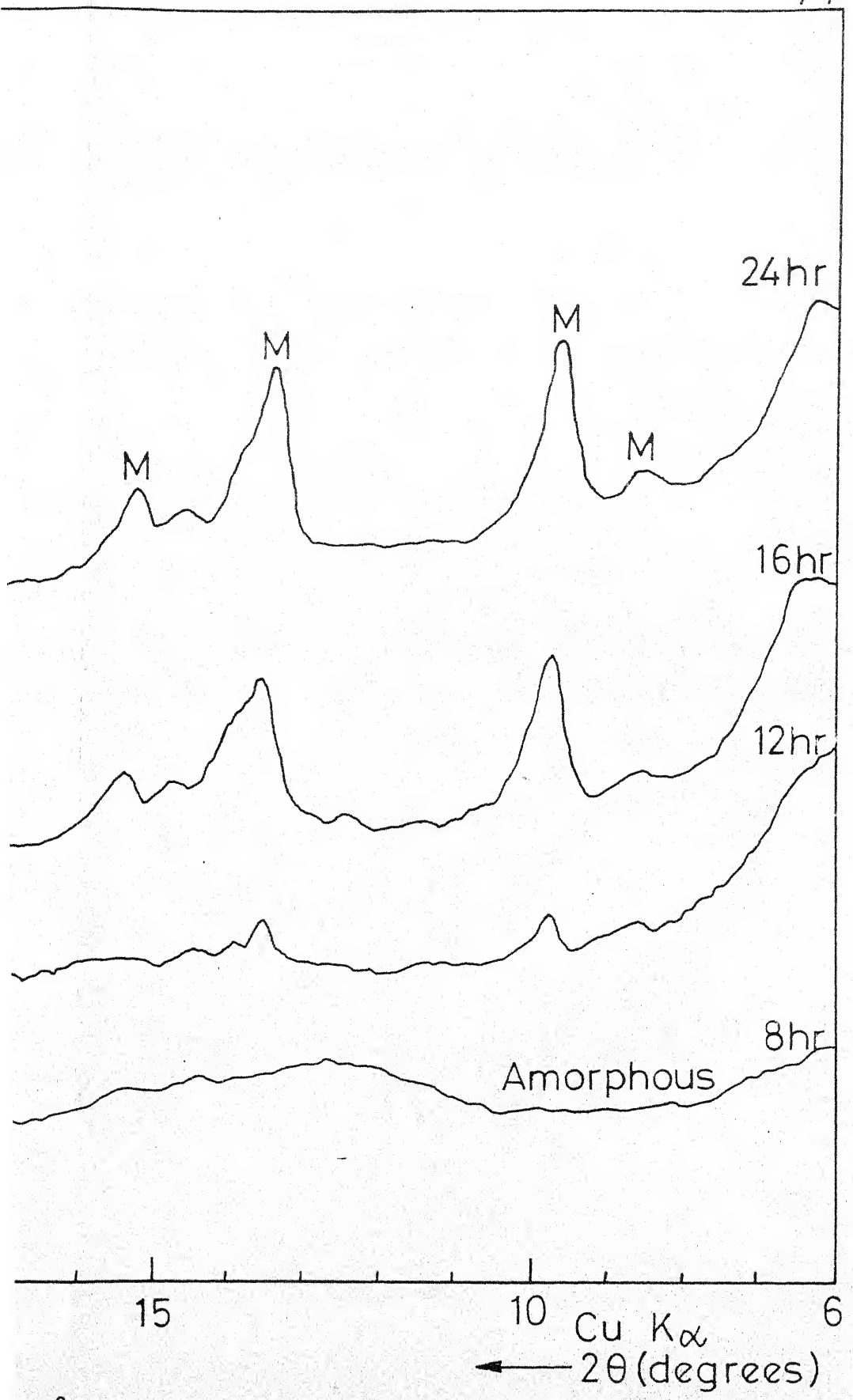

65°C with batch composition: $3.5Na_2O$·

om chemical source)

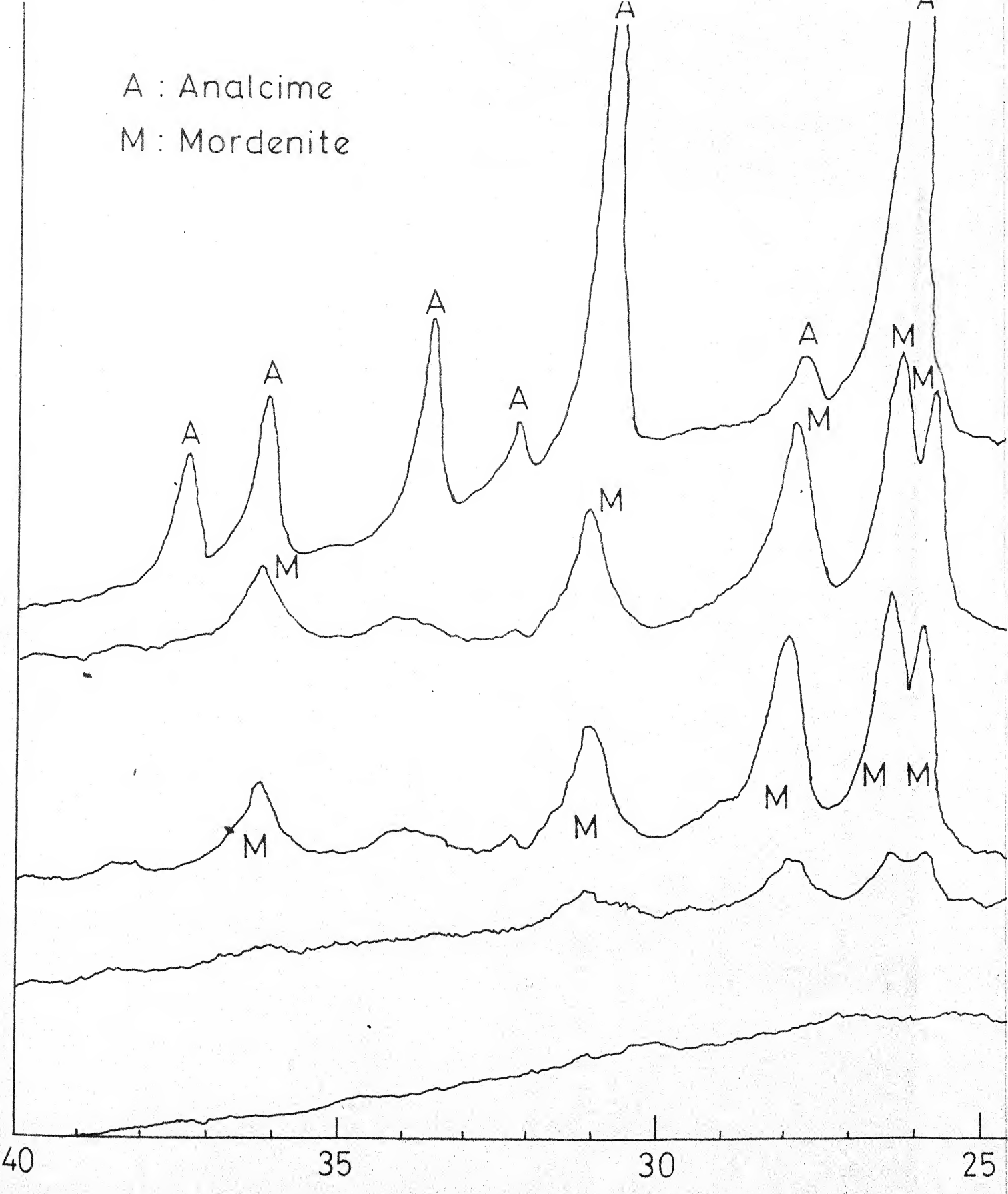

Fig.4·21– X–ray diffraction patterns of products formed

3·5 $Na_2O \cdot Al_2O$

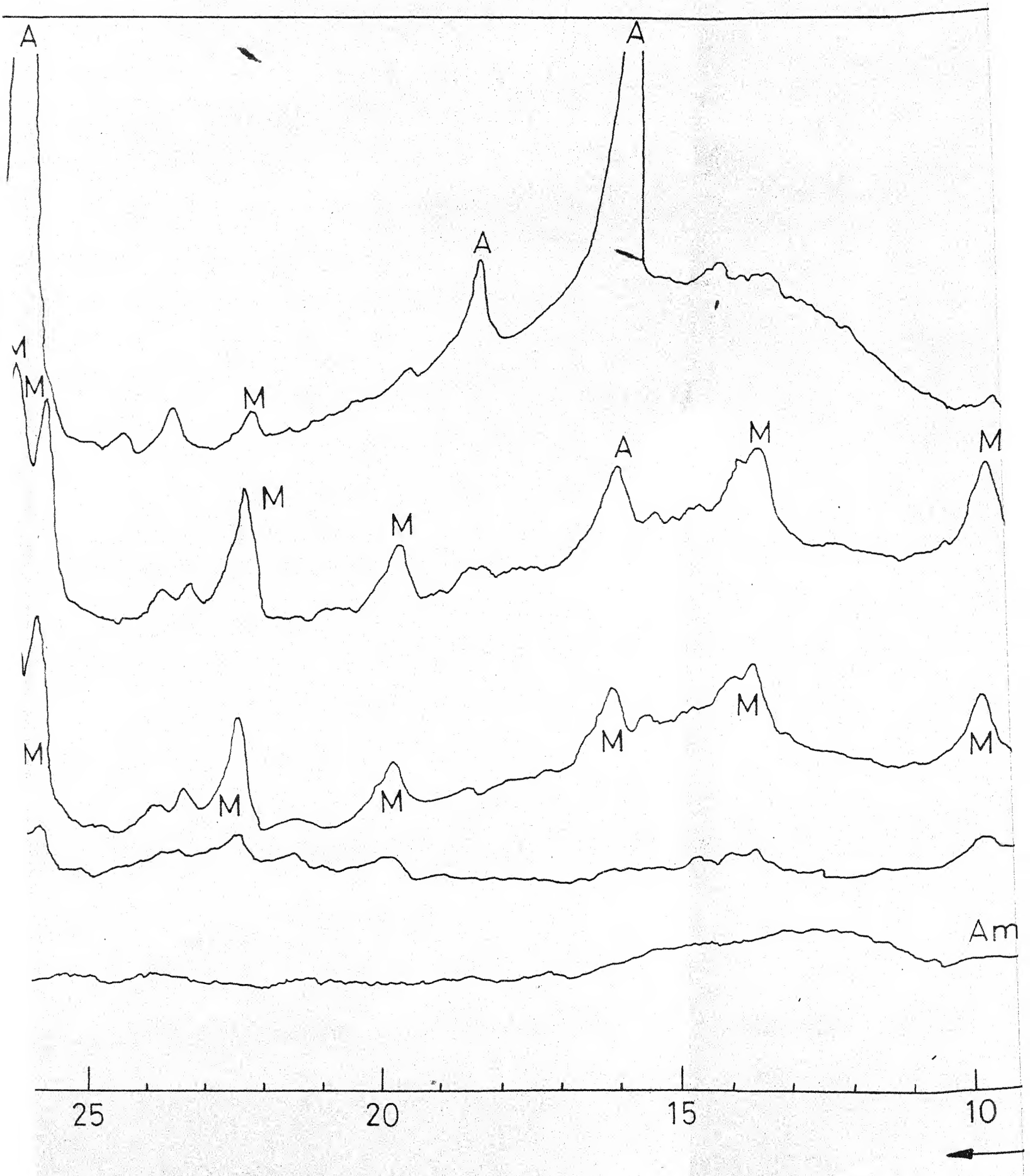

med for different reaction periods at 165°C with batch co

$Al_2O_3 \cdot 10\ SiO_2 \cdot 219\ H_2O$ (using silica from rice husk ash).

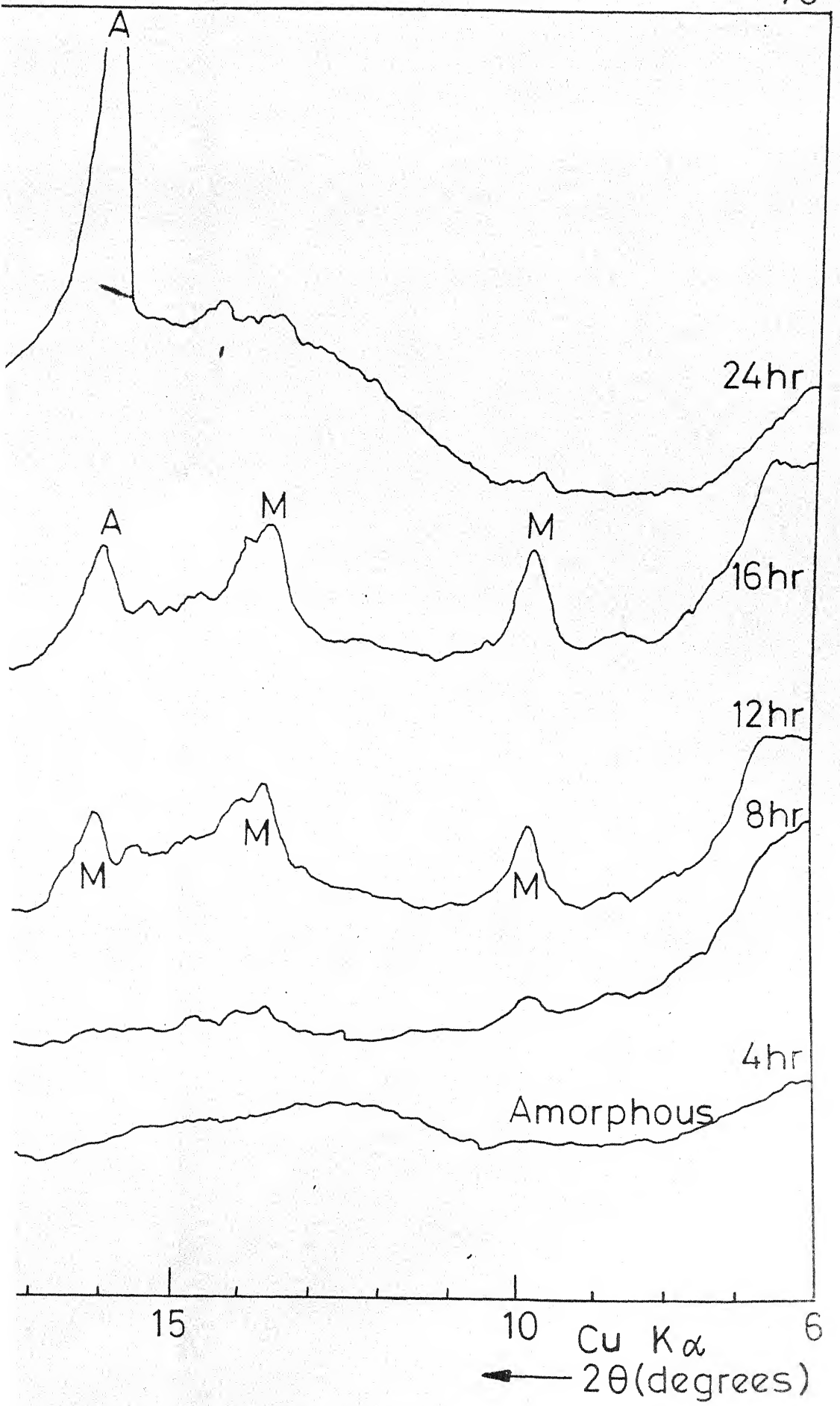

ods at 165°C with batch composition :
ca from rice husk ash).

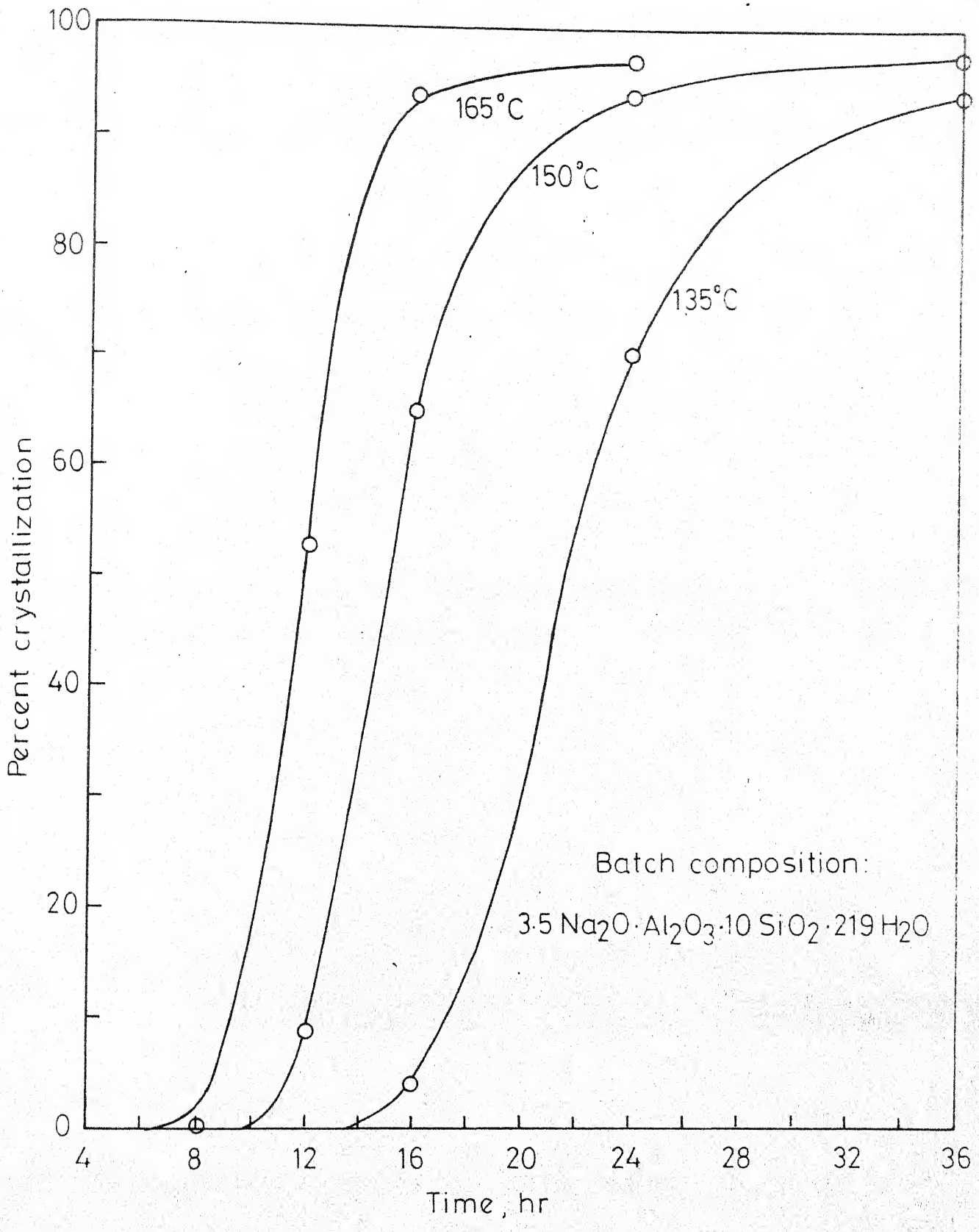

Fig.4.22- Crystallization curves of mordenite using silica from chemical sources.

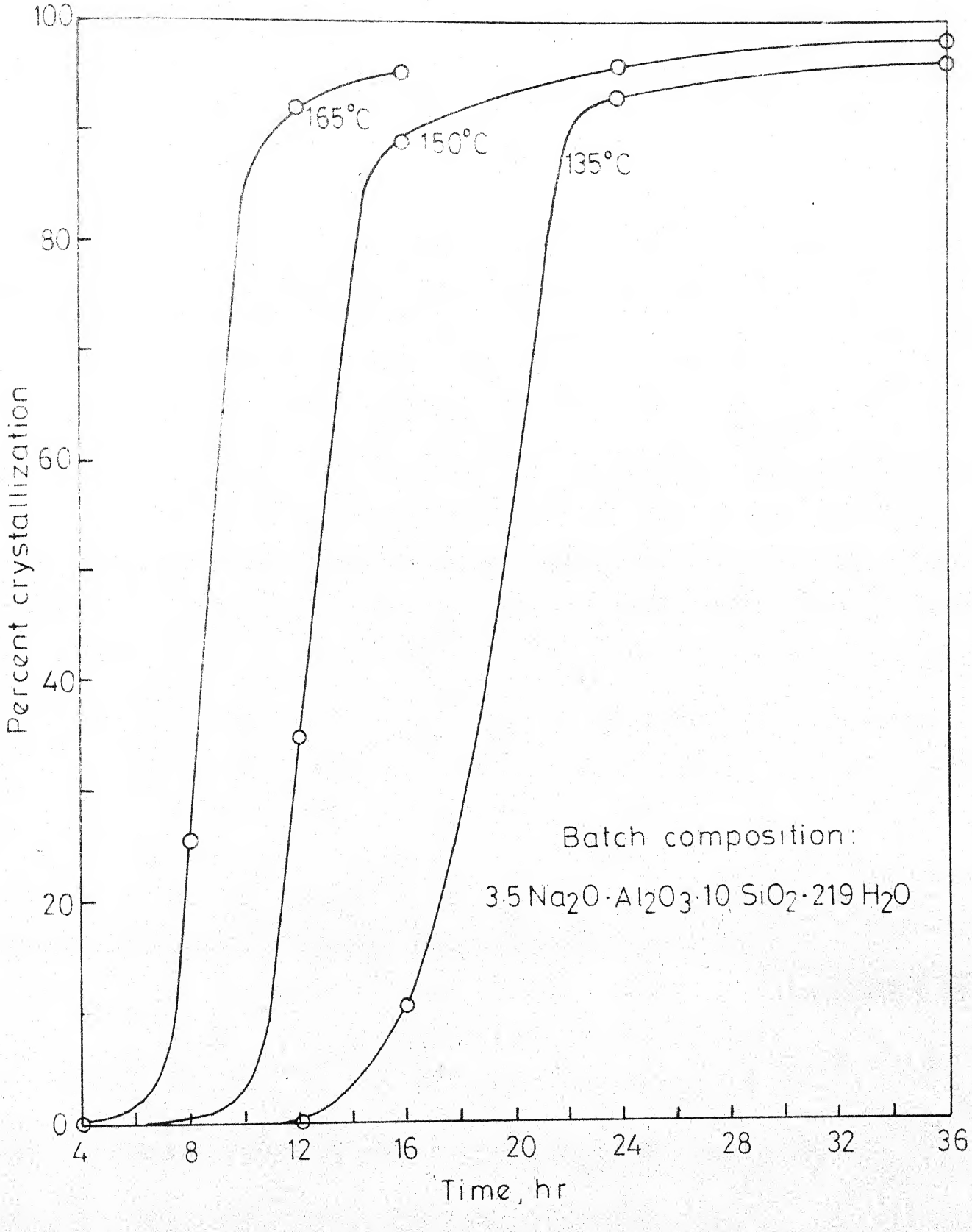

Fig.4·23 - Crystallization curves of mordenite using silica from rice husk ash.

The activation energy for the nucleation and crystal growth are determined from the crystallization curves at various temperatures with the same starting compositions. Assuming that the formation of nuclei of a stable size (which do not redissolve but grow into a crystal) is an energetically activated process and since the nucleation during the induction period is the rate determining process, the apparent activation energy for the nucleation, E_n, can be calculated from the expression:

$$\frac{d \ln (1/\theta)}{d(1/T)} = - \frac{E_n}{R}$$

where θ is the induction time i.e. the point on the crystallization curve where conversion to the crystallization phase is just starting [103].

A similar analysis is made for the crystallization rate in determining the apparent activation energy, E_c, for the crystal growth assuming that the rate limiting step is the crystal growth. This is most nearly true when the conversion rate is highest, therefore, the crystallization rate is defined as the rate of conversion at 50 per cent of the total conversion level in terms of per cent conversion/hr [50].

The results obtained from both these approaches in the present study are reported in Figure 4.24 and Table 4.10:

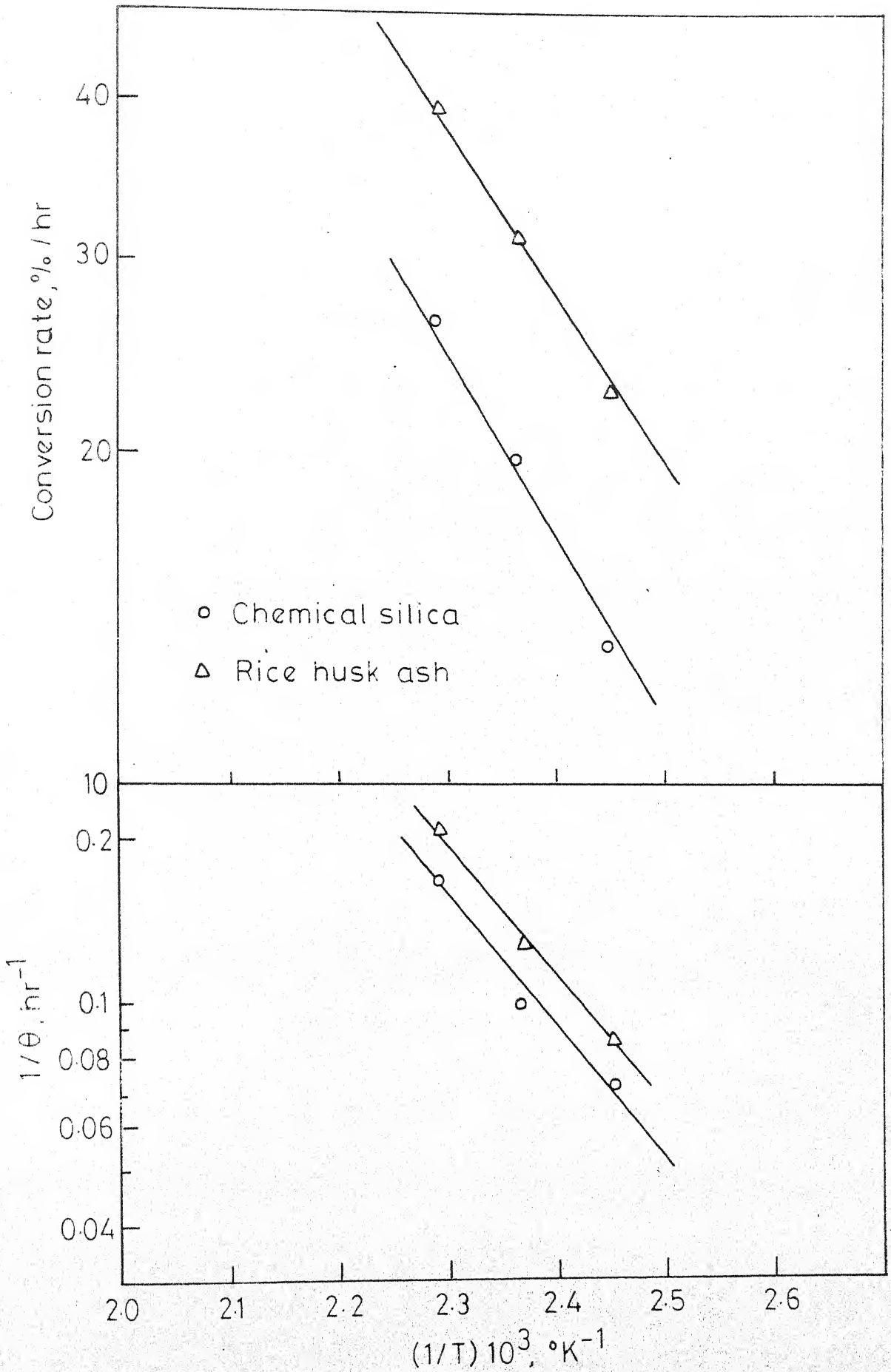

Fig. 4.24- Dependence of conversion rate and induction period on temperature for mordenite.

TABLE 4.10: ACTIVATION ENERGIES FOR NUCLEATION AND CRYSTAL GROWTH OF MORDENITE

Batch composition $Na_2O/Al_2O_3/SiO_2/H_2O$	Silica source	Temperature range, °C	Activation Energy Kcal/g.mol.	
			Nucleation En	Crystal growth Ec
3.5/1/10/219	Chemicals	135 - 165	10.2	7.56
3.5/1/10/219	Rice-husk ash	135 - 165	9.5	6.85
Ref.[47]	Chemicals	250 - 290	11.0	-
Ref.[50]	Chemicals	90 - 135	24.0	15.0

The activation energy values obtained for nucleation in the present investigations are in the range indicated by Domine and Quobex [47]. However, the values of 24 Kcal/g mol (for nucleation) and 15 Kcal/g mol (for crystal growth) reported by Culfaz and Sand [50] are too high compared to the values in the present work.

4.2 Characterization of Mordenite:

The mordenite obtained from starting materials using silica from chemical sources as also silica from rice-husk ash have been studied using several techniques for their characterization. For several samples the x-ray diffraction patterns have been obtained and on this basis the samples from two typical runs (Numbers 319 and 425) were chosen as

representative ones for detailed characterization.

4.2.1 X-ray Diffraction Data:

The d spacings for the mordenite samples (from synthesis using both types of silica) are presented in Table 4.11. The d spacings for the standard mordenite (zeolon) are also included in thesame table. The diffraction patterns for these are indicated in Figure 4.25.

The synthesized mordenites are comparable to the zeolon. Since the hydrogen form has also been prepared as a two stage process- first converting it into ammonium form of the species and later into the hydrogen form, the diffraction patterns for ammonium and hydrogen forms have been obtained. The d spacings for these forms have been presented in Tables 4.12 and 4.13. The lattice parameters for the various forms of mordenite obtained in the present study are reported in Table 4.14. The literature values for the same are also included for a comparison. It has been observed that the replacement of sodium ion with ammonium or hydrogen does not alter the lattice parameters appreciably. In the latter forms, a slight increase in 'a' dimension and a slight decrease in 'b' dimension resulted when compared to the sodium form.

During synthesis, since at some stages, phillipsite and analcime were encountered, the d spacings for these two products together with literature values on phillipsite [104] and

TABLE 4.11: X-RAY POWDER DATA FOR MORDENITE SAMPLES

hkl	Sample No. 319		Sample No. 425		Zeolon	
	d(Å)	I/I_o	d(Å)	I/I_o	d(Å)	I/I_o
1	2	3	4	5	6	7
110	13.39	25	13.39	25	13.39	25
200	9.03	15	9.03	15	9.06	15
111	6.51	45	6.51	45	6.50	45
130	6.33	30	6.32	30	6.32	30
021	6.03	15	6.03	15	6.03	15
201	5.75	20	5.76	20	5.76	20
221	5.02	3	5.04	3	5.04	3
131	4.86	3	4.85	3	4.86	3
330	4.51	40	4.51	40	4.51	40
420	4.13	5	4.13	5	4.13	5
150	3.98	70	3.98	70	3.98	70
241	3.82	20	3.82	20	3.81	20
002	3.77	10	3.77	10	3.76	10
112	3.59	5	3.60	5	3.58	5
510	3.52	5	3.51	5	3.52	5
202	3.46	100	3.46	100	3.46	100
060	3.39	65	3.39	65	3.39	65
222	3.28	10	3.28	10	3.28	10
530	3.21	75	3.21	75	3.21	75
441	3.10	5	3.10	5	3.10	5

Table 4.11 (contd)

1	2	3	4	5	6	7
531	2.93	5	2.93	5	2.93	5
402	2.89	35	2.89	35	2.89	35
152	2.73	3	2.74	3	2.73	3
621	2.69	10	2.69	10	2.69	10
370	2.63	3	2.62	3	2.63	3
461	2.54	10	2.54	10	2.54	10
442	2.51	20	2.51	20	2.52	20

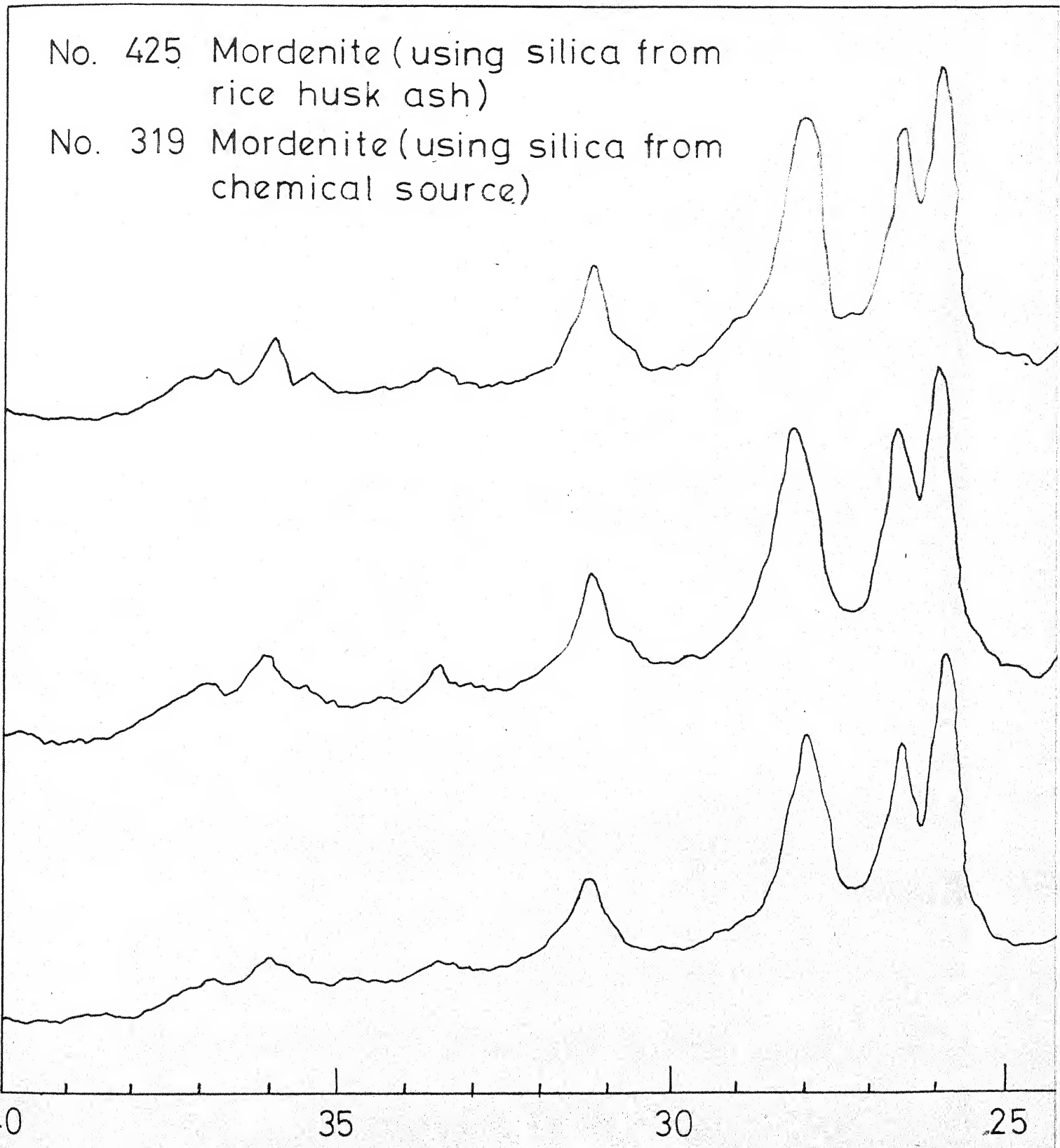

Fig. 4·25- Typical X-ray diffraction

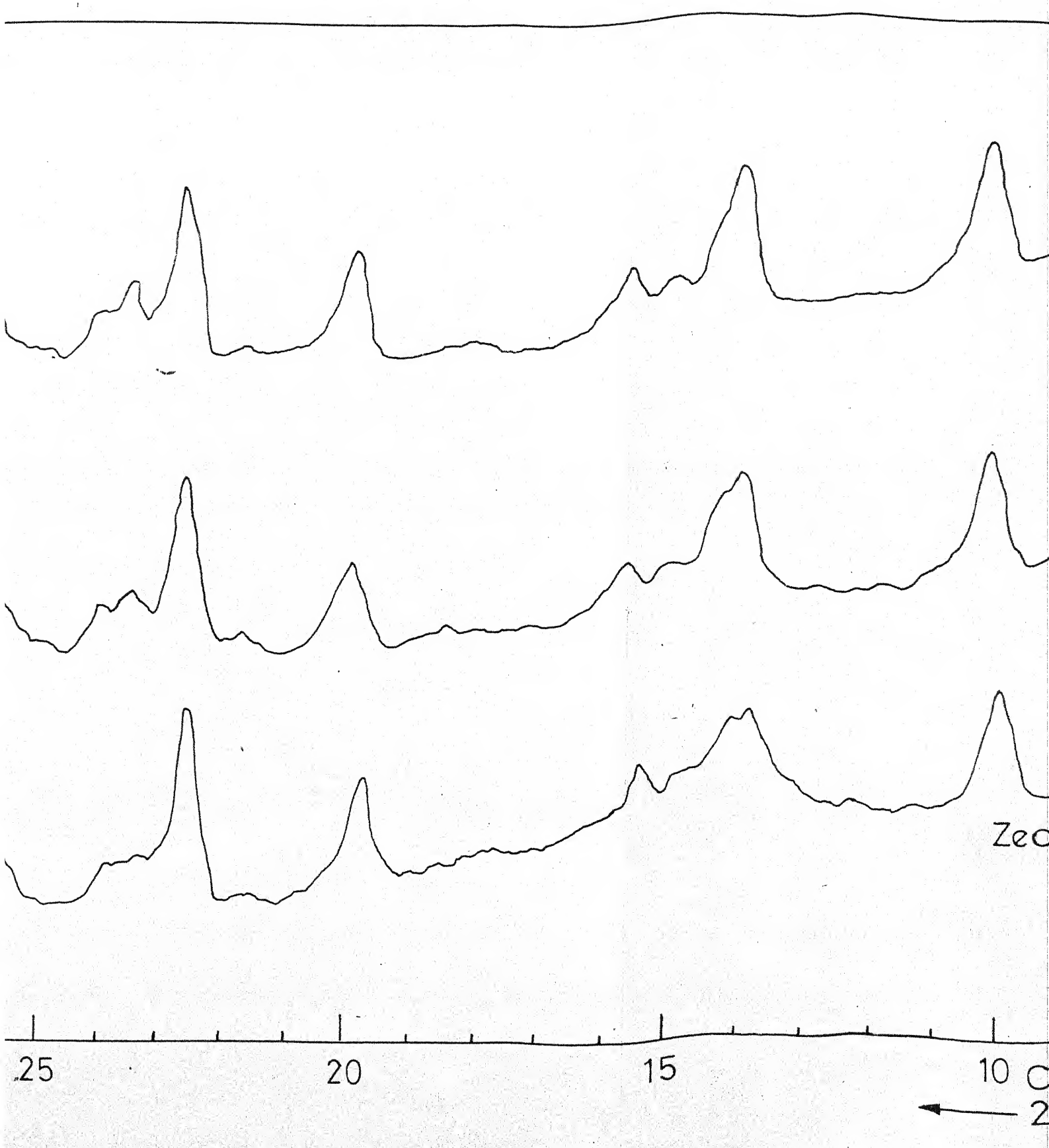

ction patterns for synthesized mordenites and standard zeolon.

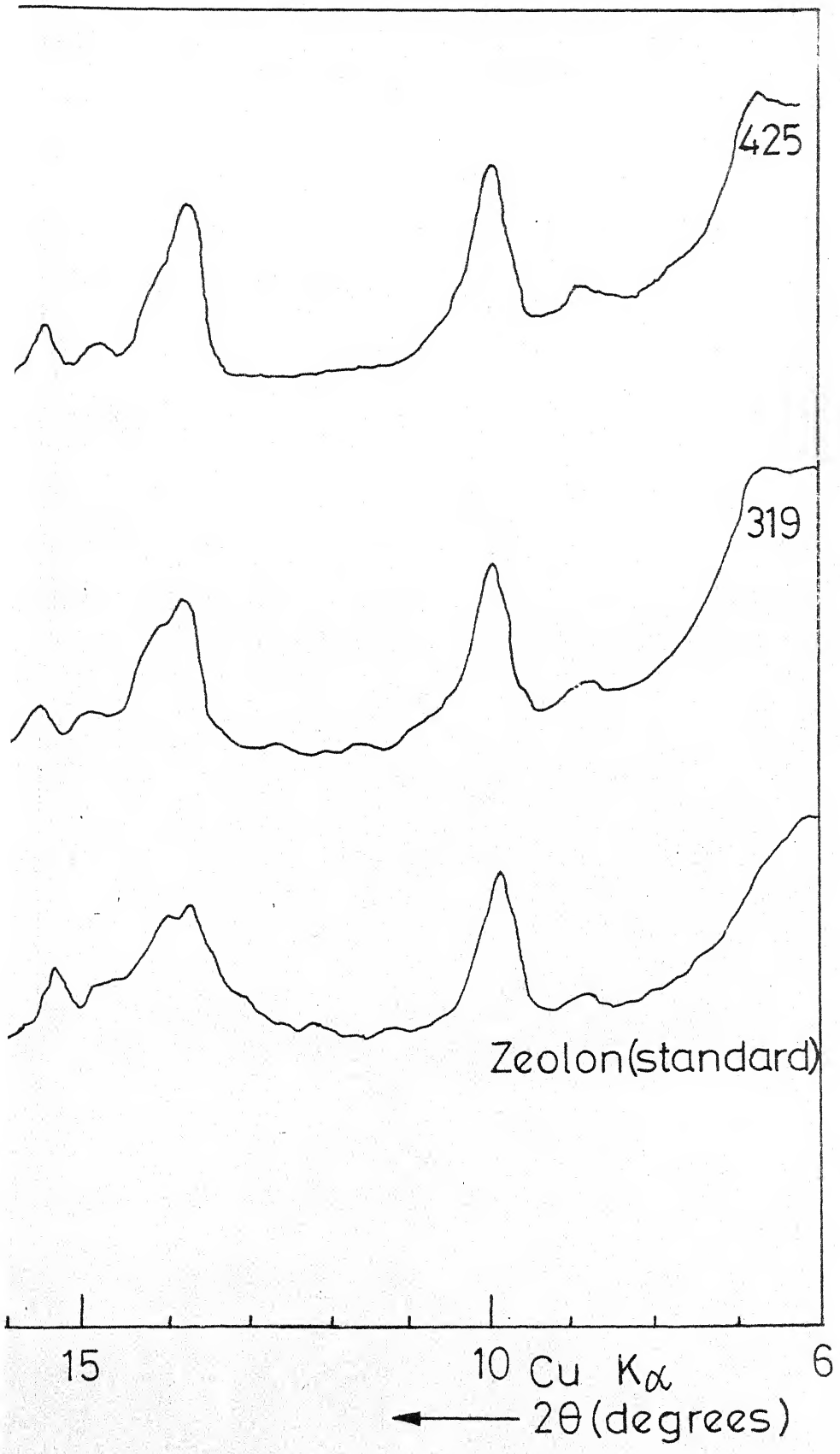

ordenites

TABLE 4.12: X-RAY POWDER DATA FOR AMMONIUM AND HYDROGEN MORDENITES SYNTHESIZED USING SILICA FROM CHEMICAL SOURCES

Ammonium Mordenite			Hydrogen Mordenite	
d(Å)	I/I_o	hkl	d(Å)	I/I_o
1	2	3	4	5
13.39	25	110	13.39	25
9.04	15	200	9.08	15
6.51	45	111	6.52	45
6.33	30	130	6.32	30
6.03	15	021	6.03	15
5.75	20	201	5.75	20
5.03	3	221	5.04	3
4.86	3	131	4.86	3
4.51	40	330	4.51	40
4.13	5	420	4.13	5
3.98	70	150	3.97	70
3.82	20	241	3.82	20
3.76	10	002	3.75	10
3.58	5	112	3.58	5
3.52	5	510	3.52	5
3.46	100	202	3.46	100
3.39	65	060	3.38	65
3.28	10	222	3.28	10

Table 4.12:(contd)

1	2	3	4	5
3.21	75	530	3.21	75
3.10	5	441	3.1[illegible]	5
2.93	5	531	2.93	5
2.89	35	402	2.89	35
2.73	3	152	2.74	3
2.69	10	621	2.69	10
2.63	3	370	2.64	3
2.54	10	461	2.54	10
2.51	20	442	2.51	20

TABLE 4.13: X-RAY POWDER DATA FOR AMMONIUM AND HYDROGEN MORDENITES SYNTHESIZED USING SILICA FROM RICE-HUSK ASH

Ammonium Mordenite			Hydrogen Mordenite	
d(Å)	I/I_o	hkl	d(Å)	I/I_o
13.39	25	110	13.39	25
9.04	15	200	9.08	15
6.51	45	111	6.52	45
6.33	30	130	6.32	30
6.03	15	021	6.03	15
5.75	20	201	5.75	20
5.03	3	221	5.04	3
4.86	3	131	4.86	3
4.51	40	330	4.51	40
4.15	5	420	4.14	5
3.98	70	150	3.97	70
3.82	20	241	3.82	20
3.76	10	002	3.75	10
3.58	5	112	3.59	5
3.52	5	510	3.51	5
3.46	100	202	3.46	100
3.39	65	060	3.38	65
3.28	10	222	3.27	10
3.21	75	530	3.21	75
3.09	5	441	3.11	5

Table 4.13 (contd)

Ammonium Mordenite			Hydrogen Mordenite	
d(Å)	I/I_o	hkl	d(Å)	I/I_o
2.94	5	531	2.94	5
2.89	35	402	2.89	35
2.69	10	621	2.69	10
2.63	3	370	2.63	3
2.54	10	461	2.54	10
2.51	20	442	2.51	20

TABLE 4.14: LATTICE PARAMETERS FOR MORDENITE SAMPLES

Sample	Source	a (Å)	b (Å)	c (Å)
Mordenites synthesized using silica from chemical source:				
Na-form	Present study	18.06	20.34	7.54
NH_4-form	,,	18.08	20.33	7.51
H-form	,,	18.18	20.26	7.50
Mordenites synthesized using silica from rice-husk ash:				
Na-form	Present study	18.06	20.34	7.53
NH_4-form	,,	18.07	20.33	7.51
H-form	,,	18.16	20.26	7.49
Zeolon (of Norton Make, U.S.A.)	Present study	18.12	20.24	7.52
Na-form	Ref.[69]	18.06	20.34	7.52
NH_4-form	Ref.[69]	18.09	20.33	7.51
H-form	Ref.[69]	18.14	20.26	7.51
Na-form	Ref.[12]	18.13	20.49	7.52

analcime [105] are presented in Tables 4.15 and 4.16.

4.2.2 Infra-red Absorption Spectra:

The infra-red patterns of synthesized mordenites along with their respective hydrogen forms and also zeolon have been presented in Figures 4.26 and 4.27 and the data are summarized in Table 4.17.

Spectra Related to Frame Work Structure:

The mid infra red region (1300-200 Cm^{-1}) of the spectra is informative in characterizing the framework structure of mordenite. The first group of frequencies of the strongest vibrations (Figure 4.26) 1250-950 Cm^{-1} and 500 - 420 Cm^{-1} can be assigned to internal tetrahedron vibrations. The strongest vibrations around 1250-950 Cm^{-1} is due to asymmetric stretching (T-O stretch) involving motion primarily associated with oxygen atom, or alternately described as an asymmetric stretching mode. $\leftarrow$ OT $\rightarrow$ $\leftarrow$ O. The strong band with in this region is observed to be at around 1050 Cm^{-1} in the present case. The position of this band has been related to the number of Al atoms in the framework structure. As the atom fraction of Al in the framework structure decreases, this band shifts to a higher frequency side. In the literature, its position has been reported to vary between 1060-970 Cm^{-1}[73]. Its occurrence around 1050 Cm^{-1} for the mordenites under study reflects the high silica and low aluminium in the framework

TABLE 4.15: X-RAY POWDER DATA FOR PHILLIPSITE

Phillipsite (Present Study)			Phillipsite (Ref.104)	
d(Å)	I/I_o	hkl	d(Å)	I/I_o
1	2	3	4	5
8.21	12	101	8.17	19
7.08	40	002	7.13	88
5.39	10	121	5.37	19
5.05	5	022	5.03	11
4.98	25	200	4.98	34
4.32	6	103	4.29	12
-	-	113	4.13	7
4.08	50	220	4.08	26
-	-	123	3.68	3
3.40	12	141	3.26	15
-	-	301	3.23	13
3.17	100	024, 133	3.18	100
3.08	8	311	3.15	16
2.92	10	321	2.94	30
-	-	240	2.89	5
2.73	8	105, 143	2.74	23
2.68	60	224	2.69	31
-	-	125	2.56	6
-	-	323	2.54	4
2.50	6	044	2.51	6
2.41	4	341	2.39	5

TABLE 4.16: X-RAY POWDER DATA FOR ANALCIME

Analcime (Present Study)			Analcime (Ref.105)	
d(Å)	I/I_o	hkl	d(Å)	I/I_o
1	2	3	4	5
-	-	200	6.87	<10
5.61	80	211	5.61	80
4.83	30	200	4.86	40
3.65	10	321	3.67	20
3.43	100	400	3.43	100
2.91	90	332	2.93	80
2.80	10	422	2.80	20
2.68	40	431	2.69	50
2.50	30	521	2.50	50
2.41	15	440	2.43	30
2.22	15	611,532	2.23	40
-	-	620	2.17	<10
-	-	541	2.12	<10
-	-	631	2.02	10
-	-	543	1.94	<10
1.90	25	640	1.90	50
1.86	15	633	1.87	40
-	-	642	1.83	< 10
1.74	35	732,651	1.74	60
1.71	10	800	1.72	30
1.68	15	741	1.69	40

Table 4.16 (continued)

1	2	3	4	5
1.66	10	820	1.67	10
1.62	5	822,660	1.62	20
1.59	15	831,743	1.60	30
1.49	5	842	1.50	20
1.48	8	761	1.48	20
-	-	664	1.46	10
1.45	5	754	1.48	10
1.41	15	932,763	1.42	40
-	-	941,853	1.39	<10
1.37	5	860	1.37	10
1.36	20	1011	1.36	40
1.30	5	1031	1.31	10
1.28	8	871	1.29	20
1.26	8	1033	1.26	20
1.22	15	963	1.22	30

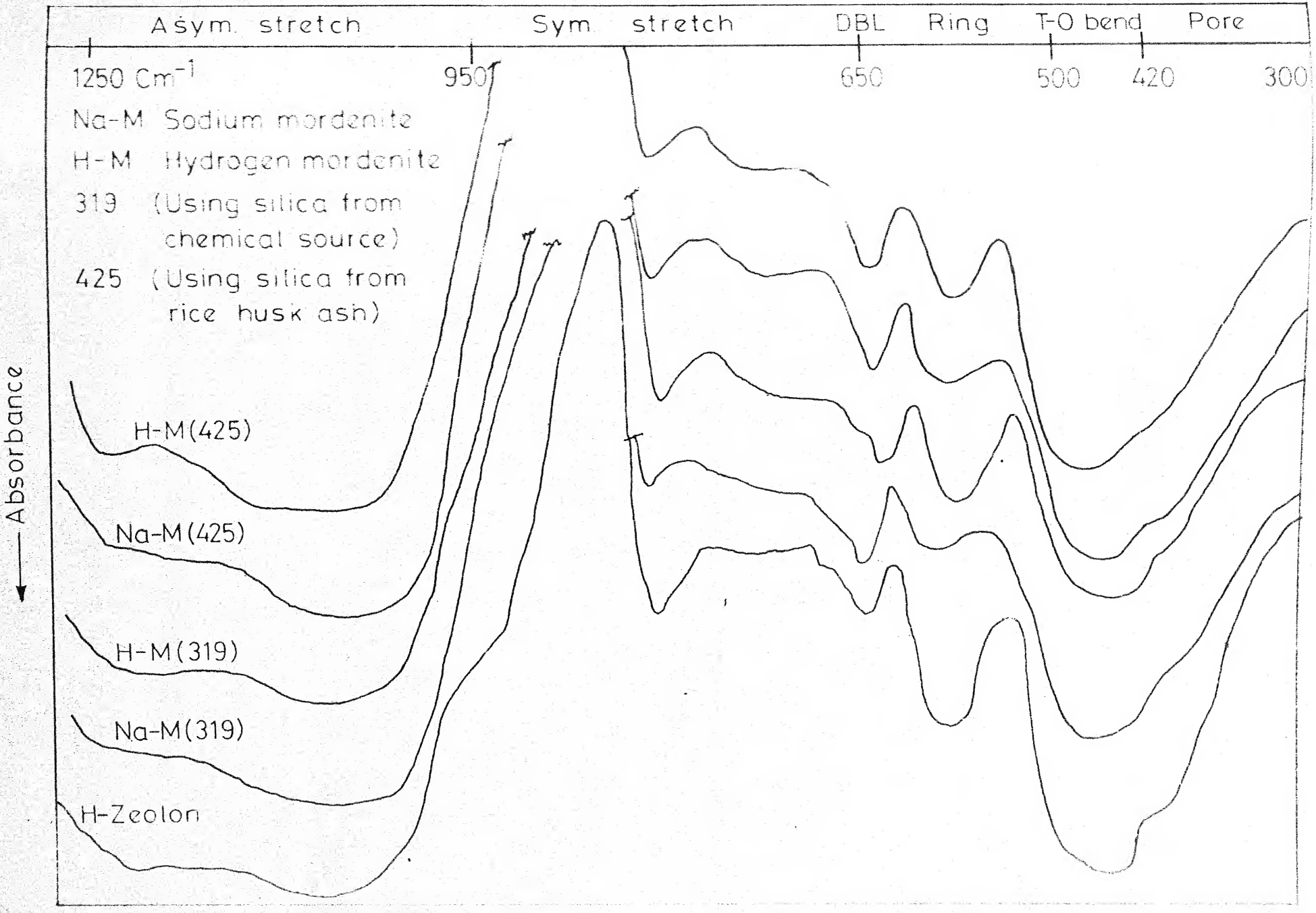

Fig 4.26 - Infrared spectra of synthesized mordenite samples (Range 1400 - 300 cm^{-1})

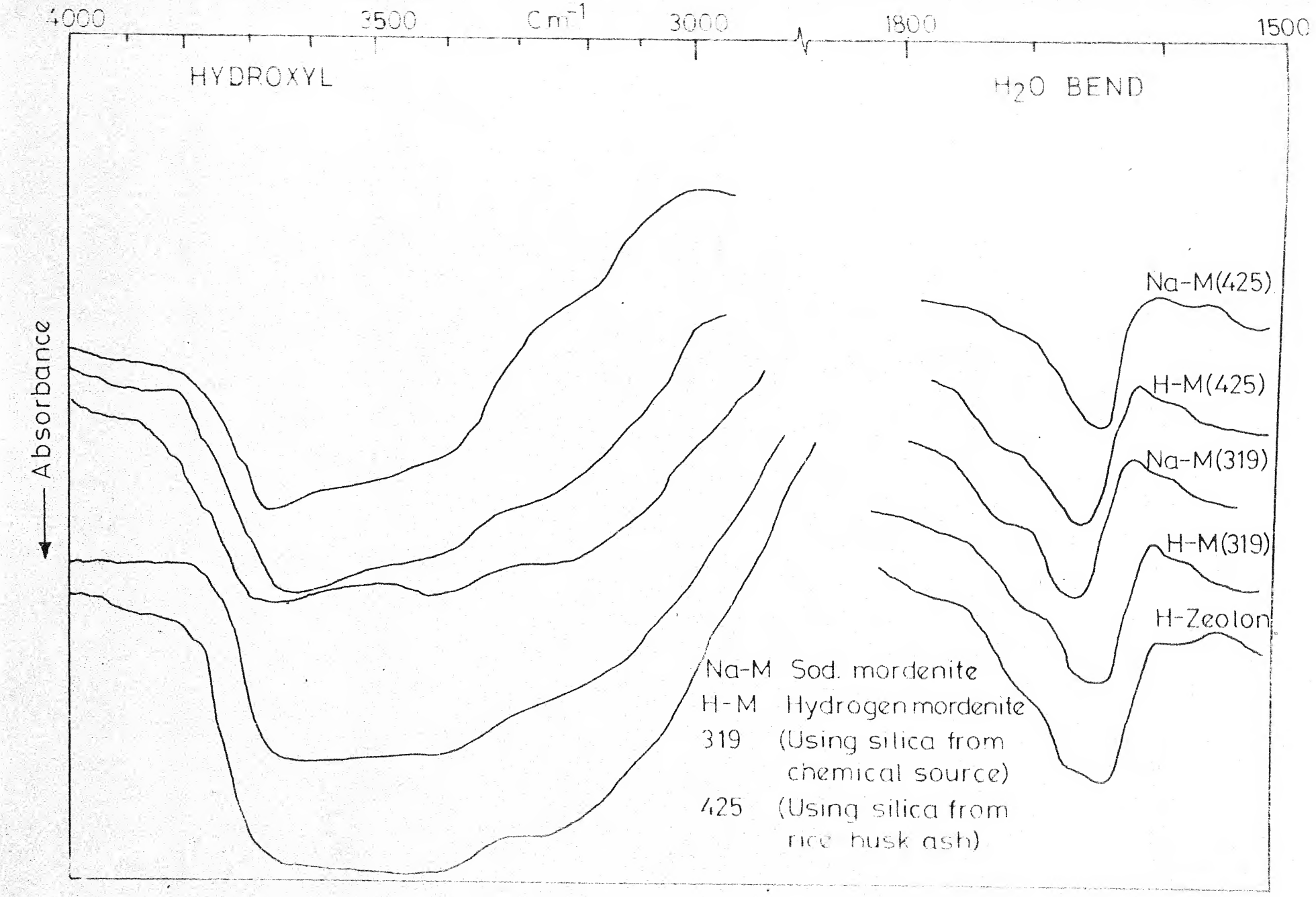

Fig 4.27 - Infrared spectra of synthesized mordenite (in region 4000-3000,1800-1500 C m⁻¹)

TABLE 4.17: INFRA RED SPECTRAL DATA FOR MORDENITE SAMPLES

Sample	Asym. Stretch		Sym. Stretch		Double Rings	T-O Bend	Pore Opening
Mordenite synthesized using silica from chemical source:							
Na-form	1210 w	1050 s	805	640	580	450 ms	390 vwsh
H-form	1220 w	1055 s	810	640	565	450 ms	390 vwsh
Mordenite synthesized using silica from Rice-Husk Ash:							
Na-form	1220 w	1060 s	810	640	580	450 ms	390 vwsh
H-form	1220 w	1060 s	810	645	580	455 ms	390 vwsh
H-Zeolon	1220 w	1060 s	810	640	580	450 ms	390 vwsh
Ref.[69]	1216 w	1080 vwsh 1046 s	795 772 wb	715 690 wb	621 w	571 555 w	448 ms 370vwsh

w= weak; s = strong; b=broad; sh=shoulder

structure. The next strongest band in the region 500-420 Cm^{-1} is assigned to T-O bending mode. Stretching modes involving mainly the tetrahedra atoms are found in the region 820-650 Cm^{-1}.

The second group of frequencies occur in the regions 650 - 500 Cm^{-1} and 420 - 300 Cm^{-1}, these are sensitive to the linkages between tetrahedra and the topology and mode of arrangement of the secondary units of structure in the mordenites. The band in the 650 -500 Cm^{-1} region is related to the presence of double rings (D4R and D6R) in zeolites [73]. The weak absorption in this region of spectrum for the mordenites in the present study reflects that these species do not contain the double rings or larger polyhedral units. The band in the frequency region 420 - 300 Cm^{-1} is assigned to external linkages. This is related to pore opening or motion of the tetrahedra rings which form the pore openings in zeolites [73]. The nature of presence of this band in any spectrum of a zeolite depends upon its structure. For example, in zeolite with cubic structure, this is very prominent and it is less distinct with a decrease in symmetry. In the present case, a feeble indication interms of a shoulder is visible for this band for the mordenites (synthesized in the present study) which are orthorhombic. Flanigen and coworkers [73] also reported a very weak band for zeolon.

Spectra of Water Adsorbed in Mordenite:

The spectra in the regions 1800-1500 Cm^{-1} and 4000 -

3000 Cm^{-1} are indicated in Figure 4.27. The band around 1645 Cm^{-1} noticed in all the samples can be assigned to the bending mode in water molecule. The broad band in the region 3400 Cm^{-1} is characteristic of hydrogen bonded OH and a sharp band around 3700 Cm^{-1} is typical of isolated OH. The isolated OH stretching is relegated to interaction of water hydroxyl with the cation. The other bands are attributed to hydrogen bonding of the water molecule to the surface oxygen and to the bending mode of the water [74].

4.2.3 Thermal Characteristics:

The differential thermal and thermogravimetric analyses were conducted for the mordenites synthesized and also their ammonium - and hydrogen forms. Although the DTA and TGA curves for synthetic mordenite are available in published reports, DTGA curves are not reported earlier.

The DTA, TGA and DTGA pattern for the mordenites synthesized using silica from chemical sources are indicated in Figure 4.28. The broad shallow endotherm starting from around 60°C with a peak maximum around 120°C is characteristic of the dehydration. Around 580°C another broad endotherm commences which was seen to continue even at 980°C. This endotherm has its maximum around 750°C and possibly due to dehydroxylation. The corresponding TGA curves show a total weight loss of 13.6 per cent upto 1000°C out of which 11.0 per cent is for the initial dehydration event. At the commencement

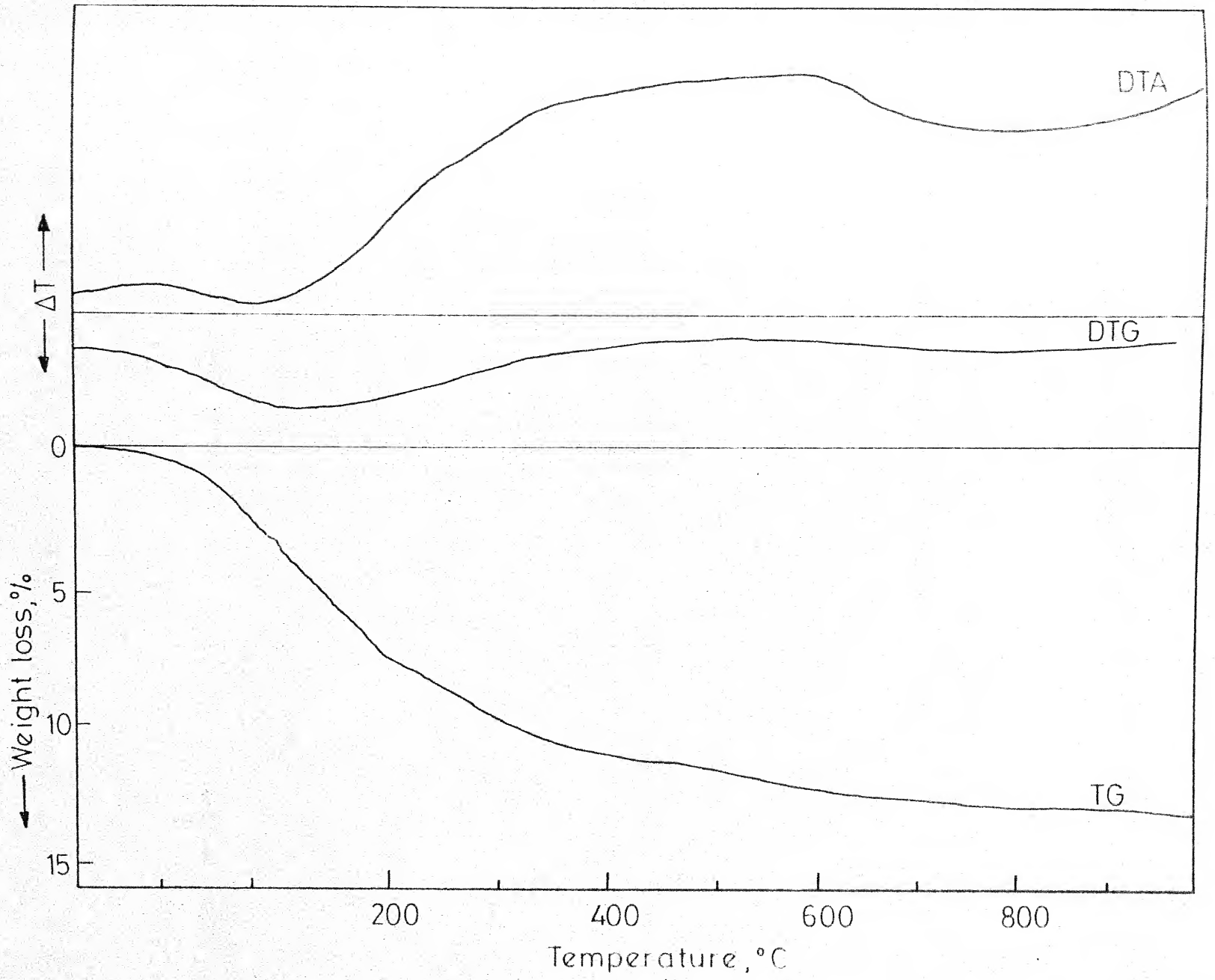

Fig 4.28 - Thermograms for Na mordenite synthesized from silica from chemical sources

of the dehydroxylation around 580°C there is a change in the slope of the TGA curve. The DTA curve for mordenite (Figure 4.29) synthesized using silica from rice-husk ash indicated the commencement of the dehydration around 60°C as indicated by an endotherm with its peak around 140°C. The peak for the dehydroxylation endotherm is around 810°C in this case. The weight loss in this case for total temperature range upto 1000°C as also for the dehydration range are similar to that of the mordenite obtained using silica from chemical sources.

The weight loss of 13.6 per cent corresponds to around 26.7 H_2O if the general formula for the mordenite is written in the following form:

$$Na_8 \cdot (AlO_2)_8 \cdot (SiO_2)_{40} \cdot 26.7\ H_2O$$

In the literature the total water in mordenite is reported as 26.8 H_2O. This is a generalized formula and the total 26.7 H_2O accounts for not only the zeolitic water but also the water of hydration of proton and the hydroxyl water.

The typical patterns for the hydrogen form of the mordenite synthesized from rice-husk ash silica source, are indicated in Figure 4.30. The peak temperature for the endotherm representing the dehydration event occurs around 120°C. The endothermic peak for the dehydroxylation has a maximum around 740°C. The weight loss for this form upto

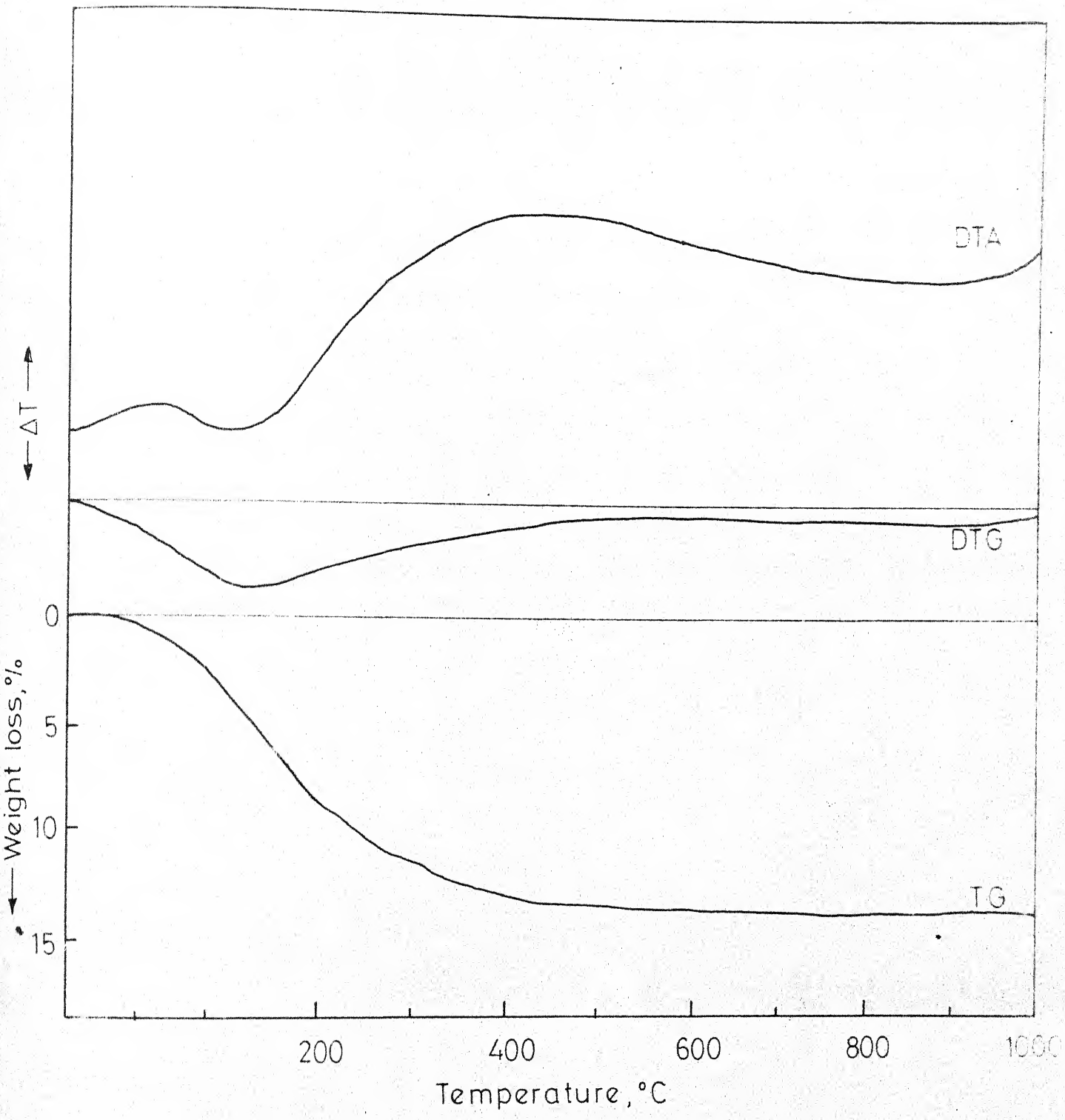

Fig. 4.29- Thermograms for Na mordenite synthesized from rice husk ash.

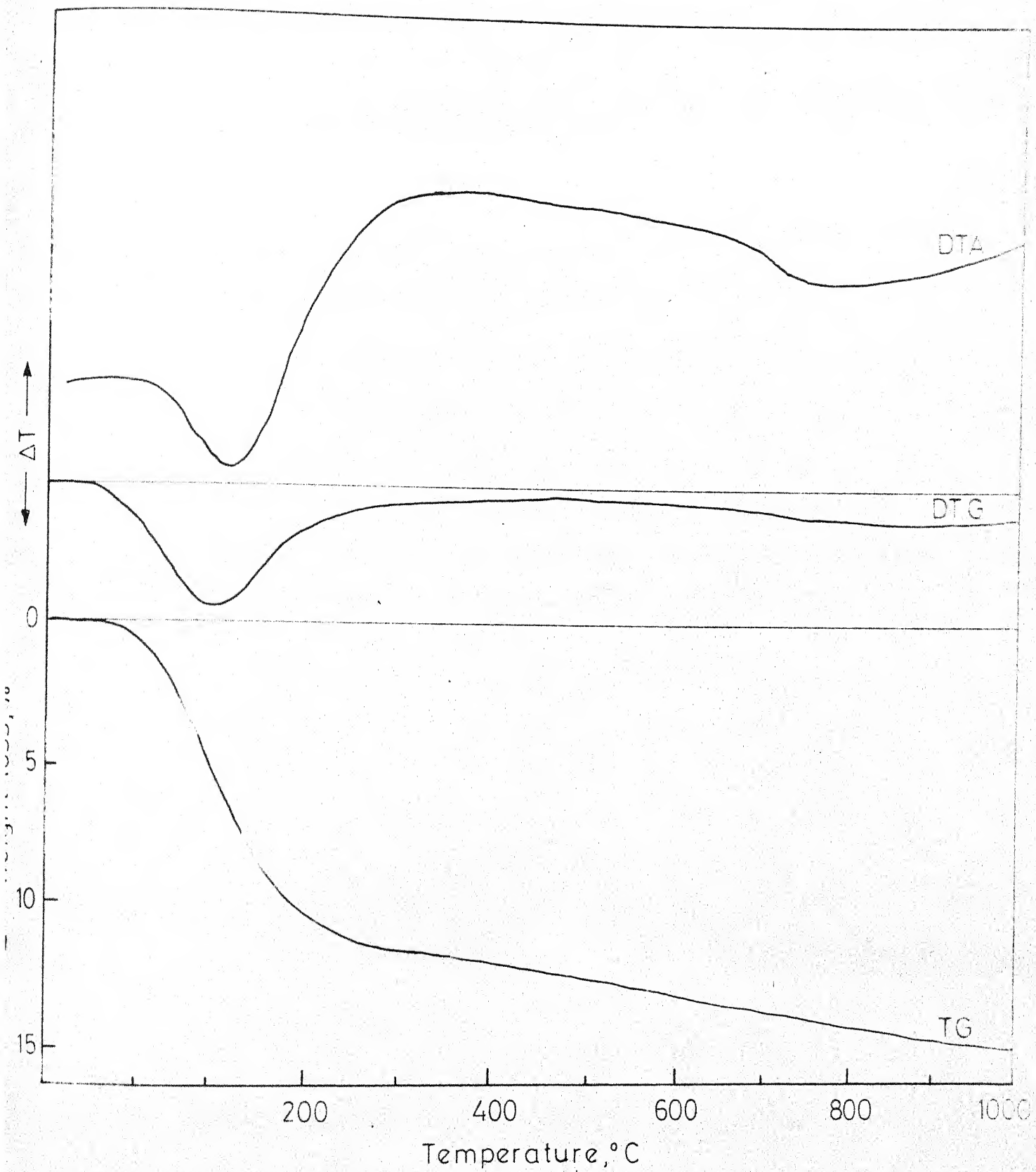

Fig. 4.30 - Thermograms for H-mordenite synthesized from silica from rice husk ash.

1000°C is around 14.8 per cent. This amount is higher than compared to its sodium form (with 13.6 per cent weight loss). It may be noted that the total weight loss for hydrogen mordenite was reported to be 15.1 per cent by Barrer and Peterson [79], although these authors have also indicated that the theoretical value as calculated from the ideal formula should be around 14 per cent for the same. For the hydrogen form of zeolon, used in the present investigations as the reference material, the thermogravimetric run (Figure 4.31) indicated the total weight loss to be around 15.1 per cent. The DTA pattern for the same contains an endothermic peak with its maximum around 730°C.

The typical DTA pattern, as obtained on Du Pont 900 DTA unit, for the ammonium mordenite form is presented in Figure 4.32. An initial endotherm with peak around 94°C is followed by minor endotherms at 390°C preceding an exotherm having its peak around 532°C. While the initial major endotherm represents the water desorption, the shallow endotherm indicates that some ammonia desorbs prior to oxidation. The exothermic peak is due to ammonia oxidation. Following this peak the broad shallow, endotherm with its peak around 680°C is for the dehydroxylation. The exothermic hump around 1062°C corresponds to the dissociation of zeolite.

A typical pattern of analcime from the present investigations is indicated in Figure 4.33. This pattern is

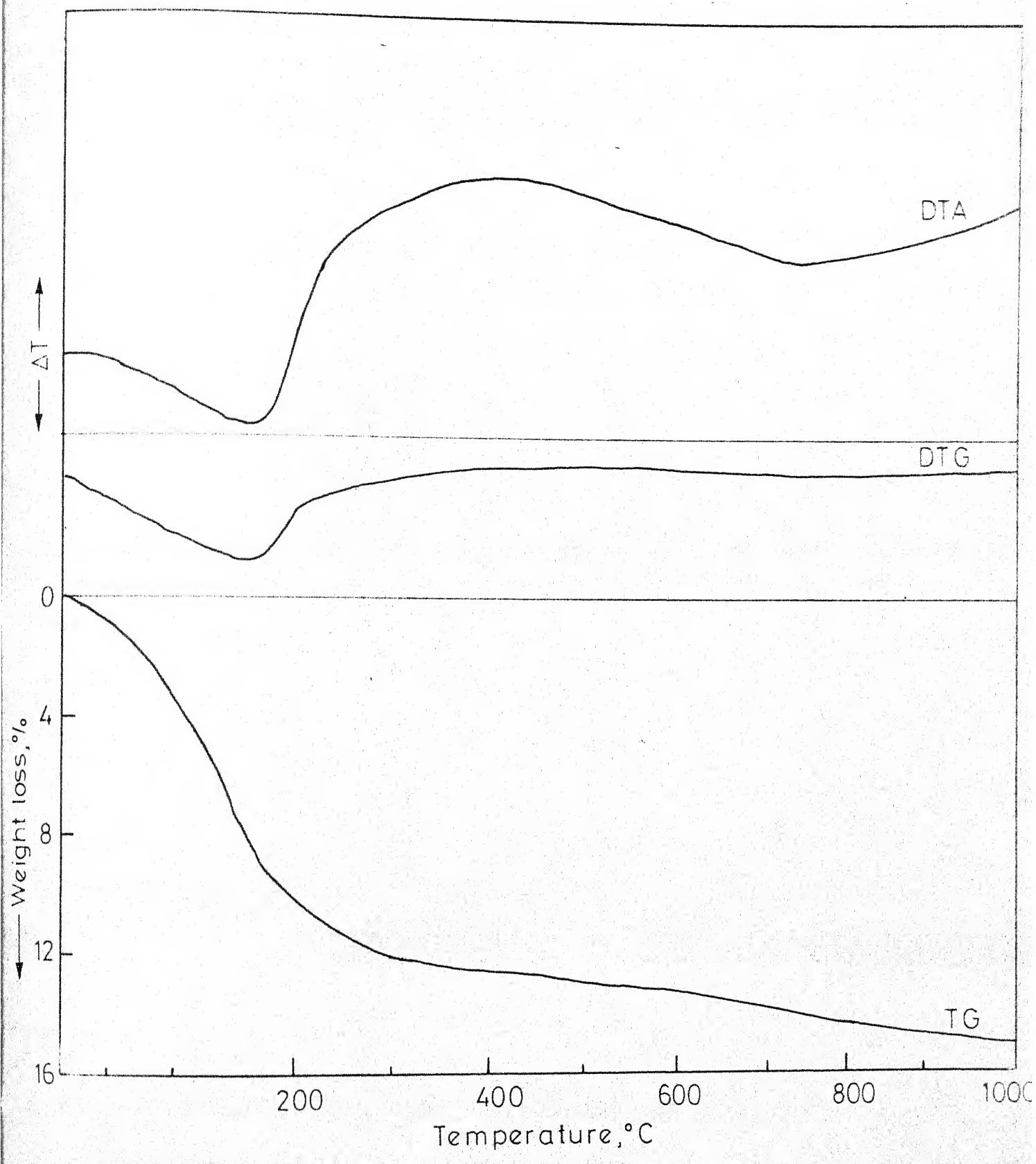

Fig. 4.31 - Thermograms for H - Zeolon (standard).

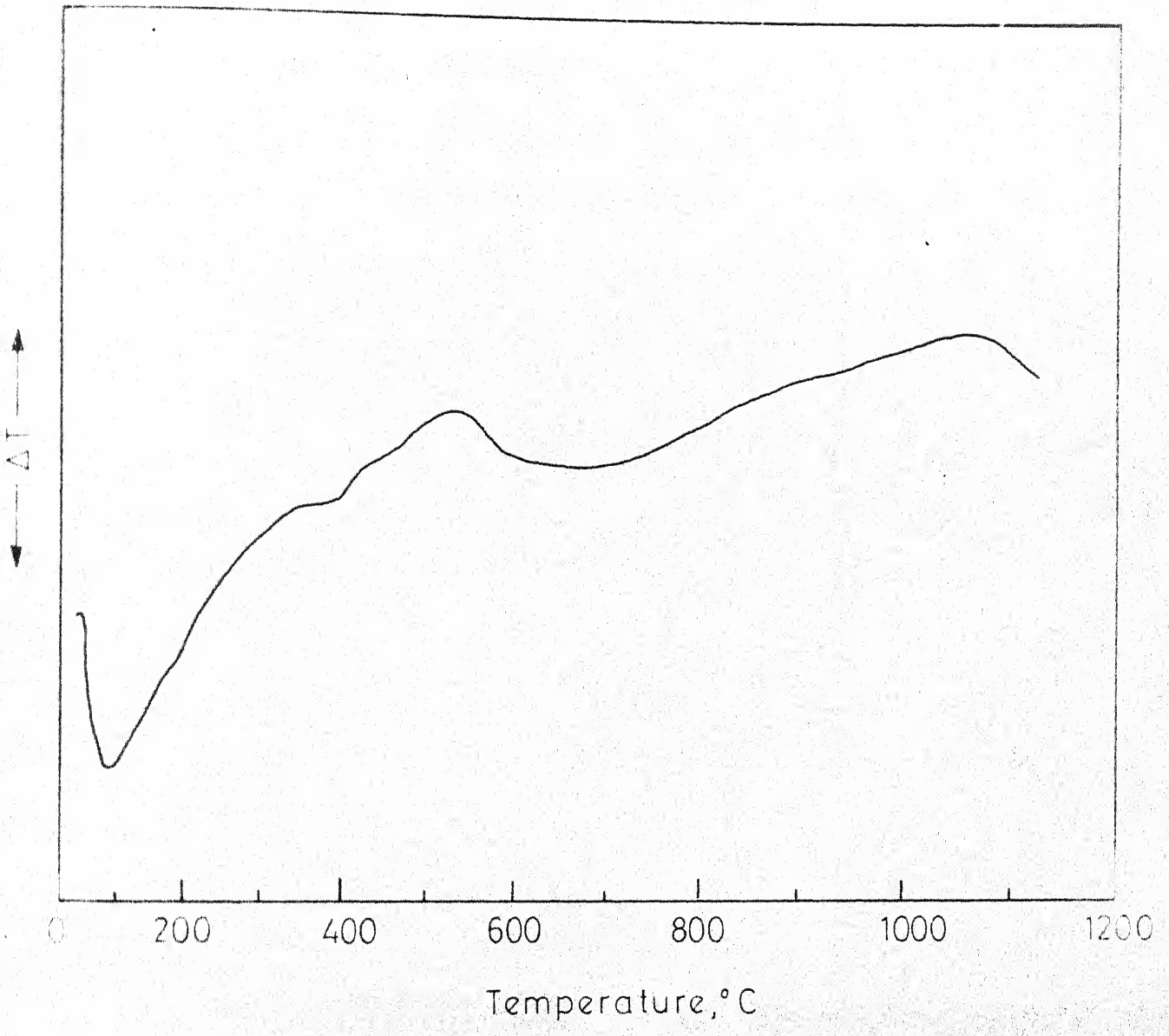

Fig. 4.32 - DTA pattern for NH_4 mordenite.

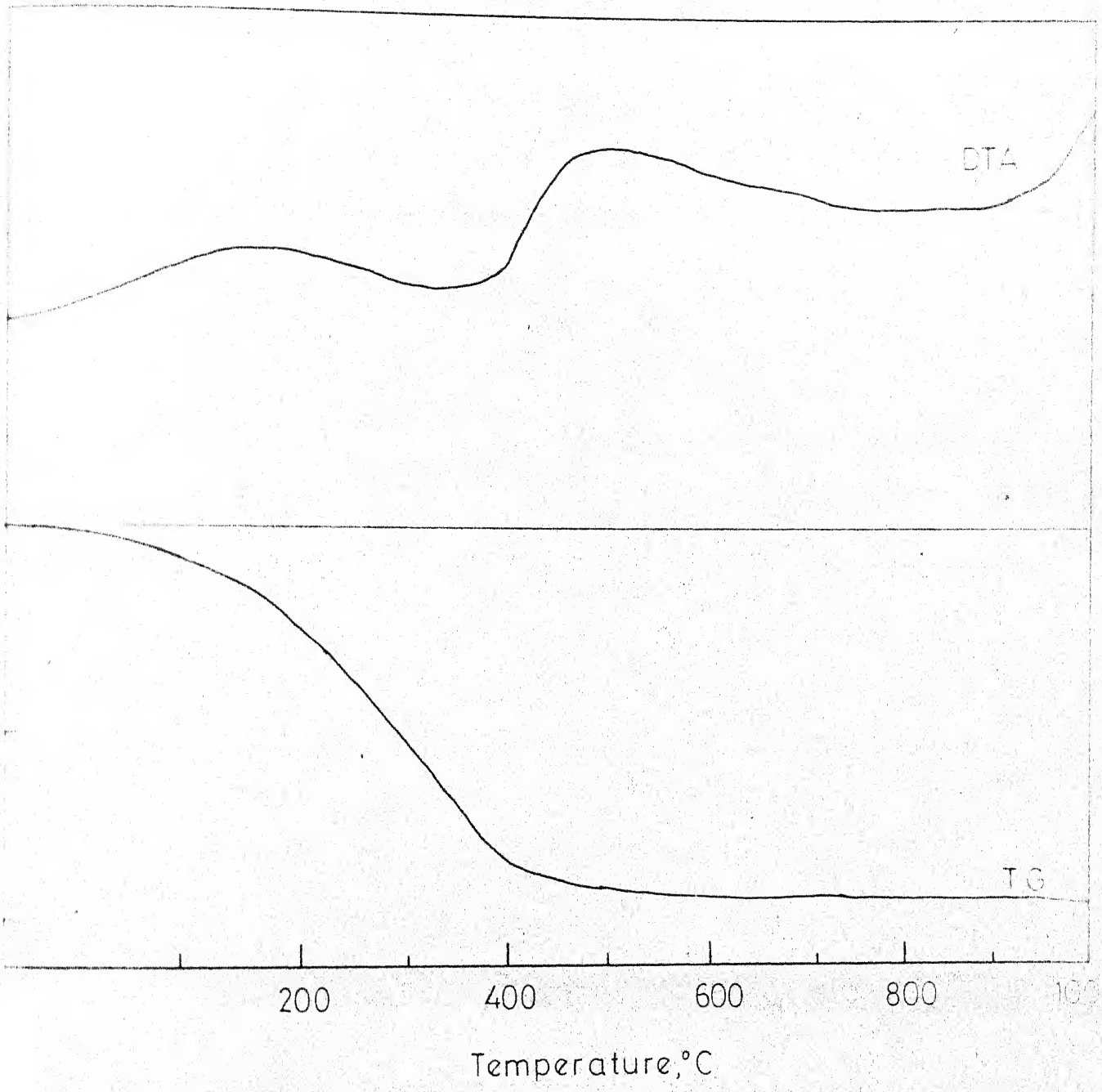

Fig. 4·33 - Thermograms for synthesized analcime

characterized by a strong conspicuous endotherm with peak around 350°C accounting for a weight loss of 9 per cent. The total weight loss observed in the TGA run upto 1000°C is 9.6 per cent (Figure 4.33). The dehydroxylation event is characterized by a broad endotherm with its peak around 740°C.

The DTA pattern for phillipsite (Figure 4.34) from the present investigations indicates a very shallow minor endothermic event around 100°C accompanied by a sharp strong endothermic event with its peak around 180°C and another small endotherm with a peak around 380°C. The sharp endothermic peak has been attributed to the formation of Wairakite [87] and the accompanying shallow endotherm being relegated to the formation of anorthite and quartz from Wairakite. The thermogravimetric run (Figure 4.34) registered a total weight loss of 17.7 per cent. The weight loss upto the end of the sharp endothermic event (340°C) is around 16.1 per cent. This tallies with the weight loss values reported in the literature [87].

4.2.4 Chemical Analysis:

The chemical compositions of the synthesized mordenites in sodium-, ammonium- and hydrogen forms are indicated in Table 4.18. For comparison the respective constituents of zeolon are also included.

The calculated composition for the sodium mordenite synthesized in the present study on the basis of its chemical constituents can be expressed as:

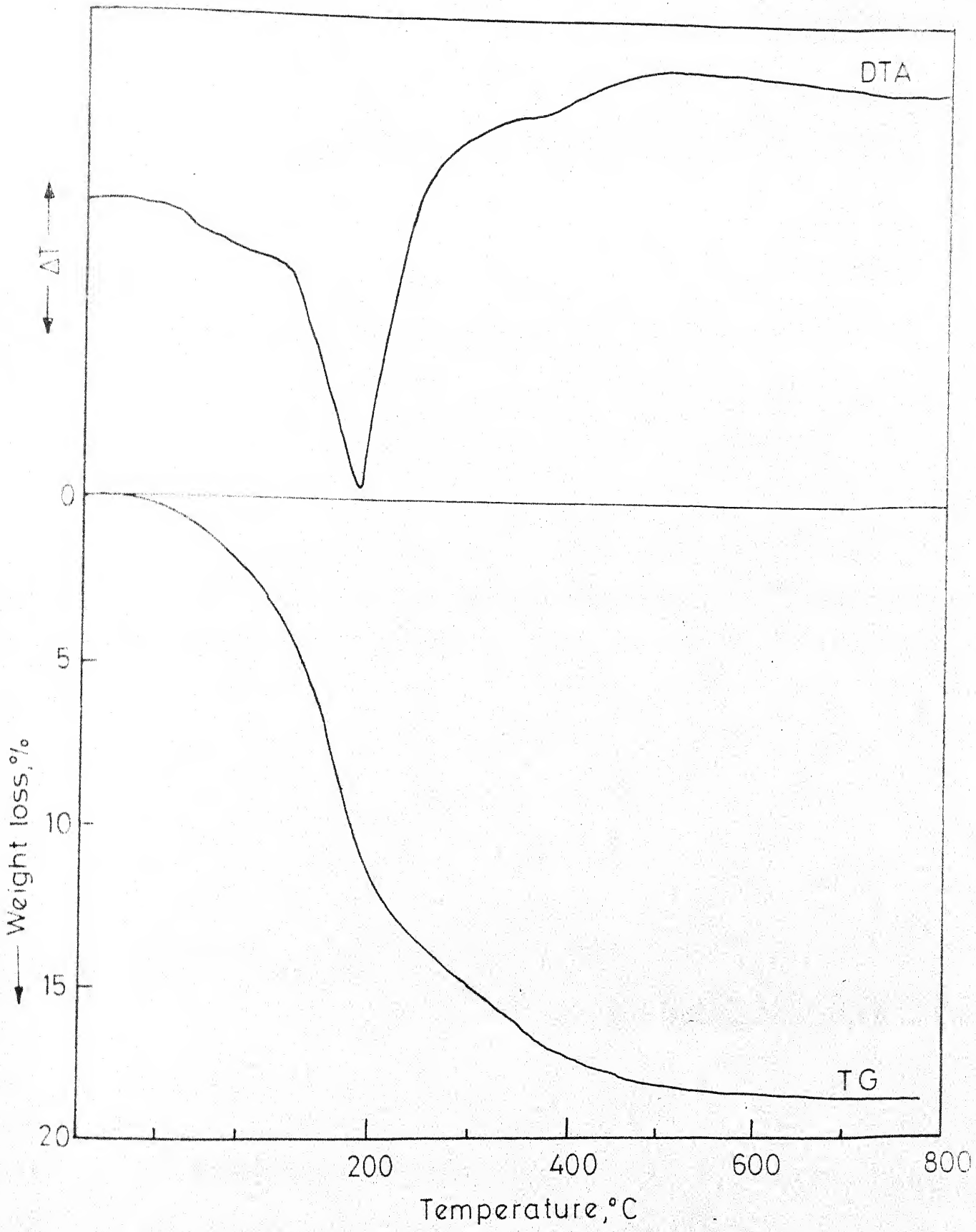

Fig. 4.34 - Thermograms for synthesized phillipsite.

TABLE 4.18: CHEMICAL COMPOSITION OF VARIOUS MORDENITE SAMPLES

Sample	Cation	Loss on ignition (wt per cent)	Composition (Anhydrous, weight per cent)			
			SiO_2	Al_2O_3	Na_2O	Impurities
Mordenites synthesized using silica from chemical sources						
319	Na^+	9.5	79.3	12.5	7.5	0.7
	NH_4^+	14.6	79.8	12.7	0.4	0.5
	H^+	10.1	87.0	12.0	0.4	0.6
Mordenites synthesized using silica from Rice-Husk Ash:						
425	Na^+	9.6	79.2	12.4	7.4	1.0
	NH_4^+	14.2	79.7	12.7	0.3	0.8
	H^+	10.0	86.7	12.1	0.4	0.8
Zeolon	H^+	10.4	87.1	12.1	0.4	0.4
Ref.[106]	Na^+	-	79.7	11.9	7.0	1.4
Ref.[69]	NH_4^+	-	79.2	12.7	< 0.1	-
	H^+	-	87.6	12.3	0.38	-

$$Na_2O \cdot Al_2O_3 \cdot 10.8\ SiO_2$$

While the sodium mordenite reported in the literature [12] has 10 SiO_2, in the present case, the silica contents appear to be a little higher than reported.

4.2.5 Ion-Exchange Characteristics:

The preparation of hydrogen form of mordenite used in the present study involves exchange of the cations in the sodium form by ammonium and subsequent heating of the ammonium exchanged mordenite at 500°C. to liberate NH_3 resulting in the hydrogen form. As stated earlier, the exchange process was repeated several times with fresh exchanging solutions to enable complete exchange to take place.

The degree of exchange was determined from the concentration of sodium ions in the equilibrating solutions using flame photometer. Although the equilibrating solutions contained sodium and ammonium ions, the varying concentrations of ammonium ions in the solutions did not effect the sodium determination as checked with several known solutions containing sodium and ammonium ions of varying concentration. The coordinates of Na^+-NH_4^+ exchange isotherm were determined adopting the method suggested by Sherry [84]. The values for the coordinates of isotherm and the corresponding degree of exchange are detailed in Table 4.19.

From the results in the Table, it is evident that the contribution of the first step towards the extent of exchange was substantial while that of the subsequent exchanges kept diminishing. This reflects that the substitution of sodium ions becomes increasingly difficult as the concentration of the residual ions in the mordenite lattice gets diminished. This is in agreement with the earlier reports [4, 77, 83, 84, 107, 108]. Further, the values of coordinates of $Na^+ - NH_4^+$ exchange isotherm indicate a higher selectivity of NH_4^+ ions in the solution phase which is due to the use of concentrated solutions in ion exchange.

In the present investigations, the exchange was achieved upto 96.8 per cent. In the literature a complete exchange of NH_4^+ for Na^+ was reported [69].

4.2.6 Surface Properties:

The nitrogen adsorption isotherms at its boiling point as obtained for the synthesized sodium mordenite and their hydrogen forms together with the hydrogen form of zeolon are presented in Figure 4.35. These isotherms have the typical shape characteristic for zeolite molecular sieve reported in the literature [4]. The nitrogen adsorption data are detailed in Table 4.20.

The surface area values as calculated by the BET method from these adsorption isotherms are indicated in Table 4.21.

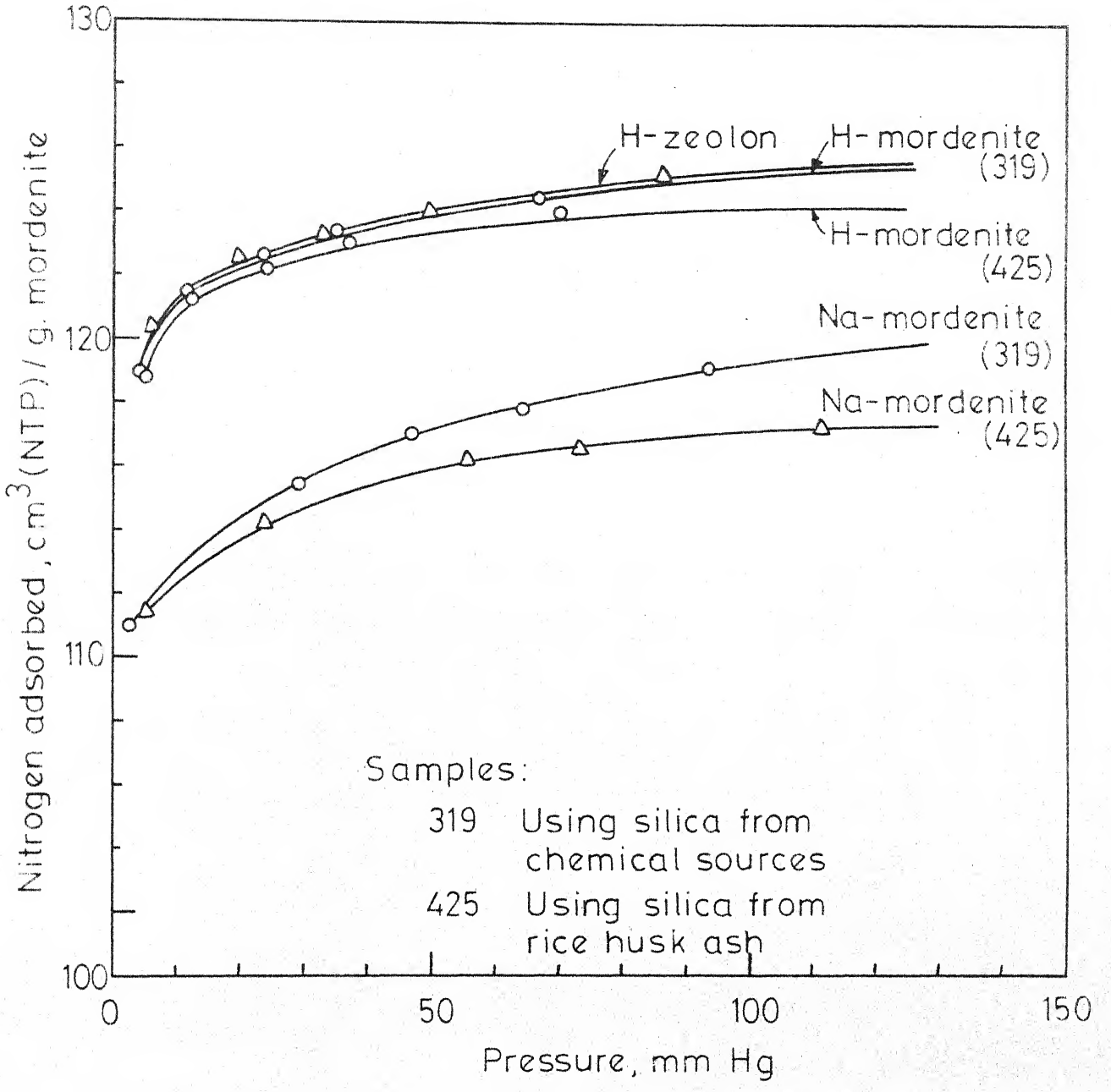

Fig. 4.35 - Nitrogen adsorption isotherms at its boiling point.

TABLE 4.20 NITROGEN ADSORPTION DATA (AT THE BOILING POINT OF NITROGEN)

Pressure (mm Hg) 1	Volume adsorbed, Cm^3(NTP)/g 2
Sample No.319	
Na-form	
2.55	111.46
29.18	115.71
47.29	117.11
64.13	117.82
93.12	119.19
190.00	121.00
H-form	
3.62	119.15
11.36	121.49
23.50	122.81
34.86	123.39
200.00	126.00
Sample No.425	
Na-form	
5.12	114.00
22.20	114.80
54.83	116.20
72.30	116.50
110.20	117.20
306.20	118.50

Table 4.20 (contd)

1	2
H-form	
4.93	118.80
11.39	121.20
23.49	122.20
37.12	123.10
69.84	124.10
272.30	124,90
H-Zeolon	
6.10	120.40
19.80	121.62
33.23	122.21
49.79	124.00
86.20	125.20
140.00	125.80

TABLE 4.21: SURFACE AREA OF VARIOUS MORDENITE SAMPLES

Sample	Cation	Surface area (m^2/g)
Mordenites using silica from chemical sources:		
319	Na^+	459
319	H^+	500
Mordenites using silica from Rice-Husk Ash:		
425	Na^+	452
425	H^+	498
Zeolon	H^+	510

The surface area values for the mordenites synthesized in the present work correspond closely to the reported values.

The water adsorption capacity values for the sodium and hydrogen forms of the synthesized mordenite were found to be 15.2 and 16 g.water/g. of zeolite respectively; for standard zeolon the same was estimated to be 16.1 g. water/g. of zeolite. These values are in accordance with the reported values [93].

The acidity measurements for the different samples of mordenite were measured with time and these results are extrapolated to zero time to eliminate the influence of

reaction between mordenite and water. These results are summarized in Table 4.22.

TABLE 4.22: ACIDITY MEASUREMENTS OF MORDENITE SAMPLES

Sample	Cation	Acidity (m.mol/g
Mordenites from chemical silica sources:		
319	Na^+	0.20
319	H^+	0.90
Mordenite from Rice-Husk Ash:		
425	Na^+	0.20
425	H^+	0.88
Zeolon	H^+	1.00

Although this method for the acidity measurement has an inherent drawback in that it can not be employed for estimation of acid sites whose strength is less than that of water, it has been adopted in the present work since it is convenient for getting an idea of Bronsted surface acidity responsible for the catalytic activity of the mordenite.

4.2.7 Molecular Sieve Behaviour and Pore Size Determination:

The sodium and hydrogen forms of the mordenite synthesized using silica from chemical sources and also from rice-husk ash have been characterized for use as molecular sieve

For this purpose mixtures of organic compounds (O-xylene and p-xylene, toluene and O-xylene, toluene and p-xylene and o-xylene and triethylbenzene) are passed through the dehydrated mordenite bed. From the adsorption or the exclusion of the individual molecules of varying sizes, the pore size for the mordenite species could be established.

The sodium mordenite could adsorb the toluene and p-xylene (molecular diameter 6.7Å) but excluded o-xylene (molecular diameter 7.4 Å). The hydrogen mordenite could adsorb o-xylene also but excluded triethylbenzene (molecular diameter 8.4 Å). Hence it is inferred that the sodium and hydrogen mordenites have the approximate pore diameters of 7 Å and 8Å respectively, and these large port variety of mordenites can be used as molecular sieves. These pore diameter values obtained are in agreement with the earlier reported values [41].

CHAPTER 5

SUMMARY AND CONCLUSIONS

5.1 Summary:

The mordenite has been synthesized with the selected concentration ratios of the constituents, in the system Na_2O-SiO_2-Al_2O_3-H_2O for which crystallization of the species is possible. Two different approaches for the synthesis have been adopted. In one, the silica from chemical sources in the form of sodium silicate and silica gel was used, in the other, silica solution obtained from rice-husk ash with sodium hydroxide leaching has been utilized. The compositional fields for the crystallization and stability of mordenite for various temperatures and periods of time of synthesis have been established.

The best temperature range for the synthesis of mordenite for the composition of the initial mixtures chosen has been observed to be 135 - 175°C. The compositions of the starting mixtures play an important role in the synthesis. When silica from chemical sources was used, mordenite started appearing at 135°C after 24 hour of reaction, its quantity increasing with time and temperature. As the temperature of synthesis increases, a shift in the crystallization field for mordenite towards higher SiO_2 and lesser Na_2O in the starting mixture

was evident. This is due to the increase in solubilities of aluminate and silicate ions at higher temperatures resulting in the modification of the concentration of the liquid phase in the gel. Thus mordenite can be synthesized from the initial mixtures of relatively lesser alkalinity at higher temperatures within the range of its stability. However, beyond 175°C mordenite rapidly disappears with the crystallization of analcime, a relatively stable species.

The aluminosilicate gels prepared using silica derived from rice-husk ash, appear to possess a greater reactivity compared to those prepared with the solutions of aluminate and silicate. This is due to the solubilization of silicate anions and their interaction with aluminate ions that make the concentrations and correlations of the components different in the liquid phase of the gel of the former type. In such cases, mordenite could be synthesized faster in the range 135 - 165°C from starting mixtures containing lesser Na_2O and greater SiO_2 at any temperature compared to the corresponding gel compositions involving silica from chemical sources. Further, analcime starts appearing early in these reactions and a complete disappearance of mordenite with the total formation of analcime at 165°C was noticed. An increase in the alkalinity of the initial gel resulted in the crystallization of analcime even at 135°C. In such cases, crystallization of phillipsite preceded that of analcime.

The rate curves for crystallization of mordenite are of sigmoidal shape with a long induction period accompanied by a rapid crystallization which attains an ultimate asymptotic value. As the crystallization starts, the fast conversion rate of amorphous batch into mordenite indicates the possibility of the rate limiting step in the overall process to be the nucleation. The activation energies for the crystallization of mordenite in the present case are estimated as 10.2 Kcal/g. mol for nucleation and 7.56 Kcal/g. mol for crystal growth from the gels containing silica from chemical sources while the corresponding values in the case of gels containing silica solutions from rice-husk ash are around 9.5 and 6.85 Kcal/g mol respectively. The value reported for mordenite crystallization from gels with silica from chemical sources is around 10 Kcal/g mol (the mechanism not specified).

The synthesized mordenites possess orthorhombic symmetry with the lattice dimensions, 'a = 18.06, b = 20.34 and c = 7.54 Å' with an assigned chemical composition of $Na_2O \cdot Al_2O_3 \cdot 10.8\ SiO_2$ on the basis of chemical analyses. From the sodium form of the mordenite synthesized, the corresponding hydrogen form was prepared through ammonium ion-exchange process. The dehydration and dehydroxylation characteristics with the weight loss patterns have been presented for the sodium and hydrogen forms of the mordenite pertaining to both the types of gels used. The sodium form has a total

weight loss of 13.6 per cent corresponding to a total of 26.7 H_2O per unit cell which accounts for the zeolitic water, water of hydration of protons and the hydroxyl water. The hydrogen form has relatively higher weight loss (around 14.8 per cent). These values correspond closely to the reported ones. The infrared spectra for the sodium and hydrogen species as related to the framework structure and the water association are presented. Within the frequency range 1050-960 Cm^{-1} common for zeolites, the occurrence of the band on the high frequency side at 1050 Cm^{-1} in the present case indicates the high silica and low aluminium in the frame work structure for the mordenite. The band in the frequency region 420 - 300 Cm^{-1} (prominent for zeolites with cubic structure) is very feeble in the present case, pointing to a decrease in the symmetry (orthorhombic).

The surface area values estimated to be around 450 m^2/g for the sodium form and 500 m^2/g for the hydrogen form are inaccordance with the reported values. The present studies indicated that exchange upto 96.8 per cent with ammonium could be achieved. The water adsorption capacity values are found to be 15.2 g.H_2O/g mordenite for the sodium form and 16.0 g·H_2O/g mordenite for the hydrogen form. The acidity measurements for these species have also been reported.

The mordenite synthesized in the present case is of large port variety. The pore diameters are found to be

7 and 8 Å for the sodium and hydrogen forms respectively. The investigations with various hydrocarbon mixtures of different molecular diameters have established that these mordenites in their sodium and hydrogen forms can be successfully used as molecular sieves.

5.2 Conclusions:

Thus in the present study, a detailed investigation on the synthesis and characterization of mordenite has been undertaken with more than one source for silica. Mordenite has been successfully synthesized both from gels containing chemical silica and also the gels with silica derived from rice husk ash. The present work is the first of its kind dealing with synthesis of a zeolite using rice husk, a low-cost agricultural waste material. Mordenites, synthesized from both these silica sources compare very well in their characteristics and were successfully demonstrated as molecular sieves.

5.3 Recommendations for Future Research:

On the basis of the present investigation, the following aspects are indicated for future work:

1. The rapid synthesis of mordenite by seeding with crystals.
2. Possibilities for the crystallization of mordenite at temperatures much below 135°C

using gels of higher alkalinity.

3. The use of the mordenite synthesized in the present study as catalyst in chemical reactions. Only the molecular sieve aspect of the study was undertaken in the present investigation.
4. Utilization of rice-husk ash in the synthesis of other types of mordenite species like Na-Li-type.
5. Synthesis of other industrially important zeolites using silica from rice-husk ash.

REFERENCES

1. Gould, R.F., Adv.Chem. Ser. 102 (1971).
2. Meier, W.M. and Uytterhoeven, J.B., Adv.Chem.Ser., 121 (1973
3. Bawa, J.S.,Shanker, U. and Bhattacharyya, J.S., Chem. Ind. Develop. VIII(7), 20 (1974).
4. Breck,D.W., 'Zeolite Molecular Sieves', John Wiley and Sons, Inc., New York, 1974.
5. Kladning, W.F.,Acta Cient Venezolana, 26, 40 (1975).
6. McBain, J.W., in 'The Sorption of Gases and Vapours by Solids', George Rutledge and Sons Ltd., Lond. 1932, Ch.5.
7. Breck,D.W., in 'Sintering and Catalysis', (Ed. Kuczynski,G.C Plenum Press, New York, 1975, p.211.
8. Eital,W., 'Physical Chemistry of the Silicates', Univ. Chicago Press, Chicago, 1954.
9. Meier,W.M., in 'Molecular Sieves', Soc. Chem. Ind., Lond. 1968, p.10.
10. Barrer,R.M.,Chem. and Ind., 7 Sept. , 1203 (1968).
11. Krainich,W.L., Ma, Y.H., Sand, L.B., Weiss, A.H., and Zwiebel, I.,Adv. Chem.Ser. 101, 502 (1971).
12. Meier, W.M.,Z. Krist. 115, 439 (1961).
13. Keough, A.N. and Sand, L.B., J.Am.Chem.Soc., 83, 3536(1961).
14. Eberly, Jr. P.E. and Kimberlin, Jr.C.N., Ind. Eng. Chem. Prod. Res. Develop. 9(4) , 335 (1970).

15. Bierenbaum, H.S., Chiramongkoi, S. and Weiss, A.H., J. Catal. 23, 61 (1971).

16. Hansford,R.C. and Ward, J.W., J.Catal. 13, 316 (1969).

17. Hopper,J.R. and Shigemura, D.S.,AIChE J. 19(5), 1025 (1973).

18. Voorhies, Jr., A. and Hopper, J.R.,Adv. Chem. Ser. 102, 410 (1971).

19. Allan,D.E. and Voorhies, Jr. A. , Ind.Eng. Chem. Prod. Res. Develop. 11, 159 (1972).

20. Brecker, K.A., Karge, H.G. and Streubel,W.D., J.Catal. 28, 403 (1973).

21. Karge,H.G., in 'Symp. on the Mechanism of Hydrocarbon Reactions', Siofok, Hungary, 5-7 June 1973, p.417.

22. Tatsuaki, Y., Hura, M. and Nobuyoshi, H., Bull. Jap. Petr. Inst., May, 12 (1970).

23. Brooks,C.S., Adv. Chem.Ser. 102, 426 (1971).

24. Kawasaki, A., Taniguchi, M. and Nishiyawa, T., Japan, 7109, 593 - 11 Mar (1971), Chem. Abstr. 75:37621c.

25. Miale, J.N. and Weisz, P.B., J.Catal. 20, 288 (1971).

26. Breck,D.W. and Flanigen,E.M., in 'Molecular Sieves', Soc. Chem. Ind.,Lond., 1968, p 10.

27. Barrer, R.M., in Molecular Sieves', Soc. Chem. Ind., Lond., 1968, p.39.

28. Bungenberg de Jong, H.G. in 'Colloid Science II', (Ed. Kruyt,W.R.), Elsevier, New York, 1949, p.2.

29. Morey,G.W. and Ingerson,E., Econ. Geol. 32 (Sup. to no.5), 607 (1937).

30. Sand, L.B., Roy,R. and Osborn,E.F., Econ. Geol. 52, 169 (1957).

31. Regis,A.J.,Sand, L.B.,Calman,C. and Gilwood, M.E.,J. Phys. Chem. 64, 1567 (1960).

32. Barrer,R.M., J. Chem.Soc. 127 (1948).

33. Barrer, R.M., J.Chem.Soc. 2158 (1948).

34. Barrer,R.M. and White, E.A.D, J.Chem.Soc. 1261(1951).

35. Barrer,R.M., and White,E.A.D., J.Chem.Soc. 1561 (1952).

36. Milton,R.M., U.S. 2,882,243 (1959), Chem.Abstr. 53:13454f.

37. Milton,R.M., U.S. 2,882,244 (1959), Chem.Abstr. 53:13454h.

38. Miyota, Y. and Okazaki,S., Kogyo Kagaku Zasshi, 73(9), 1940 (1970), Chem.Abstr. 76: 115569d.

39. Takahashi, H., Japan, 7226,598 (Cl.Colb) 18 Jul (1972), Chem.Abstr. 78:60303w.

40. Barrer,R.M. and Denny, P.J., J.Chem.Soc. 983 (1961).

41. Sand, L.B., in 'Molecular Sieves', Soc. Chem. Ind., Lond., 1968, p.71.

42. Leonard, R.J.,Econ.Geol. 22, 843 (1927).

43. Borer, H. and Meier, W.M.,Adv. Chem.Ser. 101, 122 (1971).

44. Ames, Jr. L.L. and Sand, J.B.,Amer.Mineral. 43, 476 (1958).

45. Ellis, A.J.,Geochim Cosmochim Acta 19, 145 (1960).

46. Barrer, R.M. and Marshall, D.J., J.Chem.Soc. 485 (1964).

47. Domine,D. and Quobex, J. in 'Molecular Sieves', Soc.Chem. Ind. Lond., 1968, p.78.

48. Wolf,F. and Renning, J., Ger. (East) 83978(Cl.Colb),20 Aug. (1971), Chem.Abstr. 78:113434y.

49. Wolf, F. and Renning, J. , Ger. (East), 80892 (Cl.Colb), 05, Apr. (1971),Chem.Abstr. 76: 74387x.

50. Culfaz, A. and Sand, L.B., Adv. Chem.Ser. 121, 140 (1973).

51. Sand, M.L., Coblenz, W.S. and Sand, L.B., Adv. Chem. Ser. 101, 127 (1971).

52. Sand, L.B. and Sand, M.L., U.S. 3,760,062 (Cl. 423/329, Colb), 18 Sep (1973), Chem.Abstr. 80, 49865b.

53. Kimura, K. and Nakajima, W., Kobe Daigaku Kyoikugakubu Kenkyu Shuroku 51, , 57 (1974), Chem.Abstr. 84: 152771z.

54. Cole,W. and Joh, F., Ger. Offen. 2,115,965 (Cl.colb, Bolj), 14 Oct. (1971), Chem.Abstr. 76:5429a.

55. Senderov, E.E.,Geokhim. 9, 820 (1963).

56. Saha, P.,Amer. Mineral. 44, 300 (1969).

57. Saha, P.,Amer. Mineral. 46, 859 (1966).

58. Guyer,A., Ineichen, M. and Guyer, P., Helv. Chim Acta. 40, 1603 (1957).

59. Senderov, E.E. and Khitarov, N.I., Adv. Chem.Ser. 101, 149 (1971).

60. Kim, K.T. and Burely, B.J., Can. J.Earth. Sci., 8, 311 (1971).

61. Coombs,D.S.,Ellis, A.J.,Fyfe, W.F. and Taylor, A.M., Geochim. Cosmochim. Acta. 17, 53 (1959).

62. Whittemore, Jr. D.J.,Amer. Mineral, 57, 1146 (1972).

63. Norton Company, Brit. 983756 (Cl.Colb),Feb. 17 (1965). Chem.Abstr. 62: 14217e.

64. Norton Company, Neth. Appl. 298, 606 (Cl. Colb), Aug. 10 (1965), Chem.Abstr. 64:4656a.

65. Sato, G. and Takakura, K., Japan 75,33036 (Cl.Colb) 27 Oct. (1975), Chem.Abstr. 84, 124065d.

66. Pop,E.A., Mircioiu, J., Enache,F. and Crisan,D., Rom. 57763 (Cl.Colb), 08 Oct. (1974), Chem.Abstr. 84, 137950.

67. Smith, J.V., Mineral.Soc. Am.Spec. Paper No.1, 281 (1963).

68. Fischer, K.R. and Meier,W.M.,Fortschr. Mineral 42, 50(1965).

69. Weeks, T.J., Hillery, H.F. and Bolton, A.P., J.Chem.Soc., Farad. Trans. I, 71, 2051 (1975).

70. Kiselev,A.V. and Lygin,V.I., in 'Infrared Spectra of Adsorbed Species' (Ed. Little, L.H.), Academic Press, Lond., 1967, p.361.

71. Wright,A.C.,Rupert, J.P. and Granquist,W.T., Amer. Mineral. 53, 1293 (1968).

72. Zhdanov, S.P., Kiselev, A.V.,Lygin,V.I. and Titova, T.I., Russ. J. Phys. Chem. 38, 1299 (1964).

73. Flanigen,E.M., Khatami, H. and Szymanski, H.A., Adv. Chem. Ser. 101, 201 (1971).

74. Bertsch, L. and Habgood, H.W.,J. Phys. Chem. 67, 1621(1963).

75. Rosseinsky,D.R., Chem.Rev. 65, 467 (1965).

76. Coughlan, B. and Carroll, W.M., J. Chem. Soc., Farad. Trans. I , 72 , 2016 (1976).

77. Lai, P.P. and Rees, L.V.C., J. Chem.Soc., Farad. Trans. I, 72, 1840 (1976).

78. Plank, W.A., in 'Analytical Calorimetry,Vol.3', (Ed. Porter, R.S. and Johnson, J.F.), Plenum Press, 1974, p.649.

79. Barrer, R.M. and Peterson,D.L., Proc. Roy. Soc. ,A280, 466 (1964).

80. Sherry, H.S., J. Phys.Chem. 70, 1332 (1966).

81. Barrer, R.M., Proc. Chem. Soc., April (1958), p.99.

82. Rees, L.V.C. and Rao, A., Trans. Farad. Soc. 62, 2103(1966).

83. Barrer,R.M., Davies, J.A. and Rees, L.V.C., J. Inorg. Nucl. Chem. 31, 2599 (1969).

84. Sherry, H.S., Adv.Chem.Ser. 101, 350 (1971).

85. Wolf,F., Fuertig, H. and Knoll, H., Chem.Tech. 23, 273 (1971).

86. Barrer,R.M., Trans.Farad.Soc. 67, 3565 (1971).

87. Peterson,D.L., Helfferich, F. and Blytas,G.C., J. Phys. Chem.Solids 26, 835 (1965).

88. Barrer,R.M. and Coughlan, B., in 'Molecular Sieves', Soc. Chem. Ind., Lond. 1968,p. 233.

89. Joubert, J.I. and Zwiebel, I.,Adv. Chem.Ser. 102, 209 (1971).

90. Takeishi, T. and Yusa, A., Trans.Farad.Soc. 67, 3565 (1971).

91. Beecher,R.,Voorhies, Jr. A. and Eberly, Jr., P., Ind. Eng. Chem. Prod. Res. Develop.7, 203 (1968).

92. Eberly, P.E., J. Phys.Chem. 67, 2404 (1963).

93. Norton's Chemical Process Products Division, Bulletin Z-5 (1976).

94. Freund, E.F., J.Crystal Growth, 34, 11 (1976).

95. Rao, C.N.R., 'Chemical Application of Infrared Spectroscopy', Academic Press, New York, 1963.

96. Vogel, A.I., in 'Quantitative Inorganic Analysis 3rd Ed.', ELBS and Longman, Lond. 1975, Ch.V.

97. Hillebrand, W.F. and Lundell, E.F., in 'Applied Inorganic Analysis, 2nd Ed.', John Wiley and Sons, Inc., New York, 1959, p.495 and 507.

98. Dean, J.A., in 'Flame Photometry', McGraw Hill, New York, 1960, p.295.

99. Holm, V.C.F., Bailey, G.C. and Clark, A., J. Phys. Chem. 63, 129 (1959).

100. Plank, C.J., Anal. Chem. 24(8), 1304 (1952).

101. Zhadanov, S.P., Adv. Chem. Ser. 101, 20 (1971).

102. Goldsmith, J.R., J. Geol. 61, 439 (1953).

103. Hsu, A.C.T., AIChE J. 17, 1311 (1971).

104. Kuhl, G.H., Amer. Mineral. 54, 1607 (1969).

105. Coombs, D.S., Mineral. Mag., 30, 699 (1955).

106. Chen, N.Y. and Smith, F.A., Inorg. Chem. 15, 295 (1976).

107. Dyer, A. and Molyneux, A., J. Inorg. Nucl. Chem. 32, 2389 (1970).

108. Dyer, A. and Ogden, A.B., J. Inorg. Nucl. Chem. 37, 2207 (1975).

σσσσσ

A P P E N D I X

APPENDIX A.1

X-RAY POWDER ANALYSIS

When a monochromatic beam of x-rays strikes an atom in a crystal, tightly bound electrons are set into oscillation and radiate x-rays of same wave length as that of the incident beam. This is called diffraction. Every crystalline substance scatters thex-rays in a particular diffraction pattern, depending on its atomic and molecular structure. The shape and size of a unit cell fix the angular position of peaks and relative intensities of these peaks are governed by the number and positions of atoms within the unit cell. The relationship between the wavelength of the x-ray beam, λ, the angle of diffraction, θ, and the interplanar distance, d, is governed by the Bragg equation[a]

$$2d \sin \theta = n\lambda$$

where, n, the order of diffraction, is usually first order. For a orthorhombic crystal, as in case of mordenite type zeolite lattice parameters (a,b,c), Miller indices (h,k,l) and interplanar distance (d) bear a relationship.

$$\frac{1}{d} = \sqrt{\frac{h^2}{a^2} + \frac{k^2}{b^2} + \frac{l^2}{c^2}}$$

---

[a]Bragg, W.L., 'The Crystalline State', Macmillan, New York, 1933.

APPENDIX A.2

X-RAY POWDER DATA FOR SODIUM SILICATE

d(Å)	I/I_o
7.10	20
6.65	40
6.25	100
5.68	45
5.60	35
4.49	25
4.43	15
4.15	20
4.07	60
3.90	40
3.82	20
3.76	30
3.65	25
3.32	80
3.28	70
3.16	75
3.03	30
3.00	20
2.98	20
2.85	20
2.81	35
2.73	30
2.71	45
2.65	20
2.63	20

APPENDIX A.3

X-RAY POWDER DATA FOR SODIUM HYDROXIDE

d.(Å)	I/I_o
5.75	32
4.61	35
4.01	15
2.94	7
2.81	52
2.68	4
2.58	3
2.52	10
2.34	100
2.18	8
2.03	11
1.89	24
1.71	28
1.70	29
1.65	32
1.46	13
1.34	6
1.27	10
1.20	5

APPENDIX A.4

X-RAY POWDER DATA FOR ALUMINIUM HYDROXIDE

d(Å)	I/I_o
4.70	100
4.35	65
3.19	30
2.22	60
1.71	25
1.45	10

APPENDIX A.5

X-RAY POWDER DATA FOR NATURAL MORDENITE[a]

d(Å)	I/I_o	hkl
13.70	50	110
9.10	90	200
6.61	90	111
6.38	40	130
6.10	50	021
5.79	50	201
5.03	10	221
4.87	20	131
4.53	80	330
4.14	30	420
4.00	90	150
3.84	60	241
3.76	20	002
3.62	10	112
3.56	10	510
3.48	100	202
3.39	90	060
3.31	10	222
3.22	100	530
3.10	20	441
2.95	20	531

Appendix A.5 (contd)

d(Å)	I/I_o	hkl
2.90	60	402
2.74	10	152
2.70	30	621
2.64	10	370
2.56	40	461
2.52	50	442
2.47	20	
2.44	20	
2.34	20	
2.30	10	
2.28	10	
2.23	20	
2.16	20	
2.12	10	
2.05	40	
2.02	40	
1.99	40	
1.95	40	
1.94	10	

[a]ASTM Card No. 6-0239

Date Slip A 54009

This book is to be returned on the
date stamped

.....

CME-1977-D-BAJ-SYN